

The nose knows
which way the odor flows:
spatial orientation in odor-guided
navigation.

by

J. K. LOCPORT

Submitted in partial fulfillment of the requirements for the degree of

Doctor of Philosophy

Biology Department

CASE WESTERN RESERVE UNIVERSITY

May, 2018

CASE WESTERN RESERVE UNIVERSITY

SCHOOL OF GRADUATE STUDIES

We hereby approve the dissertation of

Jamie Kendra LocPort

candidate for the degree of Doctor of Philosophy.

Committee Chair:

Mike Benard

Committee Member:

Jessica L. Fox

Committee Member:

Roy E. Ritzmann

Committee Member & Advisor:

Mark A. Willis

Outside Committee Member

Thomas L. Daniel

Date of Defense

22 March 2018

Table of Contents

<u>List of Tables</u>	3
<u>List of Figures</u>	4
<u>List of Abbreviations</u>	6
<u>Acknowledgements</u>	7
<u>Abstract</u>	8
<u>Chapter 1</u>	9
<u>Chapter 2</u>	29
<u>Chapter 3</u>	47
<u>Chapter 4</u>	82
<u>Chapter 5</u>	114
<u>Appendix i</u>	118
<u>Appendix ii</u>	127
<u>References</u>	128

List of Tables

Table	Page
<u>1.01 - Calculated Re for various animals</u>	17
<u>2.01 - Measurements of plume dynamics & geometry</u>	40
<u>3.01 - Definition of measured tracking parameters</u>	61
<u>3.02 - Grand means of track parameters</u>	62
<u>4.01 - Predicting success rate from the odor gain factor</u>	86
<u>4.02 - Predicting success rate from total antenna length in the bilateral heuristic</u>	91
<u>4.03 - Predicting inter-turn duration from the odor gain factor</u>	92
<u>A.i.01 - Credibility intervals on the difference in means between animals with only a left or right antenna</u>	118
<u>A.i.02 - Credibility intervals on the difference in means between animals with two antennae vs one antenna</u>	119
<u>A.i.03 - Credibility intervals on the difference in means between animals with different length antennae, by treatment</u>	120
<u>A.i.04 - Credibility intervals on the difference in means between animals with the same net antenna length, bilateral vs antennectomy</u>	121
<u>A.i.05 - Grand means, antennae of different lengths</u>	122
<u>A.i.06 - Grand means, number of antennae</u>	123
<u>A.i.07 - Least squares contrasts between the mean track parameters measured from cockroaches with one or two antennae but with equal total length of antennae</u>	124
<u>A.i.08 - Least squares contrasts of the effect of antennal length across all of the mean track parameters measured from cockroaches with one or two antenna equalling the same total length</u>	125

List of Figures

Figure	Page
<u>1.01 - Unknown path</u>	10
<u>1.02 - Diffusivity of CO₂ and Bombykal at different points in time</u>	14
<u>2.01 - EAG & PID recordings at different speeds and location</u>	39
<u>2.02 - 3D plume map and concentration</u>	42
<u>3.01 - Rates of Success at locating the pheromone source of the different experimental treatment groups</u>	56
<u>3.02 - Cockroach with full length antenna display a range of tracking behaviours</u>	59
<u>3.03 - Left and right antenectomized animals behave the same</u>	64
<u>3.04 - Animals with one antenna behave differently from animals with two antennae</u>	65
<u>3.05 - Most track parameters vary with antennal length, yet animals with equal total lengths of antenna are indistinguishable in their behavior</u>	66
<u>3.06 - Bilateral or antenectomized animals with different length antennae behave differently</u>	67
<u>3.07 - Animals with the same total antennae length behave broadly simmarly</u>	68
<u>3.08 - Proposed flow chart of odor-tracking behavior in <i>P. americana</i></u>	72
<u>4.01 - Success rates and linearity</u>	86
<u>4.02 - Examples of the behavior of individual simulation runs from two odor gains from the two random heuristics</u>	88
<u>4.03 - Examples of the behavior of individual simulation runs from three odor gains across the three antenna configurations from the bilateral heuristic</u>	89

<u>4.04 - Examples of the behavior of individual simulation runs from two odor gains from the two random heuristics</u>	90
<u>4.05 - The overarching flow of a trial</u>	97
<u>4.06 - Class structures</u>	102
<u>4.07 - Random heuristic</u>	103
<u>4.08 - Limited heuristic</u>	104
<u>4.09 - Bilateral heuristic</u>	106
<u>4.10 - Temporal heuristic</u>	108
<u>4.11 - Evaluating evidence</u>	109
<u>4.12 - Integration heuristic</u>	110
<u>A.i.01 - Interaction of antenna length and number of antennae with the number of stops</u>	126

List of Abbreviations

COM - Center of Mass

EAG - ElectroAntennoGram

ORC/ORN - Olfactory Receptor Cell/Neuron

PID - PhotoIonization Detector

PSP - PostSynaptic Potential

EPSP - Excitatory PostSynaptic Potential

IPSP - Inhibitory PostSynaptic Potential

HDI - Highest density interval

ECV - evidence counting variables

Acknowledgements

The list of people I need to thank is impossibly long. Below are just a few of the people I'd like to thank their invaluable support, insight, and feedback:

Current and past members of the Willis Lab:

Jen Avondet

Solomon Awe

Dana Coleman

Sean Copley

Josh Martin

Jen Milligan

Kalyanasundaram Parthasarathy

Alison Smith

Kim Thompson

Heather Voss-Hoynes

My advisor, Mark Willis

My committee: Tom Daniel, Jess Fox, Roy Ritzmann, & Robyn Snyder

The Biology Graduate Coordinator, Julia Brown-Allen, and the rest of biology department, particularly the members of the Fox Lab who were especially good at giving feedback on-the-fly.

Lastly, I need to thank my wife, Theresa LocPort; parents, Nyca & Cliff Lockey; and the rest of my family for their impeccable patience and support.

This work was supported by National Science Foundation grant IOS-1121498 to MAW, and a School of Graduate Studies-Graduate Student Travel Award.

Abstract

It has been proposed since the very beginnings of mechanistic analyses of animal orientation and navigation that bilaterally symmetrical animals had two approaches available for using sensory information - spatial and temporal. The spatial approach requires a comparison between two or more sensory inputs, whereas in a temporal approach the input from the various sensors are summed and compared across time. It has long been assumed that animals could and use both of these strategies, but these ideas have rarely been tested directly. I have chosen to address these fundamental and long standing questions directly through both behavioral experiments and computer simulations. Using the American cockroach, *Periplaneta americana* as a model organism, I have sought answers to the question of how they use the information available to them to track an odor. This required me to consider what are the physical and physiological limits of the environment and the animal ([chapter 1](#)), examine what information is available in the environment ([chapter 2](#)), what can be surmised about the information they use by studying their behavior ([chapter 3](#)), and to consider what might be the best thing to do with the information they collect ([chapter 4](#)). A brief summary tying all of this together is then given ([chapter 5](#)).

Chapter 1

Oh the places you'll go: smelling your way from A to B.

ABSTRACT

There have been many methods of chemical orientation proposed across a wide range of bilaterally symmetrical organisms, but perhaps none has been more studied or discussed than bilateral comparisons between sensors on each side of an animal. The significance and necessity of bilateral input has often been contradicted, even within the same species. By considering the context the organism has evolved in, how it moves through the environment, the morphology & physiology of the sensory structures, and the physical properties of the environment, we can design experiments that allow the animals to tell us how they orient to, and track, various chemicals.

INTRODUCTION

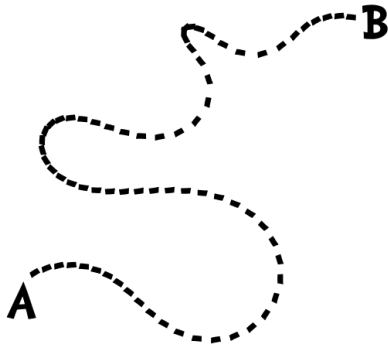


Fig. 1.01 Unknown Path. In its simplest and most abstract form, the question we seek to answer is: **How do you get from A to B?**

Imagine you are at some point, **A**, and you want to get to some other point, **B** ([Fig. 1.01](#)). How do you do it? This simple, mundane question has anything but a simple answer, involving many aspects of biology: knowing where you are (point **A**) relative to where you want to be (point **B**) is a question of sensory systems; how you locomote from **A** to **B** is a matter of physiology, biomechanics, and motor systems, cell growth, or the use of organelles like flagella. In animals, this is usually underpinned and coordinated by a nervous system where information about the environment is filtered, integrated, and processed, culminating in a chain of decisions about how to respond in moving towards **B**. You are constrained by your physiology, the biomechanics of your body's design, and how these interact with your environment. You can only move so fast, turn so sharp, and coast so far. You can only sense things within a limited range or process sensory information and motor feedback so fast. These are the constraints of the solution to the problem of how to locate the resource to which you are attracted.

To know where they are in relation to where they want to be, animals use a combination of sensory systems; the most common probably being vision, hearing, chemoreception, touch, and thermoreception. Does this place feel right? Smell or taste right? Sound right? Look right?¹ To humans, vision is perhaps our primary sense in navigating the world. We *see* where we are in relation to where we want to be, and *look*-out for obstacles and landmarks as we traverse the landscape. When trying to locate food, refuge, or other humans, vision alone can generally suffice, but is aided by other sensory modalities. For many other animals, vision has less primacy; locating food and conspecifics is often highly dependent on olfaction. Prey have distinct odors as do plants. Many species have unique pheromones meant to attract mates or aggregate conspecifics. Olfaction can play a primary role in announcing where point **B** is, and other sensory modalities such as touch and sight aid in picking a course through the terrain.

This dissertation will focus on how odor may serve as the primary sensory information, supported by others, to navigate from **A** to **B**. The goal of this manuscript is to 1) lay out how odors move through the environment, 2) examine how animals can acquire information about the odor in their environment and what limits their sensors impose, and 3) review how we think animals use the information available to them to locate an odor source.

¹ This is not to say that there aren't other forms of sensory perception that are equally, if not more, important to some animals, or that even these examples are all present or equally used by any particular species.

ODOR AND FLUID ENVIRONMENT: Diffusion is slow; turbulence is needed for timely chemical signaling across distances more than a few micrometers.

Chemo-sensation is, quite simply, the sensory perception of chemicals. Molecules must leave a source, travel through a fluid filled medium, and make contact with a sensor. While there are many ways to build a sensor to transduce chemical signals, the signals themselves are shaped along the continuum from diffusion to turbulence, and as such are always dependent on the same handful of physical principles, namely fluid dynamics.

Sensors are bathed in water-based solutions that an organic molecule must diffuse through, often with help of odor binding proteins, to make contact with a surface bound protein that will transduce a signal into electrical signals (i.e., action potentials) (Mitchell, 2009). Diffusion is perhaps best thought of as the movement of particles (molecules) in relation to each other. It is only suitable for timely communications over small length scales (i.e., sub-millimeter). Diffusing molecules move in a random walk down their concentration gradient from most to least concentrated. Any given step can be in any direction, but summed over many steps, molecules will move from where they are most concentrated towards where they are least, evening out and eventually eliminating the concentration gradient, creating maximum entropy or thermodynamic equilibrium. Once a molecule makes contact with the solvent a

sensor is bathed in, it diffuses through the solvent away from the surface where it is most abundant, towards the sensor where initially it is least abundant.

How is a chemical to make contact with a sensor's solvent? There are two main ways: first, in what we commonly think of as taste (i.e., contact chemoreception), the sensor and source are actively moved by the agent to make contact, allowing for easy transfer from source to sensor through the solvent via diffusion. Second, commonly thought of as smell, molecules evaporate from a source, travel through an intervening medium (i.e., water or air) via convective transport (i.e., mostly through bulk flow and somewhat through diffusion) before dissolving into the solvent around the sensor, and ultimately making contact with the sensor.

The chemical in the signal allows the receiver to deduce something about sender (e.g., sex pheromone signals the availability of a receptive mate). How the chemical gets to the receiver allows it to infer something about the environment between sender and receiver. If the sender, receiver, and the medium are all static with respect to each other, the signaling molecule can only travel from sender to receiver via diffusion. Diffusion from an instantaneous point source can be modeled by:

$$\rho_A = \frac{m_A}{(4\pi D_{AB}t)^{3/2}} e^{\frac{-r^2}{4D_{AB}t}}$$

The density of species A (ρ_A) at time t and distance r from the source is dependent on the mass of A injected at the source (m_A) and the diffusivity of A through species B² (D_{AB}). This equation only addresses the more familiar type of diffusion: concentration diffusion

² It should be noted that A and B are fluids here.

(movement down a concentration gradient). There is also diffusion due to temperature diffusion (movement down a thermal gradient), pressure diffusion (movement down a pressure gradient), and forced diffusion (movement caused by unequal forces)³. These others, while biologically relevant in some contexts (e.g., the Goldman–Hodgkin–Katz equation, which describes ion movement across a selectively-permeable membrane, is an example of forced diffusion), play at most a minor role in long-distance communication, which is the focus of this dissertation.

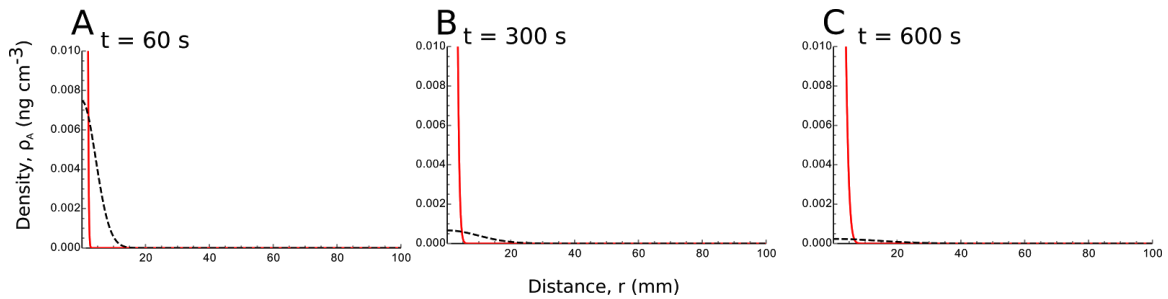


Fig. 1.02 Diffusivity of CO₂ and Bombykal at different points in time. Density (ρ_A) is given on the y-axis, and the distance from the source (r) is on the x-axis. CO₂ ($D_{AB} = 0.161 \text{ cm}^2\text{s}^{-1}$) concentrations are given in black (dashed), and the moth pheromone component bombykal ($D_{AB} = 0.003 \text{ cm}^2\text{s}^{-1}$) is in red. Three different timepoints are shown: A shows the concentration after 1 minute, B, after 5 minutes, and C, after 10 minutes.

Carbon dioxide is perhaps the lightest compound used for biological chemical signaling at 44.009 Da. Its diffusivity in air is about $0.161 \text{ cm}^2\text{s}^{-1}$, at 22.2°C (Pritchard and Currie, 1982). Contrast that with a volatile organic compound like the pheromone bombykal (236.393 Da) having a diffusivity of about $0.003 \text{ cm}^2\text{s}^{-1}$ (based on a diffusivity of $3 \times 10^{-7} \text{ cm}^2\text{s}^{-1}$ through

³These are distinct from advection: they do not create bulk flow.

sensilla liquor (Kanauija and Kaissling, 1985) and the fact that diffusion through air is roughly 10,000 times faster than through water (Vogel, 1994)). [Figure 1.02](#) illustrates the concentrations of these two compounds over a distance of 100 mm. CO₂ (black, dashed) travels considerably faster than the much heavier pheromone (red lines). As the chemical travels further from the source, the lower the peak concentration: a finite amount of mass is spreading out through a three-dimensional volume. By five minutes, bombykal has barely reached 5 mm, while CO₂ is passing 20 mm ([Fig 1.02B](#)). If we were to continue the calculations in [figure 1.02](#), it will take CO₂ 2.8 hours to reach peak concentration at 1 meter from the source and it would take another 6.2 hours to decay to half the peak concentration (contrast that with the 6.4 *days* Bombykal takes to reach peak concentration at a meter away, and the 13.7 days to decay by half). This is clearly not a good way to signal anything across a distance greater than a handful of micrometers, especially if a quick response is needed.

For most multicellular organisms, fluids, senders, and receivers are rarely all static in the same reference frame: there is usually bulk flow, or a net displacement of the fluid medium from a region of high pressure to a region of lower pressure. The fluid currents most commonly known are wind (air movement driven largely by convection), tides, and flows down a stream or river (water movement largely driven by gravity); there are currents through pipes and porous media; and currents caused by forced movements of fluids. A few examples include hearts pumping blood, animals inhaling and exhaling, and movements of the body or limbs (like flapping or swimming). These currents can reach many meters per

second, allowing for very rapid communication. All of these currents are subject to inertial and viscous forces.

Viscosity is a property of fluid that relates how much force is needed to deform a liquid at a given rate. Imagine two parallel plates sandwiching a volume of fluid, the force to move one plate past another is the shear. That force is dependent on the area of the two plates, the distance between those plates, how fast they are moving relative to each other, and the intervening fluid's viscosity. Formally, Newton's law of viscosity is: $\tau = \mu \frac{\delta u}{\delta y}$, where the shear stress (a force per unit area, τ) is related to the velocity gradient between the two areas⁴ of interest ($\frac{\delta u}{\delta y}$) by the fluid's viscosity (μ).

Inertia is Newton's second law: $\vec{F} = m\vec{a}$. The net force is a vector (\vec{F} , N) equal to the mass (m , kg) times the net acceleration vector (\vec{a} , m s⁻²).

We can define a relationship between the inertial forces and the viscous forces:

$$Re = \frac{inertia}{viscosity}$$

The Reynolds number (Re) is the ratio of the inertial force to viscosity and is defined as:

$$Re = \frac{\rho u L}{\mu} = \frac{u L}{\nu}$$

⁴ Plate one is moving at speed u relative to plate two at distance y above plate two.

Where ρ is the density of the fluid (kg m^{-3}), u is the speed of the object through the fluid (m s^{-1}), L is the length scale of the object (m); together, these account for the inertial forces ($\text{kg m}^{-1} \text{s}^{-1}$); dividing by the dynamic viscosity is μ ($\text{kg m}^{-1} \text{s}^{-1}$) gives us the dimensionless Reynolds number, Re . The equation can also be written in terms of the kinematic viscosity, ν ($\text{m}^2 \text{s}^{-1}$), which accounts for the density ($\nu = \frac{\mu}{\rho}$).

There are two extreme worlds that can be described in terms of Re : one is an inertial world, where $Re \gg 10^2$; the other is a viscous world, where $Re \ll 10$. In the inertial world, the inertial forces are so great as to overwhelm the viscous forces—viscous forces can be ignored and still yield a great deal of precision (Vogel, 1994; Weissburg, 2000; Yen, 2000). Likewise, in the viscous world, viscous forces dominate and inertial forces can be ignored and still yield good precision. It is the world between these two extremes, especially $10 < Re < 100$, that proves the most complicated and perhaps the most interesting because in this region you cannot easily ignore inertia or viscosity with much hope of making reasonable estimates. [Table 1.01](#) gives a summary of the conditions at which various organisms operate.

Table 1.01 Calculated Re for various animals (ν is taken for air or sea water at 20 °C)

Animal	L (m)	u (m s^{-1})	$\nu \times 10^{-6}$ ($\text{m}^2 \text{s}^{-1}$)	Re
Salmonella ⁵	1.4×10^{-6}	5.5×10^{-5}	1.05	7.3×10^{-5}

⁵ (Magariyama et al., 2001)

Fruit Fly ⁶	0.003	0.69	15.06	140
Cockroach ⁷	0.04	0.24	15.06	640
Hawkmoth ⁸	0.048	1.2	15.06	3.8 x 10 ³
Human (air) ⁹	1.7	1.5	15.06	1.7 x 10 ⁵
Human (water)	1.7	1.5	1.05	2.4 x 10 ⁶
Whale, blue ¹⁰	29.9	6.3	1.05	1.8 x 10 ⁸

Along with the mechanics of a fluid on an organism, it is also important to consider how the dynamics of a fluid's interaction with the environment affects the dispersal of chemical signals. Laminar flows are smooth; whatever mixing there is happens through diffusion. Turbulent flows, in contrast, are chaotic with many—typically erratic—vortices forming and slowly dissipating. We can calculate a flow's Turbulence Intensity (I) by taking a timed measurement of the flow velocity and dividing the Root Mean Squared of the velocity (u_{rms}) or the standard deviation of the fluctuations in velocity¹¹ ($\sigma_{u-\bar{u}}$) by the mean velocity (\bar{u}):

$$I = \frac{u_{rms}}{\bar{u}} = \frac{\sigma_{u-\bar{u}}}{\bar{u}}$$

⁶ (Marden et al., 1997; Vogel, 1966)

⁷ (Lockey and Willis, 2015)

⁸ (Eaton, 1988; Willis et al., 2013)

⁹ Average human height: 1.7 m, I took a slightly fast swimming speed, and a slightly slow walking speed

¹⁰ (COSEWIC, 2002)

¹¹ Some texts use the standard deviation. This should be the standard deviation of the fluctuations in the velocity (i.e., subtract the mean from the signal, before taking the standard deviation); this is equivalent to the Root Mean Squared.

The Turbulence Intensity is easy to measure and tells us how chaotic the flow is. A better, but more difficult thing to measure would be the eddy viscosity, η , which is a measure of momentum transfer (Streeter and Benjamin Wylie, 1975), and can be predicted with Prandtl's mixing-length theory ((Anderson, 2010; Prandtl, 1925).):

$$\eta = \rho l^2 \frac{du}{dy}$$

The dominant velocity gradient is assumed to be in the y direction, so du/dy is the rate of change (i.e., flow speed), ρ is the density of the fluid, and l is the mixing length. We can predict l from Von Kármán (Karman, 1934):

$$l = \kappa \frac{du/dy}{d^2u/dy^2}$$

The universal constant, κ was originally calculated by Von Kármán to be 0.38, then later revised to 0.40 (Karman, 1934). There has been much controversy surrounding the value of κ , with 0.40 being somewhere in the middle of the proposed values (Trinh, 2010). It's also worth noting that Prandtl's mixing length theory is not without its problems; it just happens to be relatively easy to calculate and reasonably accurate over a range of practical problems (Anderson, 2010).

When there is bulk flow, the chemical signal is taken from its source and carried downstream. The higher the eddy viscosity—the more mixing—the wider a plume will grow as it travels downstream. The packets of signal-laden fluid will intermingle with packets of clean air and become less concentrated. A signal released in the most turbulent environment will be spread wide, but not last very long before it dissipates below any detection threshold.

On the other hand, if a signal is released in the smoothest environment available it will be carried for a very long distance as a thin ribbon. There are pros and cons to both: in the former, the probability of a receiver crossing the plume is high, but depending on the response threshold, the sender may need to be close to the receiver if the concentration is to be high enough to detect. In the latter, the signal will travel a long ways, but the probability of a receiver crossing it (and perhaps even being able to follow it) is low.

Armed with a basic understanding of how a signaling chemical can migrate through the environment, we can make some assumptions about where B is in relation to A. In the next section, I'll examine what information organisms can access and what kinds of assumptions can be made.

USING ENVIRONMENTAL INFORMATION: comparisons will be made, either across time, space, or both

At its simplest, chemical communication is only limited by the specificity of the receptor: a signaling molecule either does or does not bind a receptor protein and initiate a transduction event. In most cases, depending on the system in question, receptor proteins are not so specific as to allow only one configuration of one molecule to bind them: there is a probability distribution on a range of molecules with similar properties, the major exception being pheromone receptors which are highly specific, the probability distribution being a sharp peak for a given conformation of the pheromone. If a given receptor has a higher affinity for molecule α than for β , then a higher concentration of β is needed to produce the

same signal using the same receptors. If we have multiple receptor types and our molecule of interest could bind to more than one receptor (with a different affinity for each type), the relative rates of bindings across receptors could be important in an organism's ability to identify the molecule. Compound this with the fact that odors can be made up of dozens of different molecules (Riffell et al., 2009) and organisms can have upwards of thousands of chemoreceptive sensillae (Schaller, 1978), and you have an excellent system for signaling. In addition to adding or removing continuants, a novel signal can evolve by simply changing the relative concentrations.

How sensors are arranged and moved through the environment matters a good deal. A chemical signal is restricted to the physical limits laid out above (diffusion is slow, turbulent mixing is (to a degree) unpredictable), but knowing¹² whether the signal is a gradient set up by diffusion or a patchwork of clean and odorous air because of turbulence, and taking advantage of it can aide you in finding B, from A.

If you want to orient to a signal with a single sensor you need to compare the signal across time, thus *requiring* memory; with multiple sensors you can instead compare the signal across space, no memory required. For example, *Escherichia coli* tracks up a chemical gradient, it does so through a series of relatively straight “runs” and tumbling-turns called “twiddles” (Berg

¹² A note of precaution: I do not mean “know” in the general epistemological sense, where knowledge is Justified True Belief (and probably a little something more, as Gettier (Gettier, 1963)). At best, here the belief is built into the system, justified by the “experience” of evolution (i.e., whatever has worked), the truth playing out as fitness. Kant (“Critique of Pure Reason” as published in (Ariew and Watkins, 2009) would most likely call this “analytical knowledge” (as opposed to “synthetic”), meaning that it is strictly causal. No agency need be ascribed to a system for it to “know” within the context of this manuscript.

and Brown, 1972). During a run, the many flagella coordinate into a bundle. This bundle will fall apart into some degree of disorder, sending the *E. coli* tumbling (the twiddle); the more disorder, the longer the twiddle. Eventually, the flagella reorganize into a bundle and send the *E. coli* off in a new direction. The length of a run, and the amount of time it takes to reorganize the flagella into a bundle to speed off again is dependent on an association with chemoreceptors. Depending on the particular attractant, both the level of association of the receptor with the flagella and the rate of change in the association can affect the stability of the flagellar bundle (Berg and Brown, 1972). The “memory” here lasts as long as it takes to clear the chemoreceptors and is found in the status of the chemoreceptors and concentrations of secondary messengers in their various states of phosphorylation (Manson, 1992). There is about a 200 ms latency between stimulation and response in the flagellar motor and the biochemical system must have a retention time of seconds (Manson, 1992).

For chemotaxis in bacteria, the organism itself is (probably) the sensor¹³, compare that to animals with nervous systems where the sensor is either a neuron or part of a neuron and there can be many sensors distributed across various parts of the body. With multiple sensors, the animal is not restricted to taking one sample at a time and being forced to compare across time; they can take two (or more) simultaneous samples and compare across space with no regard for how the signal is changing in time.

¹³ This seems like a rather large assumption, but to the best of my knowledge, there is no evidence of a bacterium making spatial comparisons (despite the theoretical possibility based on cell size and gradient steepness explored by Dusenberry (Dusenberry, 1997))—The standard dogma is that bacteria make comparisons across time and continue straight or turn based on sensory experience.

The simplest spatial comparison is between two points in space. If the organism is bilaterally symmetrical and has a sensor on each symmetrical side of its body, then bilateral comparisons are the most obvious comparison available. If you are tracking an attractive stimulus, compare the input from the sensor on the left to the one on the right and turn towards the stronger of the two inputs. An early systematic study of sensory physiology demonstrated this in the flatworm *Planaria*. (Koehler, 1932). In removing the primary chemosensory organ on one side of the worm and placing it in an arena with a chemical stimulant, Koehler found that during forward progress, the worm turned towards the remaining sensor in an attractive stimulus, and away in a repulsive stimulus, making a looping track.

Spatial comparisons can be more complicated when you have an array of more than two—symmetrically arranged—sensors, or sensors scattered across your body. A long array of many sensors (assuming they aren't organized into two meta-sensors) will require the nervous system to integrate over the array. If the tracking strategy is strictly spatial, the nervous system will need to summarize the stimulus and make a decision based on that. The stimulus can be summarized as a mean or median of relative stimulus strength or as a binary ON/OFF or different parts of the array could be weighted differently. It is worth noting that there is no guarantee that the array is represented linearly with the gross anatomy: the density or sensitivity of receptors could vary independently of surface area.

With a nervous system, animals can use temporal strategies that go beyond the biased random walks of bacteria. Changes in the stimulus can be monitored over time and correlated with known displacement vectors; something akin to path integration (Wehner et al., 1996) could be used to estimate a source's location. For example, we can imagine simple system consisting of a small collection of cells, each one representing a different compass heading. As the animal progresses, the cells corresponding to the current heading can be receiving input but not enough to trigger an action potential. When the animal senses the odor it wishes to track, additional input can be sent to all the compass cells, depolarizing the one corresponding to the current heading enough to trigger an action potential. Such cells firing would signal to the downstream nervous system that the current heading is the right one with respect to tracking the odor.

While simplistically categorizing things into spatial versus temporal makes designing and analysing studies easier, there is relatively little reason to think that most systems are restricted to just spatial or just temporal: why not both? Nervous systems interfaced with two or more distinct sensors are obviously capable of making spatial comparisons (it's at least physically possible); having neurons means you are also capable of storing information through postsynaptic potentials (PSPs)—both inhibitory (IPSPs) and excitatory (EPSPs)—as well as through synaptic modifications. Both spatial and temporal information would seem to be available to most multicellular trackers, and it would be noteworthy, indeed strange even, for a system not to take advantage of the information available to it, especially if it could be unreliant on any one source of information. Having the flexibility to make use of

spatial information when available and the ability to fall back onto something else when you lose the ability to make spatial comparisons (e.g., through injury) should increase your fitness.

WHAT THE DATA MAY BE TELLING US

When it comes to what animals actually do, the data provide a mish-mash of answers, sometimes even within the same animal. If we want to know if spatial comparisons are necessary for odor tracking, we can remove spatial information by either removing all but one sensor, or provide an environment devoid of spatial contrasts to compare between. In other words, we can force a system to use temporal methods

Most organisms that are known to use spatial information in chemotaxis are described as using bilateral comparisons to orient to an odor plume: tethered walking adult fruit flies, *Drosophila melanogaster* require bilateral input to orient to an attractive odor (Borst and Heisenberg 1982) and in tethered flying adults, bilateral input is required to orient to toward attractive (Duistermars et al. 2009) and away from repulsive odors (Wasserman et al. 2012). This is in contrast to freely moving *D. melanogaster* larva, for which bilateral input enhances chemotaxis, but is not necessary to navigate successfully in an odor gradient (Louis et al. 2008). Walking silk moths, *Bombyx mori* turn towards their antenna receiving a higher concentration stimulus or a later stimulus, and partially occluding one antenna biases turns away from that antenna (Takasaki et al., 2012). Rats require bilateral input to accurately

localize an odor (Rajan et al. 2006), and bilateral input increases the accuracy of tracking an odor trail (Khan et al. 2012). Crayfish *Orconectes rusticus* (Kraus-Epley and Moore, 2002), and the chambered nautilus, *Nautilus pompilius*, (Basil et al., 2000) have also been shown to require bilateral input to effectively track odors. Even humans perform better at olfactory tasks when bilateral information is available (Porter et al. 2005; Porter et al. 2007).

For temporal tracking, or what Fraenkel and Gunn (Fraenkel and Gunn, 1961) call “klino-taxis,” organisms are described as making a sequence of “trial movements” and the course is corrected based on the change in stimulus between trials. They provide a classic example from Mast (Mast, 1911), where maggots are stimulated with light. The maggots retreat from the light (negative photo-taxis), making slight side-to-side test movements about the axis of the light rays, and ultimately moving along the light ray away from the source. When the light source is shut off, and a new one introduced in a new location, the animal turns and retreats away from the new ray’s direction, making trial-movements about that axis. It is only by comparing stimuli across sequential samples and correlating the location with the stimuli that the correct path can be calculated. How much, and what kind of information is being retained and correlated is unknown.

By building models and testing them in simulations, we can better understand the kinds of information biological systems might be using, then use that to design better experiments, that can then provided better constraints on our models and build more realistic simulations.

SUMMARY

Information is processed through the environment and filtered by the physiology of the organism receiving it. The physical properties of the environment, the ecology of the environment, the response dynamics and arrangement of the sensors are all important.

In the following chapter I present detailed measurements of the wind tunnel environment used in the behavioral experiments ([chapter 2](#)). I note that the fluid flows in the wind tunnel are similar to what can be found in natural environments in which our test subjects (the American cockroach, *Periplaneta americana*) are found. The flow is surprisingly smooth, leading to a constant flow of odor information, rather than a turbulent, intermittent plume.

The chapter after that looks at how manipulating the sensory structure impacts the animals' ability to track an odor ([chapter 3](#)). This work extends odor-tracking work previously done in static environments (Bell and Tobin, 1981) to include the behavioral responses in fluid flows (i.e., plume following), and also examines more granular loss of antennae (not just the removal of the entire antenna(e)). As in the previous study, loss of an antenna did not bias the turning in the direction of the remaining antenna, like is seen in other organisms such as the silk moth, *Bombyx mori* (Takasaki et al., 2012), or the ant *L. fuliginosus* (Hangartner, 1967). The trait most predictive of behavior was antennae length: animals with the same total length of antenna performed similarly.

The last study presented here tests the model proposed in chapter 3, as well as several other basic models of odor tracking ([chapter 4](#)). The Integrative heuristic that was suggested in Chapter 3 was robust against any type of missing antenna segments, if inefficient. Whereas, a purely spatial heuristic that depends on bilateral input fails utterly with a loss of one of the two antennae. The purely temporal heuristic is remarkably robust, showing high levels of success in all but the highest noise trials.

Together, these studies add to our understanding of how nature has developed systems to make use of odor information filtered through an environment. It would seem that having a spatio-topic map of the location of odor sensors with respect to the body enhances a system's ability to orient to and localize an odor.

Chapter 2

Temporal and spatial distribution of airborne volatile plumes in the boundary layer

ABSTRACT:

We used a combination of Electroantennogram (EAG) preparations and a Photoionization Detector (PID) to map odor plumes in a wind flow at a typical walking experiment speed of 25 cm s^{-1} . Antennae from cockroaches (*Periplaneta americana*) were used to characterize basic plume dynamics. After verifying that the PID was able to capture the dynamics and response range of the EAGs, it was used to construct a 3D map of a boundary layer constrained plume used in my walking odor tracking experiments. At flight experiment speeds (i.e., 100 cm s^{-1}), we saw the intermittent signal expected of a turbulent plume. However, at the wind speed used for our walking plume tracking experiments (i.e., 25 cm s^{-1}) intermittency is lost. The odor plume is characterized by a slowly increasing and decreasing signal reminiscent of a drifting or “wandering baseline” signal. This is consistent with odor-bearing flows in water very close to the substrate, that has been referred to as a “viscous sublayer”.

INTRODUCTION:

Electroantennograms (EAGs) are a well established method for verifying an insect's ability to detect a chemical compound (Schneider, 1957), having been used in the lab across a wide range of arthropods (Hodgson, 1958). They have also been employed in the field to characterize natural plumes (Baker and Haynes, 1989); (Baker and Haynes, 1989; Murlis et al., 1990; Murlis et al., 2000) along with the single sensillum recording (Van der Pers and Minks, 1993); (Koch et al., 2009). The EAG works by measuring the voltage across an entire antenna: we essentially get the bulk output of all the olfactory sensory cells on the antenna, making the EAG a single-unit, multimodal sensor. The advantage in EAGs is that we get a sense of what the actual detector is experiencing. The drawback is that this limits us to the entire antenna being the unit of detection, and any sub-antennal patterns of activation are lost. The EAG has become a vital and standard tool for validating plume-tracking experiments (Grünbaum and Willis, 2015; Lockey and Willis, 2015; Willis et al., 2013); (Andersson et al., 2013).

Photoionization Detectors (PIDs) have been used to supplement EAG recordings (Daly et al., 2013). They work by passing a chemical-bearing airstream past an ionizing light source. Volatile organic molecules decompose into constituent ions that generate a current which is measured by an ammeter. By seeding a plume of a tracer molecule, we can use a PID to map a plume over an indefinite period of time. By comparison, since in most cases an EAG

preparation requires the surgical removal of the antenna, the physiological lifespan of an EAG is highly dependent on how it is prepared, with about an hour at best for an excised antenna in the studies presented here.

Electroantennograms from American cockroaches (*Periplaneta americana*), were used to make initial plume measurements and to validate that our PID sensor readings were consistent with our EAG recordings. These were followed with more extensive systematic PID recordings to generate a 3D plume map of the terrestrial plume generated by a point source in our wind tunnel. Previous work at the faster wind speeds and free-stream conditions characteristic of flying plume tracking insects have demonstrated a striking and expected highly intermittent plume structure. The results presented here characterize, for the first time, the slower wind speeds typical of a walking insect and corresponding to natural flow conditions close to the substrate where cockroaches might experience attractive odor plumes in nature. My EAG and PID measurements of odor plumes in low flow speed near the substrate were lacking in almost all sharp intermittency. Instead, they showed an extremely slowly rising and falling of odor flux more often associated with chemical plumes measured in low speed water flows in the boundary layer (Jackson et al., 2007; Moore and Crimaldi, 2004; Moore and Weissburg, 1994).

METHODS:

Electroantennograms were prepared by placing an antenna between capillaries filled with physiological saline.

Antennae were surgically removed from sexually mature adult male cockroaches (*Periplaneta americana*) that had been removed from the colony at least 1 week prior to experimentation and kept in a plastic container with food and water *ad libitum*. Animals were kept on a summer-like light-dark cycle of 16:8. All antennae were removed with a pair of dissecting scissors just above the pedicel (the goal being to avoid injuring the mechanoreceptors in the Johnston's Organ). The tip was likewise removed with dissecting scissors. The exposed ends were immediately placed into saline-filled capillaries that had silver wire electrodes placed in the other end. The capillaries were attached to an aluminum plate with red dental wax and the electrodes were soldered to an RG-58/U cable that was connected to an AC amplifier (Warner Instruments DP-304, Hamden, CT) before connecting to a data acquisition board (National Instruments USB-6221 BNC, Austin, Texas, USA). Signals were captured at 10 kHz using a custom Matlab script (Mathworks, Natick, Massachusetts, USA). Plumes were generated using 1 ng Periplanone B (one of the two components in *P. americana* sex pheromone, it is sufficient to elicit odor tracking behavior) placed on a 1 cm diameter piece of filter paper.

Electroantennograms were used to observe basic plume dynamics.

A raised aluminum platform used for walking experiments (Lockey and Willis, 2015; Willis et al., 2008; Willis et al., 2011) was placed in the wind tunnel. The EAG apparatus was placed on the aluminum floor so that the antenna (oriented vertically) was 116 cm downwind from the odor source. The apparatus started on one side of the wind tunnel well outside the expected plume envelop. A 30 s clean-air control recording was made, then the odor source was introduced, centered on the upwind end of the table. A series of 30 s recordings were made, with the EAG apparatus being moved 1 cm across the wind tunnel between recordings. Once the plume was crossed, the odor source was removed and another clean air control recording was made.

From these recordings, the flux over the sensor (ϕ), mean persistence time (\bar{t}_p), and mean interpulse time (\bar{t}_i) were calculated. Flux is measured in Webers (Wb), a unit of magnetic flux and is equivalent to volt-seconds. Because voltage should be related to concentration, this ought to be a reasonable proxy for the quantity of odor moving across the EAG preparation. The persistence time is a measure of the duration the signal is above the set threshold before dropping again, and the interpulse time is the amount of time between consecutive pulses of odor. To calculate all of these, the bandpass filtered signal (1:30 Hz) is centered on zero by subtracting its mean value. A threshold of 3 standard deviations (3σ) of the clean air signal is set, and wherever the signal increases across this threshold, an “odor-onset” is marked, and where it decreases across this threshold is marked as an

“odor-offset.” Odor-onset/offset pairs denote an odor-pulse and must span more than 250 ms or they are removed (this is to avoid noise in the signal adding many tiny odor pulses). The flux is the area under the curve between the onset and offset points, persistence time is the time between onset and offset, and interpulse time is the time between consecutive onsets.

In aggregate, these measures should provide a picture of *how much* odor is present, *how long* an odor packet is present, and *how often* packets come by. All biologically important plume characteristics with which flying moths are known to alter their plume tracking performance (Murlis and Jones, 1981; Murlis et al., 1990; Murlis et al., 2000).

Plume width was measured in the following way. First, the flux was calculated for each position in the grid. Setting a threshold of 10% the maximum flux observed, each grid position was determined to have appreciable odor present (1/true) or no odor (0/false). The plume width was determined by finding the largest cluster of positions with odor present. A cluster needed to have no more than 1 no-odor position between odor-present positions.

A Photoionization detector was used to collect data for making a detailed plume map.

The PID (Aurora Scientific model 200A: mini-photoionization detector, Aurora, Ontario, Canada) was validated as a proxy for the EAG by comparing the plume dynamics (flux,

persistence time, and interpulse time) measured using both sensors and looking for defining features indicative of the presence or absence of odor.

To map the plume, the PID was mounted on a custom built gantry together with a Kurz 490 mini-anemometer (Monterey, California, USA). Transverse slices of the wind tunnel were recorded in 10 cm steps, each slice sampled on a 1 cm by 1 cm grid, covering the region the plume is known to cover (based on preliminary recordings). Collection order (of the slices, and the order of points within a slice) was randomized to limit any possible correlations in the signal with any potential long-term drift in the baseline of the signal. Each recording lasted for 10 s to expedite the process. The recordings were taken at 10 kHz using a National Instruments USB-6002 A/D system, controlled through a custom Matlab script.

Pure ethanol was used to generate a plume for the PID. Ethanol was placed in an erlenmeyer flask, a brass tube (6 mm inside diameter) was stuffed a cotton wick and placed through a #4 stopper and into the flask. The amount of wick exposed had approximately the same cross sectional area as the filter paper disk used in the EAG measurements. The brass tube and wick reached from where the flask was placed under the aluminum floor to 2 cm above the floor, similar to the filter paper source used for the EAGs. We chose ethanol because it is the safest chemical available that provided the best response in the PID (halides would be more ideal, but their use is not safe or feasible in most facilities).

To reconstruct the map of the odor plume, the mean voltage for each recording position was calculated, then scaled from 0 to 1. Mean voltage was used rather than flux because the signal is noisier with less pronounced peaks and valleys, making contrast difficult to see.

Turbulence intensity was measured using a hot wire anemometer.

A Kurz 490 mini-anemometer (Monterey, California, USA) was mounted next to the PID's intake port. The anemometer had been modified to splice in a coaxial cable parallel to the meter-output. This allowed us to record the wind speed at 10 kHz through the NiDaq USB-6002. The wind speed was set on the wind tunnel using a Testo 425 hot wire anemometer (Sparta, New Jersey, USA). The Turbulence Intensity (TI) was calculated by dividing the root mean square of the velocity (u_{rms}) by the mean velocity (\bar{u}):

$$TI = \frac{u_{rms}}{\bar{u}} .$$

Justification for setting Wind speed to 25 cm s⁻¹.

The wind can vary quite a lot in caves and pipes, the most common homes for *P. americana* (Roth and Willis, 1960). For example, a systematic study of a cave near the southern border of Poland by Pflitsch and Piasecki (Pflitsch and Piasecki, 2003) report wind speeds ranging between $< 3 \text{ cm s}^{-1}$ and 27 cm s^{-1} . In a study of a cave near the northern border of Florida by Kowalczyk and Froelich (Kowalczyk and Froelich, 2010) report seasonal averages of 1.2, 20.4, and 53.6 cm s^{-1} in summer, autumn, and winter, respectively. A study of the Waitomo Glow Worm Caves in New Zealand by De Freitas and colleagues (De Freitas R. N. Littlejohn T.

S. Clarkson I. S. Kristament, 1982) found wind speeds ranging from 0 to 260 cm s⁻¹ with mean seasonal flows of 37 and 21 cm s⁻¹ in winter and summer, respectively.

Most of the previously published studies of the wind and odor directed orientation in *P. americana* have been conducted in laboratory arenas in which air flows ranged from 0 - 48 cm s⁻¹ (Bell and Kramer, 1979; Bell and Kramer, 1980; Bell and Tobin, 1981; Tobin, 1981; Willis and Avondet, 2005). To make our results pertinent to the earlier laboratory studies of *P. americana* orientation, and in an attempt to quantify an odor plume that may be similar to those experienced and tracked by them in nature, we have chosen to quantify a boundary layer volatile odor plume in 25 cm/s wind in our laboratory wind tunnel.

RESULTS:

EAGs of *P. americana* and the PID describe similar plumes.

[Figure 2.01C](#) is an example of a classical EAG recorded in the free stream with a wind speed of 100 cm s⁻¹. This is juxtaposed with a PID recording taken under the same conditions. Note that the PID has the temporal response needed to capture the same types of events as an EAG. At 25 cm s⁻¹ and 116 cm downwind of the odor source, the EAG showed a drifting or rolling baseline in the presence of odor with fluctuations on the order of 10ths of a Hz ([Fig. 2.01A](#)). There is no rapid depolarization followed by a long recovery typical of other published EAGs (e.g., (Baker and Haynes, 1989)), rather the response is smooth and continuous. In clean air and in a wind tunnel with no odor source at all, the EAG shows no

such response but rather a flat line with the typical background of electrical noise typical of many electrophysiological recordings. The positions where the flux was at least 10% of the maximum observed flux are denoted with an asterisk (*). In this particular sample of recordings, the plume, as defined above, is about 10 cm wide 116 cm downwind of the source ([Table 2.01](#)).

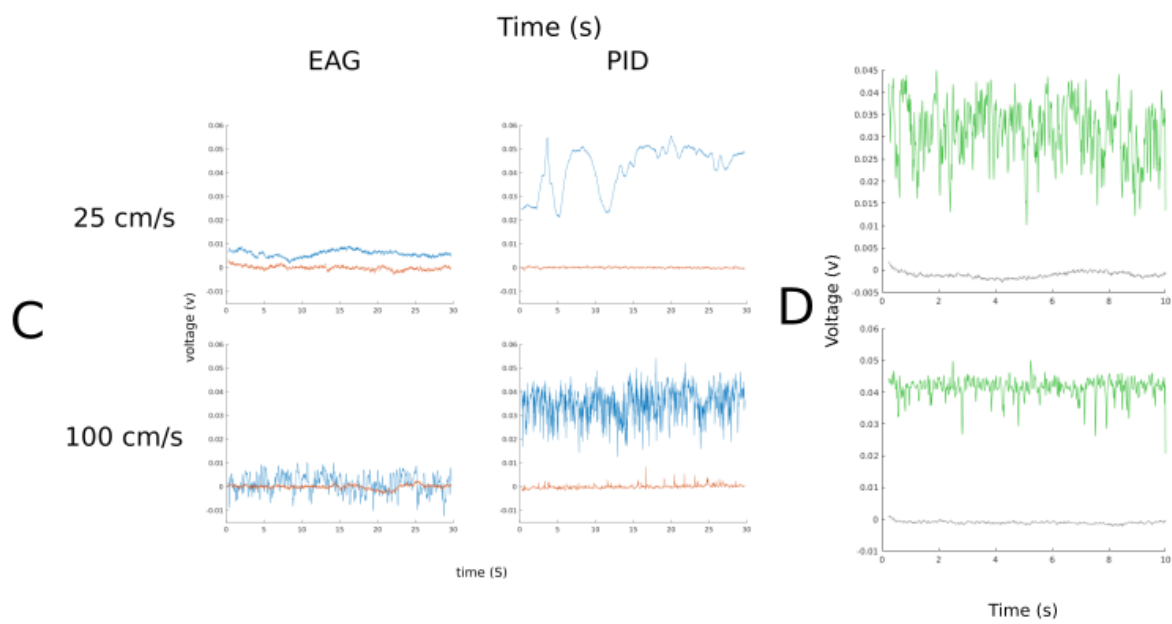
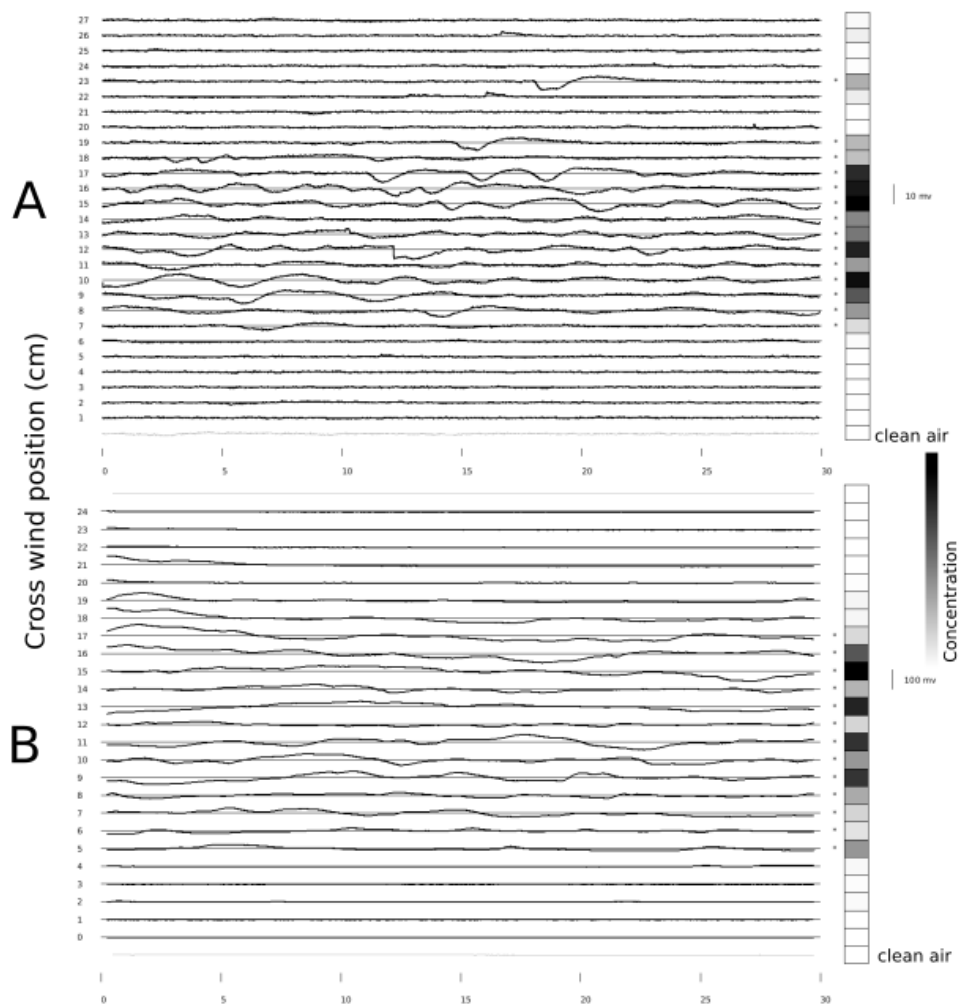


Fig. 2.01: EAGs and PID recordings at different speeds and locations.

EAG recordings (A) and PID recordings (B) at 25 cm s^{-1} are arranged in order stretching across the wind tunnel floor. On the right is a heat map representing the relative flux (scaled 0-1 for that set of recordings). EAG and PID traces are also given in C at two different wind speeds. At 100 cm s^{-1} the typical intermittent signal can be seen in both the EAG and PID, whereas at 25 cm s^{-1} a much slower signal is observed. Odor is given in blue, clean air in orange. Sample traces from the anemometer are given in D, both close to the surface of the table and in the free stream above it, at both 100 cm s^{-1} (green) and 25 cm s^{-1} (grey).

The PID recordings are broadly similar, albeit noisier ([Fig. 2.01B](#)). The flux was scaled between 0 and 1 for comparing the EAG and PID recordings because the means of signal amplification and baseline voltage were different. Over the 30 s recording, the average amount of flux was similar with a similar amount of variability. The width was also observed to be between about 9 and 10 cm for both the EAG and the PID ([Table 2.01](#)).

Table 2.01 - Measurements of plume dynamics & geometry (means \pm SD)

Parameter	EAG	PID	P-value ¹⁴
30s Flux (Wb)	144 ± 101	2968 ± 1515	0.003
30s Flux (Wb) (scaled)	0.43 ± 0.39	0.32 ± 0.42	0.68

¹⁴P-values were calculated with a t-test.

Persistence time(s)	1.38 ± 0.35	4.51 ± 1.70	0.003
Interpulse time (s)	5.37 ± 1.15	7.72 ± 1.35	0.01
Width (cm)	10.2 ± 3.3	9.2 ± 2.4	0.58

Anemometry data shows small amounts of turbulence.

A raw sample trace of the recordings from the hot-wire anemometer positioned near the PID are given in [figure 2.01D](#). The turbulence intensity observed less than 1 cm above the floor at the leading edge of the table was $3.79 \pm 0.25 \%$, and at a height of 4 cm, it was $3.82 \pm 0.22 \%$. This matches observations 50 cm downwind of the leading edge. A turbulence intensity of 3.11 ± 0.84 at the level of the floor and 3.80 ± 0.21 4 cm above the floor was observed. The maximum turbulence intensity observed was 4.94%.

Interpolation from cross-sectional analysis of the plume reveals 3D plume geometry.

Five cross-sectional segments of the plume in 25 cm s^{-1} wind were sampled three times each with the PID, each of which can be reconstructed into a 2D heat map. By stacking the heatmaps in a 3D plot appropriately spaced, the full shape of the plume becomes more apparent. [Figure 2.02](#) shows those heat maps along with approximate plume-clean air boundaries added.

Concentration modeled as a function of distance from the source.

Extracting the “hottest” point in the heat maps used to create [figure 2.02A](#), and fitting them to an exponential decay model ($N_0e^{-\lambda x}$, with x being the distance from the source), a decay rate, $-\lambda$, of 0.053 v cm^{-1} is observed with an adjusted- R^2 value of 0.94.

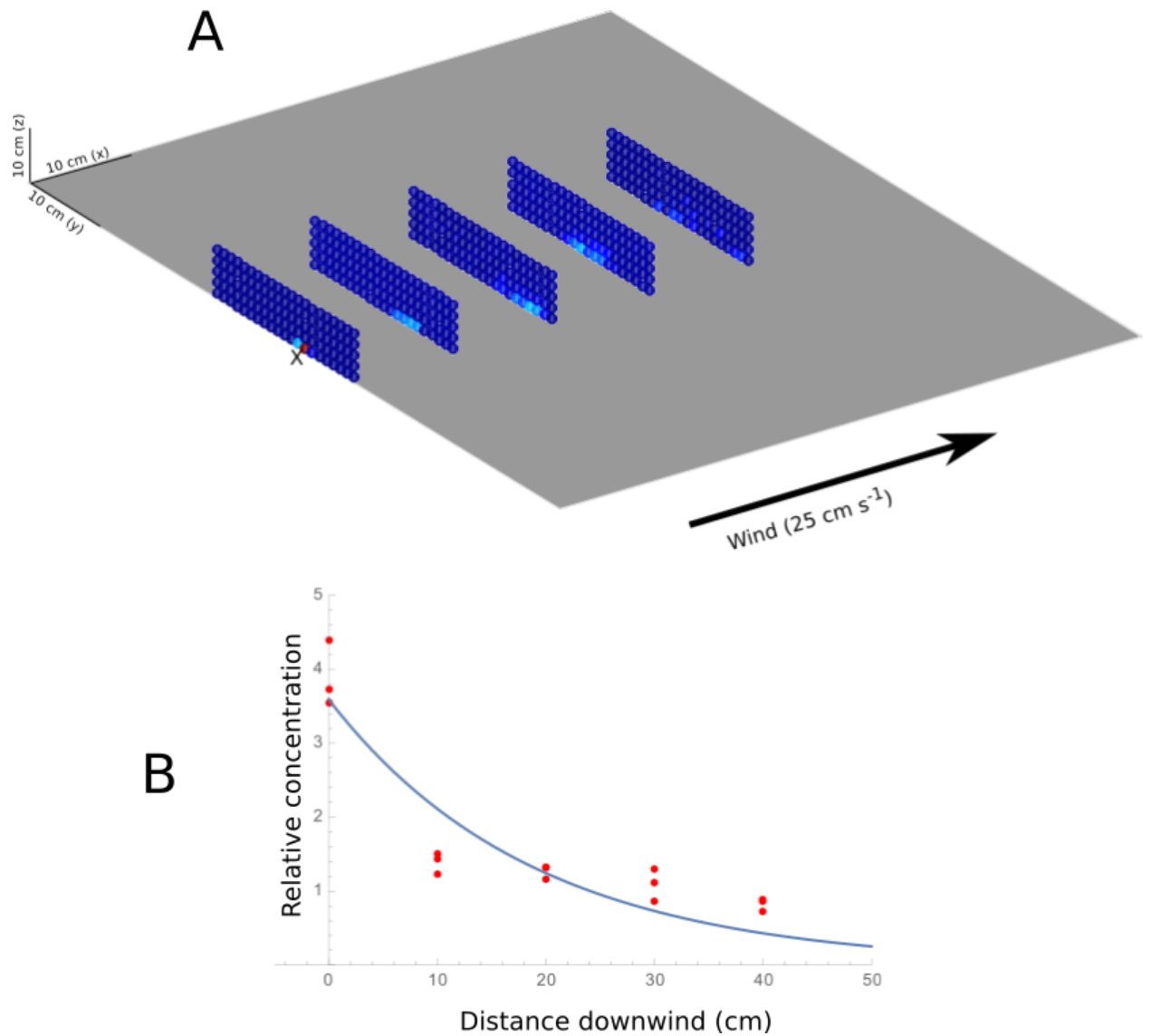


Fig. 2.02 - 3D plume map and concentration

A sample heat map from the PID recordings is given in A. Red is the highest concentration, dark blue is lowest. The source is marked with an X. B shows a plot of the max concentration across three such maps (red dots), and an exponential decay function is fitted (blue line).

DISCUSSION:

Based on previous observations, it would be reasonable to expect a turbulently-mixed, chaotic plume that would produce an intermittent EAG or PID signal (Baker and Haynes, 1989; Girling and Cardé, 2007; Murlis and Jones, 1981; Murlis et al., 1992; Murlis et al., 2000) (eg., [Fig. 2.01C](#), bottom row). However, observations here do not support this prediction, but rather, show a slowly changing signal that could easily be mistaken for a drift in the voltage signal ([Fig. 2.01](#) A & B, C, top row) were it not for its remarkable consistency using very different sensors in correlating with the presence or absence of odor in an otherwise stable signal. Importantly, this consistent signal also disappears when the odor source is removed from the wind tunnel. If the plume is turbulent the odor should exist as thin ribbons or small packets that stretch, curl, and tumble through otherwise clean air, creating a very intermittent signal (Murlis et al., 1992). What is observed in the boundary layer above the surface of our experimental arena in our laboratory wind tunnel at a speed appropriate for a walking, cave dwelling insect is a more homogeneous plume.

The plume is wider than would be expected due to diffusion alone. Given that the pheromone Bombykol has a diffusivity of about $9 \times 10^{-7} \text{ cm}^2 \text{ s}^{-1}$ (Kaissling, 2009), and that

periplanone is of a similar size (bombykol is $238.42 \text{ g mol}^{-1}$ & periplanone B is $248.32 \text{ g mol}^{-1}$), the plume should have diffused by less than 20 nm in cross section in the 4.6 s it takes the wind to carry it from the source to the recording location. Clearly, there is another transportation phenomenon happening to expand the plume as wide as it is.

The best explanation is that what little turbulence there is ([Fig. 2.01D](#)), is creating some mixing, but it's not enough to create large enough pockets of clean air to register on the sensors. The EAG and PID are most likely sampling from too large an area to register a clean pocket of air. Perhaps across one or a few small sensilla, the intermittency of the plume can be registered. For the animals to make use of this, the central nervous system would need to be able to register such differences. This is not outside the realm of possibilities, as *P. americana* can tell the difference between dorsal, ventral, anterior, and posterior surfaces of the antennae (Nishino et al., 2015), which is ca. 900 micrometers at the base and narrows towards the tip.

Alternatively, the odor could be getting trapped in the viscous-sublayer. This is a layer of liquid close to the substrate that is dominated by slow, laminar flows—no turbulence. However, this seems unlikely, as Crimaldi et al. (Crimaldi et al., 2002) measured the viscous-sublayer it at 0.1 cm thick, in a 9.84 cm/s flume, and Weissburg and Zimmer-Faust (Weissburg and Zimmer-Faust, 1994) measured it at 0.8cm in a 1 cm/s flume and it just got thinner with a rougher bed or higher velocity flow. Following this, if the higher Re (from a faster flow) means a thinner viscous sublayer, then in the flows in the wind tunnel the

viscous sublayer should be incredibly thin—too thin for us to measure with the tools available.

The sensilla of *P. americana* are better described as odor on-off detectors than concentration detectors (Tichy et al., 2005). This would seem adaptive over the concentration gradient observed across most of our experimental arena ([Fig. 2.02B](#)). Concentration does not vary a great deal over the region observed except very near the source.

This would all suggest that, from the perspective of a cockroach walking upwind, they experience the plume as an ever-narrowing swath of space filled with odor. From overhead, the plume would look like a solid triangle, the apex being the odor source, reminiscent of the simplistic plumes diagrammed in many odor tracking papers (Lochmatter and Martinoli, 2009; Lockey and Willis, 2015; Willis et al., 2011). The edge of the plume probably provides the strongest stimulus available to orient to, it could be an important “olfactory landmark” (Steck et al., 2009). From the measurements here, it is clear that the edge of the plume is about 1 cm wide (i.e., moving within a crosswind span of a centimeter, we transition from being embedded in odor to clean air). The distance between the tips of the antennae varies, but averages around 5 cm (Willis and Avondet, 2005), meaning the cockroach’s sensors can easily span this olfactory landmark and follow it.

Cockroaches have been observed tracking along where we believe the edge of plumes to reside (Lockey and Willis, 2015; Willis and Avondet, 2005), suggesting that they may indeed

be making use of this olfactory landmark. If *P. americana* has an odor map along their antennae, a tracking strategy making use of the edge of a plume could be fairly simple and straightforward. All the system would have to do is maintain contact with that edge, noting the position of the edge along the odor map, and turning appropriately to maintain contact. If the edge moves to the right, turn right, etc. With a mean antennal span of about 5cm it would be easily possible for a walking cockroach to walk upwind along the edge with one antenna embedded in the odor plume and one in clean air.

Chapter 3

One antenna, two antennae, big antennae, small: in odor tracking insects,
bilateral input isn't all¹⁵.

ABSTRACT

Determining the location of a particular stimulus is often crucial to an animal's survival. One way to determine the local distribution of an odor is to make simultaneous comparisons across multiple sensors. If the sensors detect differences in the distribution of an odor in space, the animal can then steer toward the source. American cockroaches, *Periplaneta americana*, have 4 cm long antennae and are thought to track odor plumes using a spatial sampling strategy, comparing the amount of odor detected between these bilateral sensors. However, it is not uncommon for cockroaches to lose parts of their antennae and still track a wind-borne odor to its source. We examined whether bilateral odor input is necessary to locate an odor source in a wind-driven environment and how the loss of increasing lengths of the antennae affects odor tracking. The tracking performances of individuals with two bilaterally symmetrical antennae of decreasing length were compared with antennal length-matched individuals with one antenna. Cockroaches with one antenna were generally able to track an odor plume to its source. In fact, the performances of unilaterally

¹⁵ This chapter has been published as (Lockey and Willis, 2015)

antennectomized individuals were statistically identical to those of their bilaterally symmetrical counterparts when the combined length of both antennae equaled the length of the single antenna of the antennectomized individuals. This suggests that the total length of available antennae influences odor tracking performance more than any specific piece of antenna, and that they may be doing something more complex than a simple bilateral comparison between their antennae. The possibility of an antenna-topic map is discussed.

KEY WORDS: Olfaction, Spatial orientation, Tracking behavior, Antenna map, Spatial tracking

INTRODUCTION

An animal's survival and reproductive success often depend on its ability to localize resources. For animals using olfaction to seek food or mates, multiple strategies can be used to determine the location of an odor source (Bell and Tobin, 1982; Fraenkel and Gunn, 1961; Kennedy, 1978; Weissburg, 2000). In fluid environments (i.e. air and water) with zero flow, odor is dispersed by diffusion and will have a gradient in which the concentration of odor near the source is greater than the concentration far away. In environments with moving fluids, diffusion is trumped by turbulent mixing, creating pockets of clean fluid intermixed with fluid bearing odor of different concentrations (Campbell, 1977; Weissburg, 2000). These pockets of odor decrease in concentration as they are carried away from the source (Murlis and Jones, 1981; Murlis et al., 2000; Webster and Weissburg, 2001). In either

flow condition, an animal must be able to adapt its behavior as it moves and use the information available to navigate to the source.

Orientation responses of animals to environmental information are thought to fall into two rough categories: indirect and direct. In indirect responses, an animal's rate of locomotion or turning is modulated by the intensity of a specific sensory input (i.e. light, chemicals, sound, etc.). These responses have been termed kinesis with modulation of locomotion rate termed ortho-kinesis and that of turning rate termed klino-kinesis (Fraenkel and Gunn, 1961). Animals might also alter their movement by steering directly toward or away from a stimulus. These orientation movements have been termed positive or negative taxes, respectively. Animals controlling their locomotion directly with respect to stimuli use two well described methods: spatial and temporal comparisons (Bell and Tobin, 1982; Fraenkel and Gunn, 1961).

A tracking strategy using spatial comparisons requires an organism to sample simultaneously from two or more sensors distributed on their body to make instantaneous comparisons of at least two points in space (Moore and Lepper, 1997; Weissburg and Dusenbery, 2002)(Willis, 2008). In tropotaxis, perhaps the best understood method of making spatial comparisons, the signal from one bilaterally symmetrical sensor is compared with the signal from its contralateral sensor. For example, in the fly *Drosophila melanogaster*, bilateral input is required for odor-guided steering in adults while either walking (Borst and Heisenberg, 1982) or flying towards an attractive odor (Duistermars et al., 2009) or away

from a repulsive odor (Wasserman et al., 2012). This is in contrast to the larva, where bilateral input enhances, but is not required for, odor tracking (Louis et al., 2008). *Drosophila melanogaster* larvae with two intact dorsal organs (i.e. larval antennae) typically turn towards the organ detecting the higher concentration of an attractive odor. When one dorsal organ is functionally removed, they meander more (Louis et al., 2008). Many other species have likewise been reported to make use of bilateral spatial comparisons to orient toward attractive odors. The crayfish *Orconectes rusticus* requires input from both antennules to successfully orient to a food source (Kraus-Epley and Moore, 2002), and the chambered nautilus, *Nautilus pompilius*, requires both odor-detecting rhinophores to track a plume of food odor (Basil et al., 2000). Similarly, the ant *Lasius fuliginosus* steers towards the remaining antenna when one has been removed, generating a predictably asymmetric and looping track depending on the antenna that has been removed (i.e. turning toward the intact antenna – a classic prediction of unilateral ablation in tropotactic animals). Their ability to track a pheromone trail is disrupted when the detected position of the trail in space is flipped by crossing their antennae (Hangartner, 1967). The silkworm *Bombyx mori*, turns towards the antenna receiving delayed input or a higher odor concentration relative to the opposite side (Takasaki et al., 2012). Rats require bilateral input to accurately localize an odor (Rajan et al., 2006), and bilateral input increases the accuracy of tracking an odor trail (Khan et al., 2012). Even humans track an odor faster and more accurately when bilateral information is available (Porter et al., 2005, 2007). In radially symmetrical animals such as sea stars, this comparison may be across multiple sensors (Moore and Lepper, 1997).

Temporal tracking requires an organism to take sequential samples as it moves, compare those samples across time, and alter its course in the direction of the larger stimulus (Bell and Tobin, 1982; Kennedy, 1978). Animals using this strategy could sum or average readings across multiple sensors to determine whether the stimulus intensity has increased or decreased and steer accordingly (Schöne, 1984). The classic example of temporal tracking is transverse klinotaxis, whereby animals symmetrically zig-zag across their net displacement vector by changing their turning angle, sampling transverse slices of the odor plume and adjusting their net displacement vector towards the stimulus source (Kennedy, 1978), effectively constructing the spatial information over time that would otherwise be available instantaneously in tropotaxis. The side-to-side head motion of a nematode tracking a chemical (Ward, 1973), as well as the casting behavior of various moth species (Kennedy and Marsh, 1974; Vickers and Baker, 1991; Willis and Arbas, 1991), are exemplars. This is in contrast to longitudinal klinotaxis, where animals continue forward so long as stimulus intensity is increasing. When there is a decrease in intensity, a series of turns are executed and samples are compared between headings to determine the direction of increasing stimulus (Bell and Tobin, 1982; Kennedy, 1978).

Recent studies of the blue crab, *Callinectes sapidus*, show that this animal uses both temporal and spatial strategies to guide its walking path while tracking a plume of food odor, and that these two strategies are supported by different odor-sensing structures (Page et al., 2011a,b). It has been proposed that the crab's brain compares the inputs from the chemoreceptor hairs on the distal tips of the crab's walking legs to decide what direction to

steer to remain in the center of the odor plume (Page et al., 2011b). The speed of walking during plume tracking is correlated with the rate at which the crab's antennules encounter filaments of odor in the plume (Page et al., 2011a). The associations between the odor signal, sensory appendage and motor performance of the crabs was made possible by video recording the fine structure of a fluorescent dye that had been formulated with the attractant odor and co-released. Although insects do have chemosensors on other parts of their bodies, including their feet, most of these are contact chemosensilla that are typically less centrally organized than the olfactory sensilla on the antennae, and none are known to be used in long-distance orientation like plume tracking (Resh and Cardé, 2009).

American cockroaches (*Periplaneta americana* L.) are attractive models for studying odor plume tracking because they are champions of olfactory behavior and the olfactory epithelium on their 4 cm long, filamentous antennae is easily accessible. These antennae are each made up of more than 150 segments called annuli, and each annulus is covered in olfactory sensilla of multiple types. In males, about half of these sensilla are selectively sensitive to the female sex attractant pheromone periplanone (Schaller, 1978).

The long linear array of odor sensors characteristic of *P. americana*'s antenna could allow spatial, temporal or both strategies to be used simultaneously for odor localization. Previous work in an environment with no predictable flow has suggested that *P. americana* with two antennae use a spatial tracking strategy, in which the insects compare the olfactory signal on one antenna with the olfactory signal on the other (Bell and Tobin, 1981, 1982). Individuals

with only one antenna are thought to switch to using a temporal tracking strategy as comparisons between the antennae are no longer possible (Bell and Tobin, 1981, 1982). In this case, steering is thought to depend on changes in the olfactory input detected by the intact antenna being compared across two or more consecutive time points. Locating an odor source with only one antenna is likely to be a requirement of *P. americana* outside of laboratory experiments. It is not uncommon to find adult *P. americana* in our laboratory colony with all or part of an antenna missing, and it should not be surprising to find cockroaches in their natural, crowded, habitats suffering similar damage (Guthrie and Tindall, 1968; Roth and Willis, 1960). Until the study presented here, the impact of partial antenna loss on odor-guided navigation strategies had not been addressed systematically.

In principle, the long antennae of *P. americana* gives the animal the ability to obtain a significant amount of spatial information about its odor environment. This holds true even if one of the antennae is missing, so long as the system is able to discriminate zones of sensation along an antenna. Previous work by Hösl (1990) has shown that the firing frequency of a subset of interneurons in the processing center for female pheromone in the antennal lobe of *P. americana* males, the macroglomerular complex (MGC), is dependent on the location of pheromone stimulation along the antenna. This suggests the presence of an antenna-topic olfactory map of each antenna in the brain. The MGC is a specialized collection of glomeruli in the antennal lobe where all sex pheromone-sensitive olfactory neurons from the antenna converge (Ernst and Boeckh, 1983; Watanabe et al., 2010, 2012), and is the first possible place where intra-antenna comparisons or integration can occur. If

an antenna-topic map is utilized, information on the spatial distribution of odor and subsequent steering and ultimately the tracking performance should be influenced by the size and spatial resolution of the available map.

To better understand whether *P. americana* males use spatially sampled odor information from across their antennae to track a windborne odor, we challenged animals with both bilaterally symmetric and unilaterally ablated antenna of different lengths ([Fig. 3.01](#)) to track a plume of female sex attractant pheromone in a wind tunnel. If *P. americana* use bilateral comparisons between their antennae to steer upwind in an odor plume then unilaterally ablated individuals should be unable to track the odor or show predictable behavioral deficits such as looping toward the intact antenna (Hangartner, 1967). In contrast, individuals with bilateral input should be able to track the plume, regardless of antennae length as long as they can still detect the odor. We found that unilaterally ablated individuals were able to track odor nearly as well as their bilateral counterparts with the same total antennal length. This shows that they can track a plume when bilateral comparisons are unavailable to them. However, decreasing the length of the antennae also affected the plume tracking ability of cockroaches, with individuals with shorter antennae being less successful at locating the odor source. While the role of temporal information is still not clear, these results show that bilateral comparisons are not a requirement for odor plume tracking in *P. americana*. Further, these results show that, for male *P. americana*, the total amount of olfactory epithelium providing odor information is predictive of successful orientation to odor plumes, regardless of whether that epithelium is on one antenna or two. The fact that cockroaches with only

one antenna perform as well as those with two totaling the same length suggests either that they switch from using spatial to temporal comparisons when they lose an antenna or that spatial information continues to be available to them through a single antenna.

RESULTS

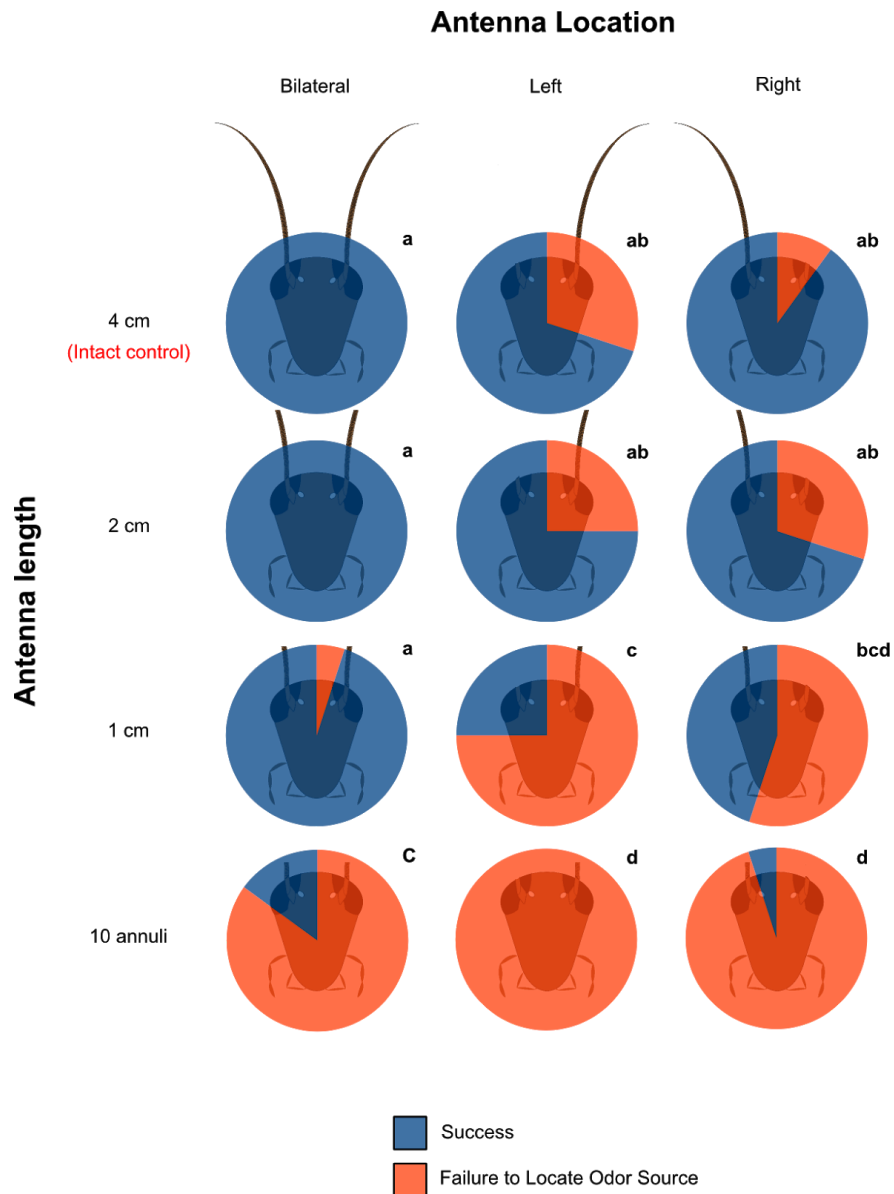


Fig. 3.01. Rates of success at locating the pheromone source of the different experimental treatment groups.

Diagram of *Periplaneta americana* with both antennae (bilateral input, left column), with the right antenna removed (left antenna remaining, middle column) and with the left antenna removed (right antenna remaining, right column). The first row represents animals with intact 4 cm antennae and antennae length decreases from top to bottom (2 cm, 1 cm, 10 annuli). Success rates for locating the odor source are presented in the superimposed pie charts. A Fisher's exact test for all groups was highly significant ($P=1.0\times 10^{-4}$). Sub-sampling the contingency table to compare each group shows that, in general, animals with the longest antennae have higher success rates than those with the shortest antennae. Groups with the same letter are similar after a Bonferroni correction for 12 groups ($P<0.00417$).

Successful plume tracking continues with only one antenna

We first determined the percentage of animals in each group that were able to complete the odor-tracking task and navigate to the odor source. Out of 20 individuals in each treatment group, at least one tracked the odor plume to its source except for the group with only 10 annuli remaining on the left antenna. The animals with longer antennae had higher success rates (up to 100%) than those with shorter antennae (as low as 5%) ([Fig. 3.01](#)). The percentage of animals tracking the plume to the source was significantly different for each treatment group according to Fisher's exact test ([Fig. 3.01](#)). The 10 annuli treatment length was excluded from further statistical analysis because of low success rates yielding such a small sample size.

Next, we observed the behavior of the cockroaches as they navigated towards the odor source. The trajectories of our treatment groups showed considerable variability ([Fig. 3.02](#)), consistent with results from other plume-tracking experiments in cockroaches (Willis and Avondet, 2005; Willis et al., 2008). Each group had animals with a high linearity score that

walked up the plume to the source with few (if any) turns or excursions out of the plume ([Fig. 3.02](#), top row) as well as animals with low linearity scores that made many turns or excursions out of the plume ([Fig. 3.02](#), bottom row). Visual inspection of the tracks revealed no obvious trends in turning direction or exits from the plume for any group so we could not visually discriminate between the treatment groups based on their tracks. Furthermore, loss of left or right antenna did not obviously bias subsequent behavior in the direction of the intact or removed antenna (see below).

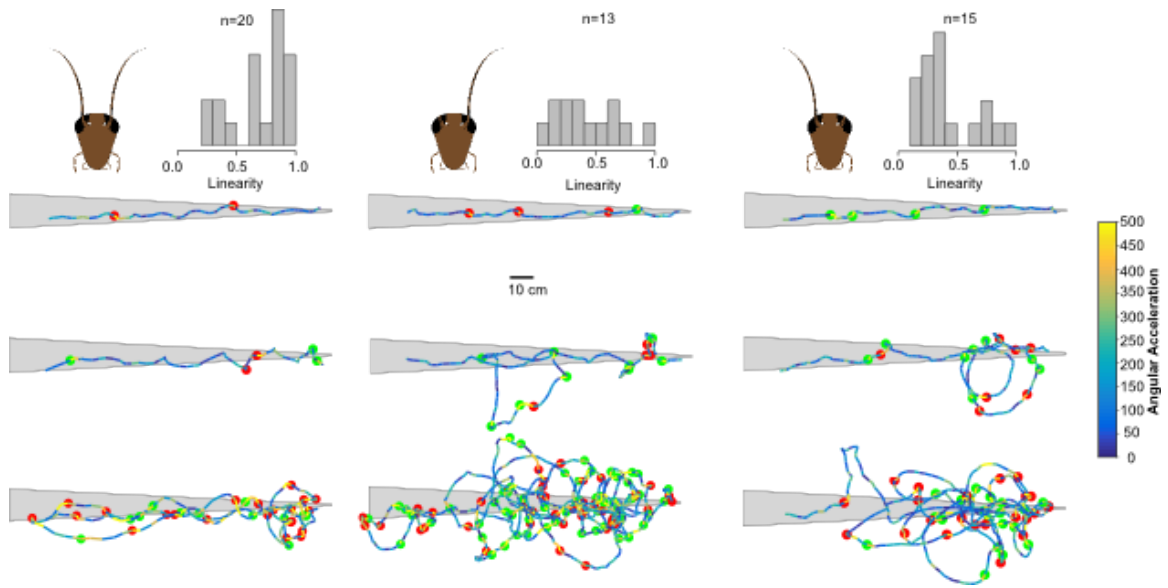


Fig. 3.02. Cockroaches with full-length antennae display a range of tracking behaviors.

Tracks for animals with two antennae (left column), a left antenna (middle column) and a right antenna (right column) are shown. In each column, the top trace represents the track with the highest linearity score (the straightest track), in the middle is a track with the median linearity score for that treatment, and on the bottom is the track with the lowest linearity score. The distribution of linearity scores for the treatment groups is given in the inset histograms. The time-averaged plume boundaries (as measured by electroantennograms) are represented by a light gray triangle. The trajectory follows the cockroach's head position and the color is scaled to the animal's angular velocity. Turns were defined as points where the angular acceleration was either $> 360 \text{ deg s}^{-2}$ or $< -360 \text{ deg s}^{-2}$. Left and right turns are denoted by red and green circles, respectively. Wind blows from right to left at 25 cm s^{-1} .

There is no effect of left versus right antenna loss, but animals with two antennae versus one antenna of the same matched length show considerable differences in behavior

A detailed computer analysis of the tracks was performed using custom-written MATLAB scripts to calculate 16 different track parameters and Bayesian estimation was used to compare groups in R (see Materials and methods and [Table 3.01](#) for track parameter definitions, and [Table 3.02](#) for grand means \pm s.d.). These results were further corroborated with hierarchical Bayesian models and one-way and two-way ANOVA (see Materials and methods, and supplementary material [Tables A.i.05](#), [A.i.06](#) for the one-way ANOVA tables, and [Tables A.i.07](#), [A.i.08](#) for the two-way ANOVA). Within each antenna length grouping (i.e. 4, 2 and 1 cm), the performance of individuals with only one antenna (either left or right) was statistically identical ([Fig. 3.03](#)). Further, a one-way ANOVA showed six of the 16 track parameters to be different between all one and two antennae individuals, regardless of length (supplementary material [Table A.i.06](#)). Individuals with one antenna were pooled into groups by length and compared with animals with two antennae of that same length (e.g. one versus two 4 cm-long antennae) ([Fig. 3.04](#)). This comparison reveals that in the 2 cm and full-length (4 cm) groups, the animals with only one antenna performed differently from those with two antennae on most parameters, the main exception being average body angle and its derivatives. A one-way ANOVA and post hoc tests likewise showed the 4 and 2 cm groups to vary on 10 of the track parameters, regardless of the number of antennae (supplementary material [Table A.i.05](#)). The 1 cm group had fewer differences in track

parameters between one and two antennae individuals. This may be due to the low number of tracks and the higher variability in the behavior of animals with shorter antennae.

Table 3.01. Definitions of measured tracking parameters

Term	Definition
Time to source	The time (sec) from leaving the release cage to finding the source.
Walking speed	The mean ground speed (distance/time).
Walking distance	The total distance traveled by the animal.
Linearity	The walking distance \div the straight line distance from the release point to the source.
No. Stops	No. of times the animal moved less than 0.2 cm in > 0.133 s
Stop duration	The mean time spent during each stop.
Total stop time	Sum of all time spent not moving.
No. backtracks	No. of down excursions > 8 cm (two body-lengths).
No. left turns	No. of spikes in the angular acceleration $< 360^\circ/\text{s}^2$.
No. right turns	No. of spikes in the angular acceleration $> 360^\circ/\text{s}^2$.
Inter-turn duration	The mean time between turns.
Magnitude body angle	The mean absolute value of the body angle.
Body angle	The mean angle between the head-thorax axis of the animal and the central axis of the plume.
Angular velocity	The mean change in body angle.
Angular acceleration	The mean change in angular velocity.

Table 3.02. Grand means \pm s.d. of track parameters (with number of individuals in each group)

	Bilateral			
	Full length (20)	2 cm (20)	1 cm (19)	10 annuli (3)
Time to source (s)	9.24 \pm 5.26	29.7 \pm 38.6	39.3 \pm 41.7	69.9 \pm 14.9
Walking speed (cm/s)	23.9 \pm 7.59	21.6 \pm 6.68	21.6 \pm 4.87	22.9 \pm 10.5
Track width (cm)	3.28 \pm 1.84	4.17 \pm 2.19	5.46 \pm 1.48	6.63 \pm 2.87
Walking distance (cm)	205 \pm 123	737 \pm 1140	862 \pm 963	1500. \pm 380.
Linearity	0.68 \pm 0.24	0.45 \pm 0.32	0.24 \pm 0.15	0.08 \pm 0.023
No. stops	4.65 \pm 3.82	5.45 \pm 4.70	10.6 \pm 14.5	15.7 \pm 11.9
Stop duration	0.11 \pm 0.15	0.11 \pm 0.084	0.13 \pm 0.095	0.10 \pm 0.060
Total stop time	0.57 \pm 0.59	0.87 \pm 1.45	2.14 \pm 3.83	1.98 \pm 1.68
No. backtracks	1.15 \pm 1.69	9.25 \pm 16.4	12.4 \pm 12.7	23.3 \pm 4.51
No. left turns	4.65 \pm 5.43	24.2 \pm 38.8	26.2 \pm 27.9	39.7 \pm 2.52
No. right turns	4.40 \pm 3.80	21.5 \pm 34.0	28.6 \pm 34.0	43.7 \pm 21.2
Inter-turn duration	1.43 \pm 1.23	0.85 \pm 0.53	0.78 \pm 0.23	0.87 \pm 0.35
Magnitude body angle	31.4 \pm 20.7	49.4 \pm 27.7	66.0 \pm 15.3	78.4 \pm 5.07
Body angle	3.10 \pm 11.6	-0.54 \pm 8.11	-2.77 \pm 9.12	-0.20 \pm 7.88
Angular velocity	6.54 \pm 22.8	-0.42 \pm 17.6	-0.62 \pm 23.2	6.57 \pm 42.9
Angular acceleration	-4.24 \pm 9.91	-0.52 \pm 7.00	0.60 \pm 5.51	-1.00 \pm 3.03
	Left			
	Full length (13)	2 cm (15)	1 cm (4)	10 annuli (0) [†]
Time to source (s)	23.0 \pm 17.0	53.5 \pm 38.0	73.1 \pm 73.4	NA
Walking speed (cm/s)	18.6 \pm 6.30	14.5 \pm 4.85	17.4 \pm 4.69	NA

Track width (cm)	5.33 ± 2.36	6.04 ± 1.82	7.50 ± 1.91	NA
Walking distance (cm)	419 ± 355	691 ± 413	1190 ± 396	NA
Linearity	0.42 ± 0.26	0.23 ± 0.16	0.10 ± 0.034	NA
No. stops	9.46 ± 7.64	22.7 ± 21.5	32.5 ± 28.4	NA
Stop duration	0.14 ± 0.14	0.15 ± 0.084	0.17 ± 0.052	NA
Total stop time	2.13 ± 3.16	4.53 ± 5.06	5.85 ± 6.22	NA
No. backtracks	4.92 ± 6.44	11.5 ± 7.74	20.8 ± 5.50	NA
No. left turns	10.6 ± 11.4	17.9 ± 13.0	30.3 ± 7.09	NA
No. right turns	12.6 ± 15.6	20.2 ± 12.3	30.5 ± 4.12	NA
Inter-turn duration	1.32 ± 1.01	1.43 ± 0.74	1.22 ± 0.72	NA
Magnitude body angle	51.1 ± 20.6	66.0 ± 16.4	76.3 ± 6.13	NA
Body angle	1.29 ± 11.7	3.91 ± 10.4	4.52 ± 7.06	NA
Angular velocity	0.68 ± 21.4	-11.6 ± 14.1	1.71 ± 15.86	NA
Angular acceleration	1.32 ± 7.85	0.38 ± 3.68	1.84 ± 2.93	NA

	Right			
	Full length (18)	2 cm (14)	1 cm (9)	10 annuli (1) [‡]
Time to source (s)	21.6 ± 12.9	57.8 ± 55.1	72.6 ± 38.4	$33.9 \pm \text{NA}$
Walking speed (cm/s)	18.3 ± 5.06	14.4 ± 5.86	11.8 ± 2.56	$3.5 \pm \text{NA}$
Track width (cm)	5.23 ± 2.31	6.10 ± 1.87	6.95 ± 2.10	$19.0 \pm \text{NA}$
Walking distance (cm)	$370. \pm 219$	681 ± 504	903 ± 584	$120. \pm \text{NA}$
Linearity	0.42 ± 0.25	0.30 ± 0.25	0.22 ± 0.25	$0.94 \pm \text{NA}$
No. stops	10.2 ± 9.58	30.6 ± 24.4	31.6 ± 36.4	$9.00 \pm \text{NA}$
Stop duration	0.16 ± 0.10	0.18 ± 0.091	0.19 ± 0.090	$0.11 \pm \text{NA}$
Total stop time	2.10 ± 2.39	7.03 ± 6.88	6.35 ± 8.43	$1.00 \pm \text{NA}$
No. backtracks	4.50 ± 4.22	11.1 ± 10.0	18.4 ± 15.3	$1.00 \pm \text{NA}$

No. left turns	8.78 ± 6.34	20.9 ± 18.4	22.3 ± 17.1	$1.00 \pm \text{NA}$
No. right turns	8.78 ± 5.94	21.9 ± 19.0	21.1 ± 18.3	$2.00 \pm \text{NA}$
Inter-turn duration	1.42 ± 0.92	1.71 ± 1.07	3.01 ± 3.37	$11.1 \pm \text{NA}$
Magnitude body angle	54.1 ± 26.19	62.7 ± 23.2	69.0 ± 23.5	$81.2 \pm \text{NA}$
Body angle	0.16 ± 11.6	1.33 ± 11.5	1.40 ± 3.68	$60.3 \pm \text{NA}$
Angular velocity	7.43 ± 16.7	1.37 ± 19.3	0.23 ± 10.8	$-4.06 \pm \text{NA}$
Angular acceleration	1.36 ± 5.06	-1.05 ± 4.40	-0.068 ± 2.59	$-0.66 \pm \text{NA}$

[†]No Animals in the 10 annuli, left antenna group tracked (See [figure 3.01](#))

^{*}Only one animal in the 10 annuli right antenna group tracked (See [figure 3.01](#))

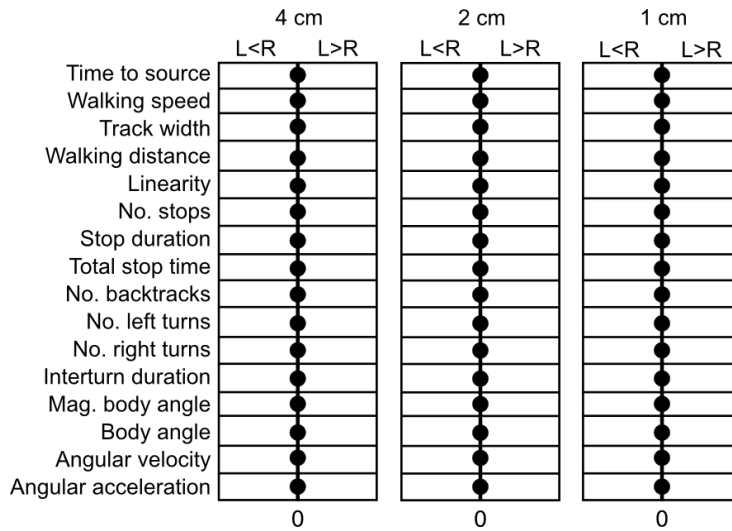


Fig. 3.03. Left and right antennectomized animals behave the same.

This figure presents credibility intervals on the difference in means between animals with only a left or right antenna. See [Table 3.01](#) for a definition of the tracking parameters. Mag., magnitude. A dot to the left of the 0 line indicates that the credibility interval is to the left of zero (negative), a dot on the 0

line indicates that the credibility interval includes zero (the groups are practically equivalent) and a dot to the right of the 0 line indicates that the credibility interval is to the right of zero (positive). A negative credibility interval indicates that the first group in the comparison is smaller than the second group whereas a positive credibility interval indicates the first group is larger than the second. In this case, we compared left with right, and all groups were equal for all track parameters. See supplementary material [Table A.i.01](#) for the highest density intervals (HDIs) used to compile this figure.

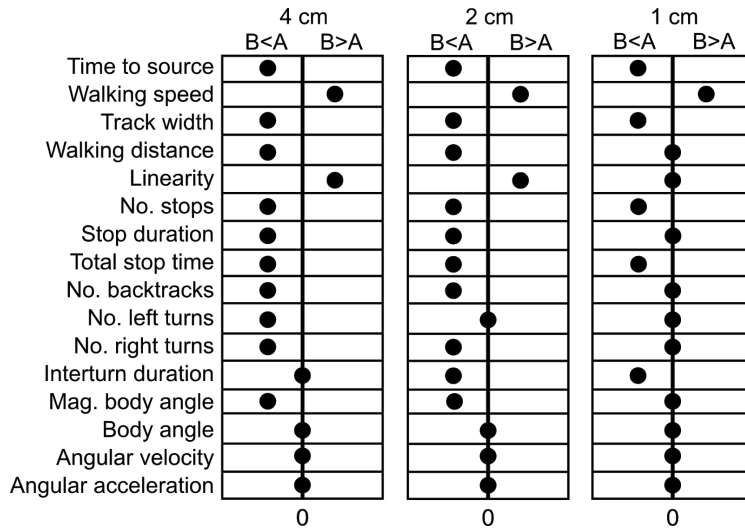


Fig. 3.04. Animals with one antenna behave differently from animals with two antennae.

This figure presents the credibility intervals on the difference in means between bilaterally symmetric animals (B) and antennectomized animals (A). In this case, we compared bilateral with antennectomized animals. The

first row of the first column should be interpreted as ‘individuals with bilateral input took less time to walk to the source than antennectomized individuals’. See legend to [figure 3.03](#) for a more complete explanation of the interpretation, and supplementary material [Table A.i.02](#) for the HDIs used to compile this figure. Means (\pm s.d.) of these values can be found in [Table 3.02](#).

Animals with longer antennae perform better

Animals with longer antennae had a higher success rate at finding the source than animals with short antennae, regardless of antennae group (left, right or bilaterally symmetric) ([Fig. 3.01](#)). Groups with longer antennae found the source faster than those with shorter antennae ([Fig 3.05A](#) and [Fig 3.06](#)). This is due in large part to animals with longer antennae having narrower tracks, ([Fig. 3.05B](#)), and making fewer turns, backtracks, or stops ([Fig. 3.06](#), [Table 3.02](#); supplementary material [Table A.i.03](#)). They walked more directly to the source ([Fig. 3.05D](#)).

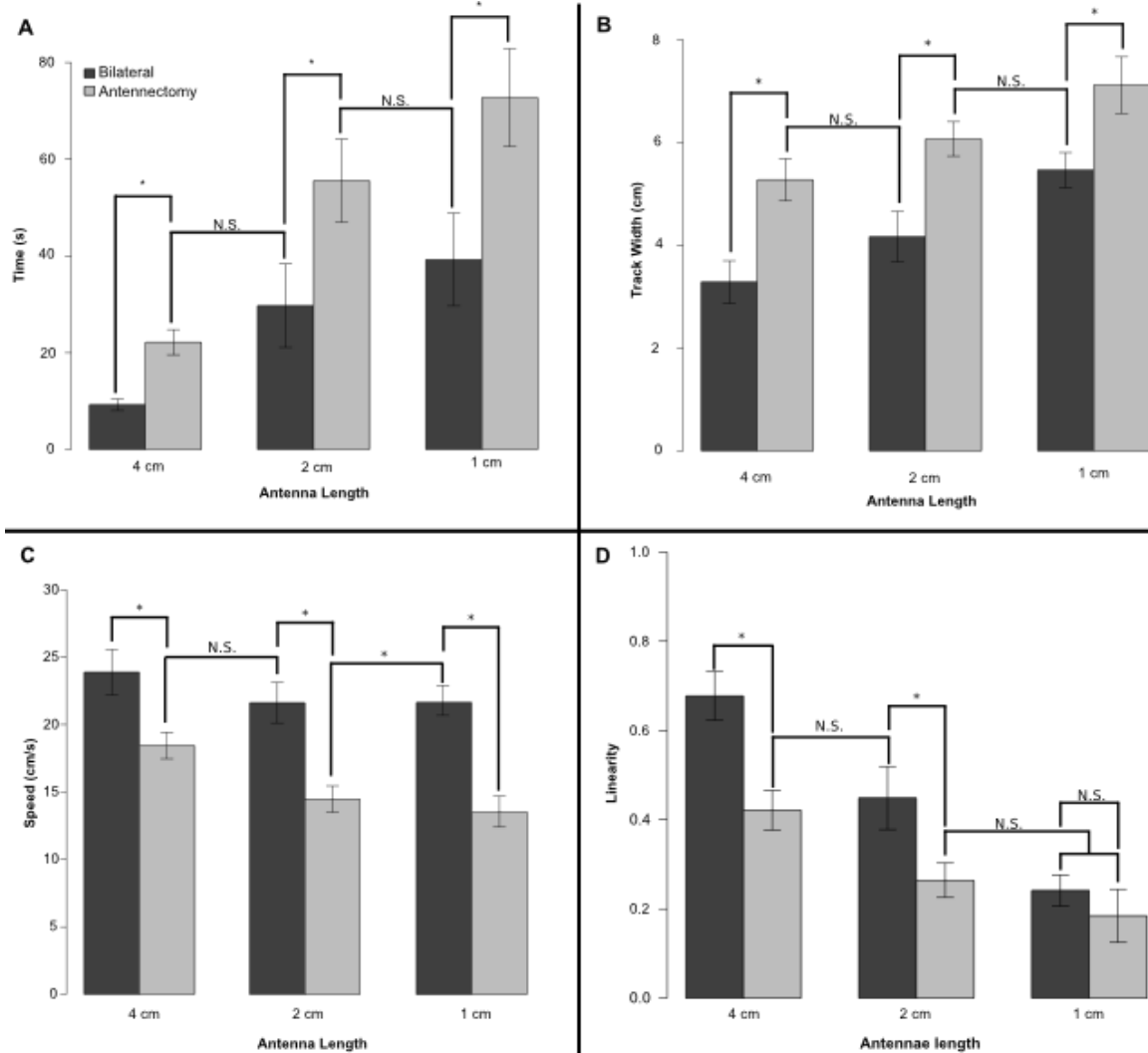


Fig. 3.05. Most track parameters vary with antennal length, yet animals with equal total lengths of antenna are indistinguishable in their behavior.

For example, tracking time was shorter (A), track width was narrower (B), walking speed was faster (C) and tracks were straighter (D) in all bilateral individuals with two antennae than in those with one antenna of the same length (paired bars) – except for linearity for 1 cm individuals (D). Animals with the same total antenna length (4 cm antennectomy and 2 cm bilateral, or 2 cm antennectomy and 1 cm bilateral) had statistically identical tracking times (A), track widths (B), speed (C) and linearity (D), except for total 2 cm individuals on speed (C). Bayesian estimation for two groups (BEST package in R) was used to measure effect size and differences between means; asterisks denote groups with no overlap in the 95% credibility interval on the means, indicating that the groups are significantly different. Likewise, N.S. denotes groups that have overlapping credibility intervals, indicating that the groups are practically equivalent. For comparisons on all track parameters, see [Figs 3.04](#), [3.06](#), [3.07](#).

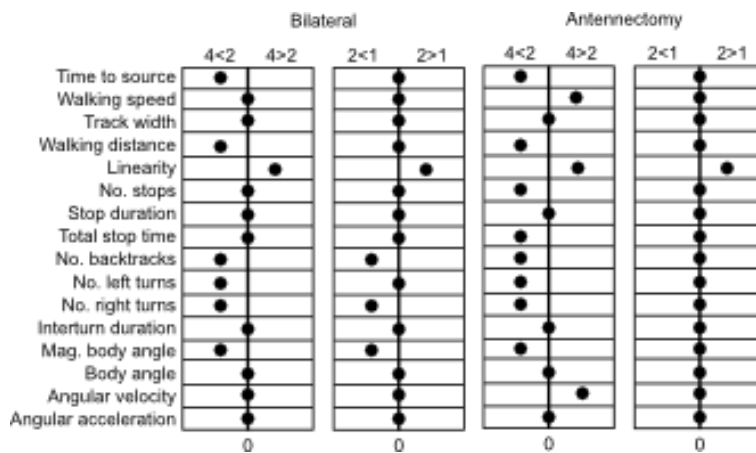


Fig. 3.06. Bilateral or antennectomized animals with different length antennae behave differently.

This figure presents credibility intervals on the difference in means between animals with different length antenna (4 cm versus 2 cm, 2 cm versus 1 cm) within treatment groups (bilateral and antennectomy). See legend to [Fig. 3.03](#) for a more complete explanation of

the interpretation, and supplementary material [Table A.i.03](#) for the HDIs used to compile this figure.

Animals with the same total length of antennae are broadly similar in their behavior

We found few differences in performance between animals with the same total amount of olfactory epithelium, regardless of where that epithelium was located (e.g. two 2 cm-long antennae and one 4 cm long antenna, both have a total of 4 cm of antenna) ([Fig. 3.07](#)). The only difference in individuals with 4 cm of total antenna is those with bilateral input had a shorter interturn duration, made fewer stops and correspondingly spent less total time stopped. The same was true of individuals with 2 cm total antenna with the addition that those with bilateral input also walked faster. The only significant interaction between number of antennae and antenna length revealed by the ANOVA was in the number of stops (see supplementary material [Fig. A.i.01](#)). This was consistent with results from the Bayesian

hierarchical model. No other interactions between antennal length and bilateral symmetry were found.

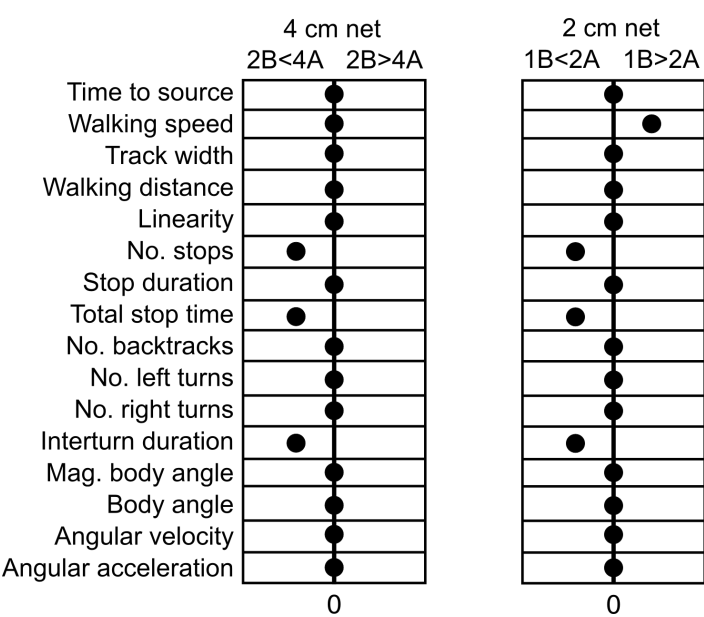


Fig. 3.07. Animals with the same total antennae length behave broadly similarly.

This figure presents credibility intervals on the difference in means between animals with the same total length antenna (2 cm bilateral versus 4 cm antennectomy, 1 cm bilateral versus 2 cm antennectomy). See legend to [Fig. 3.03](#) for a more complete explanation of the interpretation, and supplementary material [Table A.i.04](#) for the HDIs used to compile this figure.

DISCUSSION

One antenna is sufficient for odor tracking

Our results clearly demonstrate that *P. americana* males can track a wind-borne odor with only one antenna, and thus bilateral input is not necessary for successful odor tracking when directional information is provided by the wind. By this observation alone, we can reject bilateral chemo-comparisons as the sole means of odor guided navigation in *P. americana*. They do not need to make a comparison between their two antennae, which is consistent with previous work by Bell and Tobin (1981) done in a zero-wind environment. Our

observation that there are no appreciable differences in the behaviors performed by left and right antennectomized animals is likewise consistent with the findings of Bell and Tobin (1981). While intact animals could make bilateral comparisons, they are not a requirement to successfully track a wind-borne odor plume. Unilaterally antennectomized *P. americana* do not loop toward their intact antenna like the ant *L. fuliginosus* (Hangartner, 1967). Looping toward the intact sensor is an obvious sign that an organism is comparing one sensor with the other across the midline of the body (Schöne, 1984). The cockroaches also made similar numbers of leftward and rightward turns, regardless of which antenna had been removed ([Table 3.02](#) and [Fig. 3.03](#)) – a further indication of a lack of directional bias.

Total antenna length may determine spatial information for odor tracking

We present evidence that antennal length makes a significant contribution to tracking ability in *P. americana*. The tracking behavior of animals with only a left or only a right antenna was remarkably similar, and was also similar as a group to individuals with bilaterally symmetric antennae of the same total length (e.g. one 4 cm-long antenna versus two 2 cm-long antennae). These results suggest that the total length of the antennal epithelium defines the size of the cockroach's window on the olfactory world. Restricting the size of the window reduces its ability to track odors rapidly and effectively. Cockroaches with less antennal surface spend significantly more time tracking the plume ([Fig. 3.05A](#)), stop more frequently and spend more time stopped ([Fig. 3.07](#)). It is particularly telling that cockroaches

with shorter antennae generate wider overall tracks, suggesting that a smaller olfactory ‘window’ must be moved through a larger space to inform appropriate steering maneuvers. There are at least two other ways to achieve the odor information necessary to track a plume. The first could be to move each antenna through space using the antennal muscles. While previous studies have observed intact *P. americana* males to hold their antennae in a stereotyped posture during plume tracking (Willis and Avondet, 2005), it may be that animals with missing antennae do not hold a stereotyped posture, but resolution of our video recordings precluded these measurements. Ongoing studies will address the question of antennal scanning movements in animals with different antennal lengths. A second possible way *P. americana* could be informing steering maneuvers is through a temporal tracking strategy such as transverse klinotaxis (see below).

Potential use of olfactory spatial maps

Previous work by Hösl (1990) demonstrated that some projection neurons in the MGC of *P. americana* describe overlapping, spatially distinct receptive fields on the antenna that could form an antennatopic map of odor space in the brain. An anatomical map of olfactory receptor neurons was recently demonstrated by Nishino et al. (2015), lending support to Hösl's work. Given our observations, if *P. americana* continue to use instantaneous spatial information for olfactory tracking after the complete loss of one antenna, it must be through comparison between zones or integration across zones along the length of the remaining antenna. An antenna-topic map as suggested by Hösl's (1990) study and demonstrated by

Nishino et al. (2015), provides a possible neural mechanism to support this behavior. If the animal is able to compare olfactory inputs across such a map, it could still make spatial comparisons similar to those following the classical idea of tropotaxis using bilateral comparisons. However, such a spatial map could be far more flexible than a two input bilateral comparison system, as much of the antenna could be lost, yet still provide enough information for chemotaxis. At a bare minimum, the animal would need enough antennae remaining for there to be two distinct receptive fields to compare across.

Alternatively, *P. americana* could be integrating across the map (see Eqn 1 below, and [Fig. 3.08](#)), using an additive rather than a comparative olfactory tracking strategy. This integration could be over two maps, one for each antenna as described by Hösl (1990), or one continuous map stretching across both antennae made from the maps present in each MGC. Such an additive model has been shown to enhance directional olfactory performance in fruit fly larvae (Louis et al., 2008), rats (Khan et al., 2012; Rajan et al., 2006) and humans (Porter et al., 2005, 2007). In each of these studies, one sensor was sufficient to complete the olfactory task, and the availability of a second (bilaterally symmetric) sensor decreased the amount of wandering the animal did. If *P. americana* can integrate odor information detected across the span of one or both antennae and keep track of where on the antennal map the odor is detected, it could use the change in the pattern of activation to orient within the plume. Detecting changes in the encountered odor distribution would require a short-term memory to be generated as odor tracking progresses. For this to be successful, a temporal component would be required.

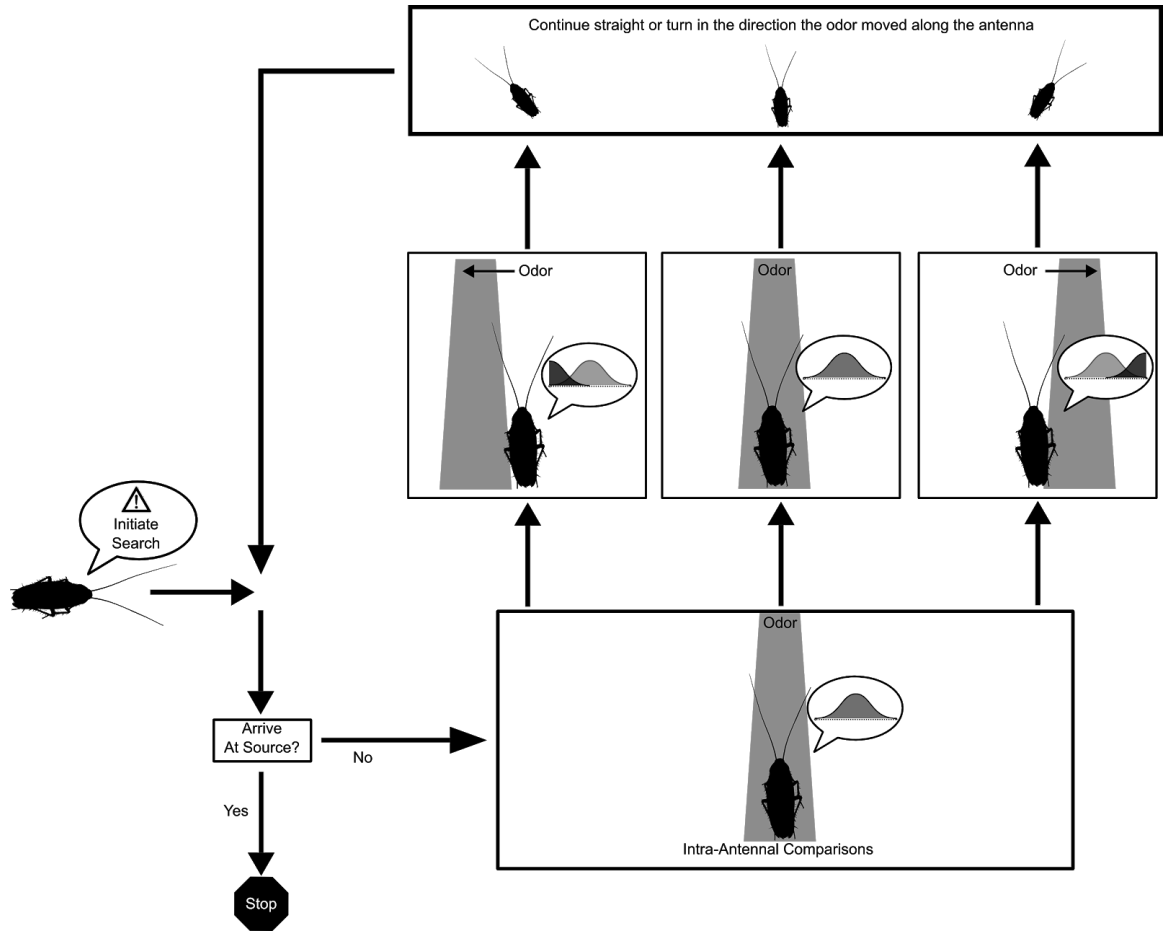


Fig. 3.08. Proposed flow chart of odor-tracking behavior in *P. americana*.

When the animal is tracking an odor, turning is dependent on changes in the center of the stimulus. If the odor moves to the right along the antenna, the animal should turn to the right, whereas if the odor moves to the left, the animal should turn to the left. The inset distributions show possible activation patterns across the antenno-topic map.

Potential for a switch to temporal comparisons

An alternative hypothesis to using a spatial map could be that *P. americana* use klinotaxis (temporal tracking) upon loss of bilateral odor inputs. For *P. americana* to track an odor using a temporal tracking strategy, they would need to store information about the location of odor encounters and the displacement of their odor sensors through the environment, either

by moving their antennae relative to their head or by walking or flying. Whole body displacement information could be gained through a visual (optomotor) response (Marsh et al., 1978) or through a proprioceptive pedometer (e.g. step counting) (Buehlmann et al., 2012; Collett and Collett, 2000; Wittlinger et al., 2006). Previous work by our lab has demonstrated that *P. americana* successfully track an odor plume with their eyes (both compound eyes and ocelli) covered with black paint (Willis et al., 2011), suggesting that a visually guided temporal search strategy is not being used by these cockroaches. Antennal movement information could be gained through processes like proprioceptive feedback or efference copies. Future investigations into potential evidence for temporal tracking in *P. americana* will begin with the search for their ability to calculate displacement via a pedometer. The antennal movement hypothesis seems unlikely, as previous work has shown that intact *P. americana* hold their antennae in a stereotyped posture and move them very little (Willis and Avondet, 2005), but could be tested in the various antennae manipulation groups by tracking antennae movement through a known odor distribution. The experiments presented here were done with freely behaving animals with no control over exactly when and where the stimulus was encountered by the antennae. Future experiments will determine the contribution of any potential spatial map by experimentally applying odor to specific points on the antennae and measuring steering responses.

Proposed model

Prior to the publication of Hösl's work, Bell and Tobin (1981) suggested that *P. americana* with an antenna removed must use a temporal tracking strategy, and went on to suggest that cockroaches normally may use a combination of both instantaneous spatial comparisons (tropotaxis) and temporal comparisons (longitudinal klinotaxis) (Bell and Tobin, 1982). Briefly, they proposed a flow chart in which instantaneous left– right comparisons of the gradient were used to steer left or right (towards whichever concentration was higher), and that temporal comparisons were made along their track to determine whether the heading should be maintained (i.e. concentration is increasing) or to make an abrupt sharp turn (i.e. concentration is decreasing) (Bell and Tobin, 1982). It should be noted that this flowchart assumed zero-wind conditions with a detectable concentration gradient.

In light of our results and in consideration of Hösl's (1990), we propose a new flow chart featuring integration across the antenna olfactory receptor array ([Fig. 3.08](#)). Specifically, the animals could use changes in the pattern of excitation across the antenna to inform turning (i.e. which odor receptive fields on the antenna are receiving odor versus which are not). One way to summarize this pattern of excitation would be to calculate a central 'balance point' along the sensory array. If this balance point moves to the left along the antennae, the animal should adjust its course to the left, and likewise to the right (see insets in [Fig. 3.08](#)). This can be modeled mathematically by Eqn 1, where c is the center of olfaction, n_a is the number unique olfactory receptive fields on the antennae, $q(a)$ is the density of sensory input

across the receptive fields and r is a binary (0/1) input indicating whether a given zone detects odor:

$$c = \frac{1}{n_a} \int_{ant} \rho(a) r \delta a \quad (\text{eq. 1})$$

This is analogous to the center of mass for a one-dimensional system, only instead of applying weights along a line, we are interested in odor detection along the array of sensors. The turns we observe would be due to large course corrections (if c made a large shift along the antennae), or if odor was lost and searching behavior was initiated. Such a tracking strategy could be particularly effective at tracking the high-contrast edge encountered at the plume's lateral margins. The transition from odor plume to clean air at the lateral edge typically occurs within ca. 1 cm (Willis et al., 2013; see also plume measurements in this study in Materials and methods, below). In support of this idea, it is noteworthy that the narrowest tracks generated by *P. americana* males are in response to the narrowest pheromone plumes (Willis and Avondet, 2005).

Our integration model is similar to the proposed behavioral tracking strategy in the crab *C. sapidus* (Page et al., 2011b), but with key differences. Page et al. (2011b) describe the crabs as detecting the distribution of odor concentrations, calculating a center-of-mass (COM), and steering towards that center of the distribution. Odor concentration is not directly measured by *P. americana* olfactory sensilla but rather threshold changes in concentration (Tichy et al., 2005). This is the rationale for treating r as binary and merely measuring the distribution of odor in space, invariant of concentration (either it is above the necessary threshold or it is not). Moths flying and crabs walking upcurrent while tracking odor plumes both reveal that the temporal structure of the plume (i.e. odor onset, offset and

interval duration) and changes in that structure have a greater effect on the tracker's behavior than the odor concentration in the plume (Mafra-Neto and Cardé, 1995; Page et al., 2011a). Odor concentration is trumped by encounter rate in predicting *C. sapidus* odor-tracking velocity (Page et al., 2011a). Further, the balance point *c* is only a summary statistic of the pattern of activation along the antennae. There are other statistics a nervous system could encode to yield a similar result, but we cannot say without proper neurophysiological recordings what is encoded by the nervous system. By focusing on changes in the pattern of activation, the integration model would expect animals to maneuver through the plume in no particular position. They could follow the edge of the plume or walk up the center – both of which have been observed in plume-tracking *P. americana* (Willis and Avondet, 2005), including the present study ([Fig. 3.02](#)). In contrast, in the COM-tracking strategy described by Page et al. (2011b), the animals' steering tends towards the center of the plume. If integration happens continuously across both antennae, it would have further explanatory power in that it accounts for the observed similarity in behavior of animals with antennae of the same total length ([Fig. 3.05A,B](#), [Fig. 3.07](#)). Loss of receptive fields would decrease the accuracy of *c* in describing the plume, and presumably decrease the effectiveness of the animal's tracking behavior. This is consistent with our observation that cockroaches with shortened antennae generate wider walking tracks, perhaps increasing their lateral movements to move their remaining antennal receptive fields across more of the environment.

This model is consistent with our observations and the observations of others and supports the idea that it does not matter if you have one big antenna or two small antennae:

it is the total amount of available olfactory epithelium that is important in the odor-tracking performance of *P. americana*.

MATERIALS AND METHODS

Study animals

Adult, male *P. americana* were removed from our lab colony and held for 1 week to increase their sensitivity to female sex attractant pheromone. They were then placed in an environmental chamber on a 12 h:12 h light:dark cycle for a minimum of 2 days before experimentation.

Treatment groups and odor challenge

For each experimental day, 24 animals were divided into three groups 1 h before the onset of the dark phase (scotophase): left antenna (right antenna removed), right antenna (left antenna removed) and bilateral (two bilaterally symmetric antennae). Each group was further subdivided into four groups by antenna length: 4 cm (full length), 2 cm, 1 cm and 10 annuli (ca. 0.5 cm). Each of these 12 treatments was represented by two individuals on each experimental day. Complete antennectomies were performed by cutting the antenna between the pedicel and the first annulus. This removes all olfactory sensilla while preserving the mechanoreceptive Johnston's organ. The full length group had intact antennae with no apparent missing segments. The remaining groups were cut to the appropriate length with

micro-scissors. Ten annuli was chosen as the shortest length because previous work suggested that a minimum of 8–14 segments are needed for *P. americana* to track the female sex pheromone (J.K.L., unpublished). Cutting just above the tenth annuli should result in a more consistent number of olfactory sensilla being included than using a total length of 0.5 cm. Counting annuli in the treatments with longer antennae was not possible within a reasonable time

At the scheduled onset of scotophase, the animals were placed under red and infrared lighting (i.e. wavelengths thought to be undetectable by the eyes of *P. americana*). Behavioral recordings were conducted from 2 to 4 h post-sunset, centering the experiments on male *P. americana*'s peak behavioral response time to female sex attractant pheromone (Zhukovskaya, 1995). The testing arena consisted of a raised aluminium platform (91×152 cm) in a laminar flow wind tunnel (25 cm s⁻¹). Periplanone B (0.1 ng) (Kitahara et al., 1987; Kuwahara and Mori, 1990) was placed on a filter paper disk (diameter 1 cm) held 2 cm above the platform and centered at the upwind end. The filter paper was oriented perpendicular to the direction of flow, yielding a plume 14.2±2.3 cm wide (mean±s.d.) at the downwind end of the platform. Experiments began and ended with intact control (full-length antennae) trials to verify that the odor source was viable and the cockroaches were still responding. All other trials were done in random order and the treatment was not known to the experimenter. Trials began by placing the animal in its release cage centered at the downwind end of the platform. After 30 s of acclimation time, the individual was released from its cage to track the plume.

Infrared camera recording and digitization of pheromone plume-tracking behavior

Behavior was recorded on an infrared camera at 30 Hz. The video was sub-sampled at 15 Hz because the animals moved slowly enough to yield sufficiently high resolution of the behavior for our analysis. The video was digitized in MATLAB (MathWorks, Natick, MA, USA) with the DTLdv5 application (Hedrick, 2008). Track parameters were calculated using a custom-written MATLAB script (modified from Rutkowski et al., 2009). All trials where the animal tracked the odor plume to the source were digitized, save for one full-length, left antenna individual because the video file was corrupted. The track parameters we measured are described in [Table 3.01](#).

Electroantennogram preparation

The time-averaged plume boundary in the track figures ([Fig. 3.02](#)) was determined using an electroantennogram preparation, similar to previous work in our lab (Willis et al., 2013; Talley, 2010). Because *P. americana* antennae are too slender to accept a fine silver wire into their lumen, we placed them between saline-filled capillaries, connected to silver-wire electrodes. The preparation was then moved across the wind tunnel in 1 cm steps and a 30 s sample of the response was recorded. The boundary coordinates of five separate antennae were averaged to give a mean (\pm s.d.) width of 14.2 ± 2.3 cm, and the plume envelope displayed in the figures ([Fig. 3.02](#)).

Bayesian estimation reveals treatment effects in behavioral patterns

Statistics were performed in R (R Core Team, 2014) using the BEST package (Kruschke and Meredith, 2014). The BESTmcmc function was used to compare groups. This function uses Bayesian estimation to compare two groups (analogous to Student's t-test; Gosset, 1908). The results were corroborated with a hierarchical Bayesian model with two nominal predictors (antenna length and ablation) and a metric predicted variable (a track parameter); this is analogous to an ANOVA with a post hoc test (Kruschke, 2014). Bayesian approaches are used because they are less sensitive to outliers, allow us to accept the null hypothesis (that two groups are practically equivalent), are robust in estimating effect size, and are generally more conservative than traditional Frequentist methods (Kruschke, 2013, 2014). The reported statistic in [Figs 3.03](#), [3.04](#), [3.06](#) and [3.07](#) (the columns of dots next to track parameters) are a graphical representation of the 95% credible interval (highest density intervals, HDI) on the difference between means with a Bonferroni adjustment for eight groups (Gelman et al., 2012). If this HDI excluded zero, it is analogous to significance at the 0.05 level (Kruschke, 2014); this is represented by a dot to the left or right of the zero line. The placement of the dot is determined by the difference between means: a dot to the right indicates that the first group has a greater estimated value for the given track parameter than the second, and vice versa to the left. The groups are indicated at the top of each column. Conversely, if the credible intervals contain zero (the dot straddles the zero line), the groups are practically equivalent (i.e. we can accept the null hypothesis; Kruschke, 2013, 2014). The

HDIIs used to generate the tables are supplied in supplementary material Tables A.i.01–A.i.04, as well as the corroborating statistics from the hierarchical model and the ANOVA (supplementary material [Tables A.i.05](#), [A.i.06](#)).

Supplementary material

Supplementary material available in [Appendix i](#).

Chapter 4

Bunches of hunches: agent-based models of insect odor tracking based on behavioral experiments.

ABSTRACT:

Previous behavioral studies with American cockroaches, *Periplaneta americana*, show that they can track an odor plume even when all but a small portion of one antenna has been lost, and that bilateral symmetry is not predictive of behavior. Their tracking performance improves with increasing amounts of antenna present whether bilateral symmetry is preserved or not. Moreover, published neural recordings and histological data suggest there is a spatial map of the antenna in the antennal lobe of the animal's brain. These observations, combined with our behavioral data lead us to propose a heuristic featuring spatial integration across an antenno-topic map to describe how *P. americana* tracks an odor plume. This study uses an agent-based model to test the proposed heuristic along with several other heuristics describing “classic” tracking strategies. We tested agents with nine different antennae configurations consisting of three arrangements (two bilaterally symmetric antennae, one antenna on the left, or one on the right), with three different lengths (10 mm, 20 mm, and 40mm). The Integrative heuristic is relatively inefficient, but robust against any type of missing antenna segments. Whereas, a purely spatial heuristic that depends on bilateral input

fails utterly with a loss of one of the two antennae. Meanwhile, the purely temporal heuristic is remarkably robust, showing high levels of success in all but the highest noise trials.

Keywords:

Olfaction, odor, tracking, spatial, antennae

INTRODUCTION:

In contrast to using either purely spatial or purely temporal information when tracking an odor, we previously reported behavioral evidence suggesting the use of a spatio-topic olfactory map (SOM) in an integrated tracking strategy in the American cockroach, *Periplaneta americana* (Lockey and Willis 2015). We proposed a model describing how *P. americana* could be making use of a SOM in its odor tracking strategy (Lockey and Willis, 2015). Our goal in the present study is to test the viability of our model and compare it to several variations (bunches) of purely spatial and purely temporal tracking strategies, or heuristics (hunches).

The hypothesis for a SOM is based on the previous behavioural study mentioned above, intracellular recordings of interneurons in the antennal lobe that rate-encode locations along an antenna (Hösl 1990, (Nishino et al., 2018), and anatomical stainings that show olfactory receptor cells (ORCs) project in patterns that uniquely describe both location along the

length of the antenna (i.e., along proximal-distal axis of the flagellum) (Nishino and Mizunami, 2007) as well as the dorsal, ventral, posterior, or anterior surfaces of the antenna (Nishino et al. 2015). In short, the *P. americana* control system may have access to an incredible amount of spatial odor information. The question examined here is if *P. americana* is making use of this abundance of information? and if they do, then how?

A simulation has been developed to test five different tracking heuristics based on various tracking strategies described in the literature (Fraenkel and Gunn, 1961). We compare the results of our simulations to each other and then discuss how they compare to the available tracking data from freely behaving animals.

RESULTS:

Five different heuristics were tested: two controls: Random and Limited, and three proposed tracking strategies: Bilateral (spatial), Temporal, and Integration (a combination proposed in (Lockey and Willis, 2015)).

Fig. 4.01 - Success rates and linearity

Each major column outlined in black indicates the odor gain factor used. The odor gain factor indicates what proportion the heuristic (ω_h), labeled in each major row, makes up of the angular velocity (ω). This denotes the relative influence of the odor input signal on the heuristics decisions (i.e., 0.1 means less effect from the odor and 0.9 means more). Within each tile of the major grid, are nine pie charts, indicating the success rate of the 100 trials run under each sensor/antennae condition. Each row indicates the sensor length (40 mm, 20 mm, and 10 mm, from top to bottom, as indicated on the left of the first major column). Each column indicates which sensor structure was present (both (Bi), just left (L), or just right (R) , from left to right, as indicated at the top of the first major row). The blue portion of the pie chart indicates the proportion of successes for that given set of parameters. Behind each pie chart is a rectangle, shaded to indicate the mean linearity index for the successful tracks, with 0, dark grey, indicating long tracks with many turns, and 1, white, indicating very straight tracks with few or no turns (there is no rectangle if there were zero successes).

The controls performed as expected, showing little success in finding the source (Fig. 4.01, top two rows). The Random heuristic showed an overall mean success rate of 9.4%, while the Limited heuristic (a biologically constrained version of the Random heuristic) showed a mean success rate of 14%. Both showed a small correlation with gain factor (Table 4.01). There are no consistent patterns of turning observable in the tracks (Fig 4.02). The agents always start in the same location with the same heading, and the tracks diverge from there, the simulations using the Limited heuristic diverge less quickly because they are limited in the range they can adjust their angular velocity (ω) in a single step.

Table 4.01 - Predicting success rate from the odor gain factor

Heuristic	β -weight	Adjusted R^2	p-value
Random	-0.0467	0.20	<0.01
Limited	0.0644	0.18	<0.01

Bilateral	0.28	0.01	>0.2
Bilateral (2 antenna only)	0.88	0.64	<0.01
Temporal	0.56	0.62	<<0.01
Integration	0.68	0.65	<<0.01

The Bilateral heuristic was the most successful of all we tried when both left and right sensors were present ([Fig. 4.01](#)). If one sensor was completely removed, the system nearly always failed to locate the source. With a sensor on only one side, the agent would turn in the direction of that sensor until leaving the arena or run out of time ([Fig. 4.01](#)). As the gain factor (GF_r) for the random component of the angular velocity (ω_r) increased (and the gain factor on the odor heuristic component GF_h decreased), the turns became less tight, so much so that it becomes possible in at least a few cases for the agent to loop past the target close enough to be considered a success (Fig 4.01 - Bilateral, Odor gain factor 0.1). The gain factors only had a significant impact on the success rate when the 1 antenna treatments were dropped ([Table 4.01](#)).

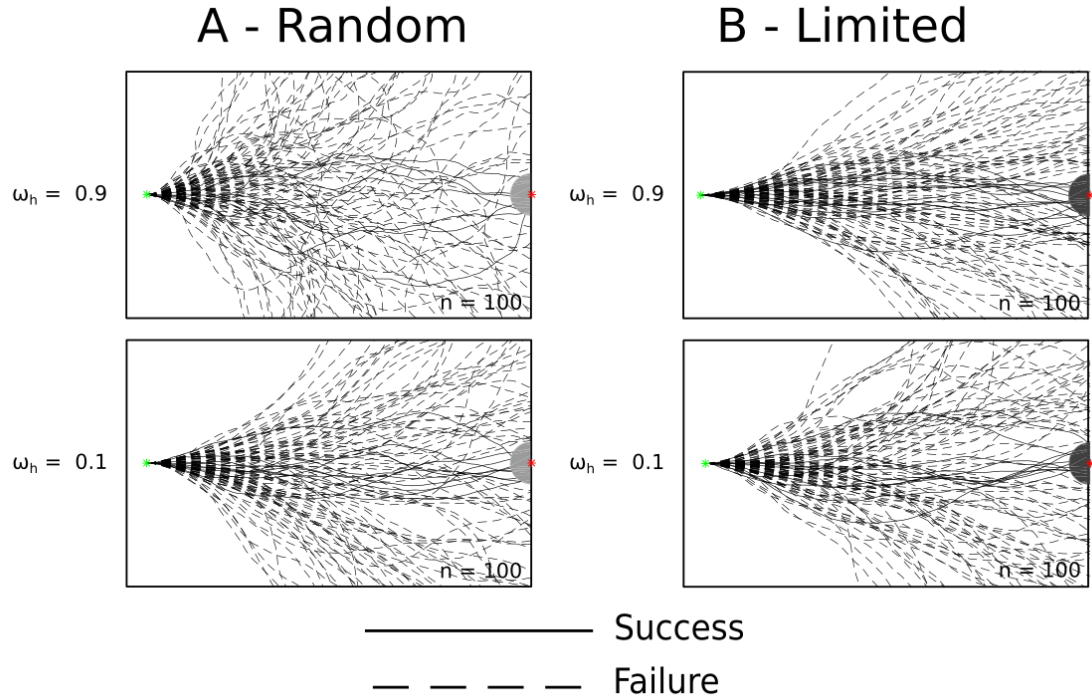


Fig. 4.02 - Examples of the behavior of individual simulation runs from two odor gains from the two random heuristics.

In all figures, the starting location and source are marked with green and red asterisks, respectively. The target area is indicated by the shaded semi-circle. All agents started moving from the left to the right, the ones that managed to hit the target area were considered successes, and their tracks are indicated by solid lines. The agents that failed to locate the source/hit the target region, are indicated by dashed lines. The corresponding heuristic is indicated by the subfigure letter: A - Random, B - Limited (see also [figure 4.03](#) - Bilateral, [figure 4.04A](#) - Temporal, and [4.04B](#) - Integration). A & B both show all 100 tracks for the agents with two full-length antennae and an odor gain factor indicated by the ω_h to the left.

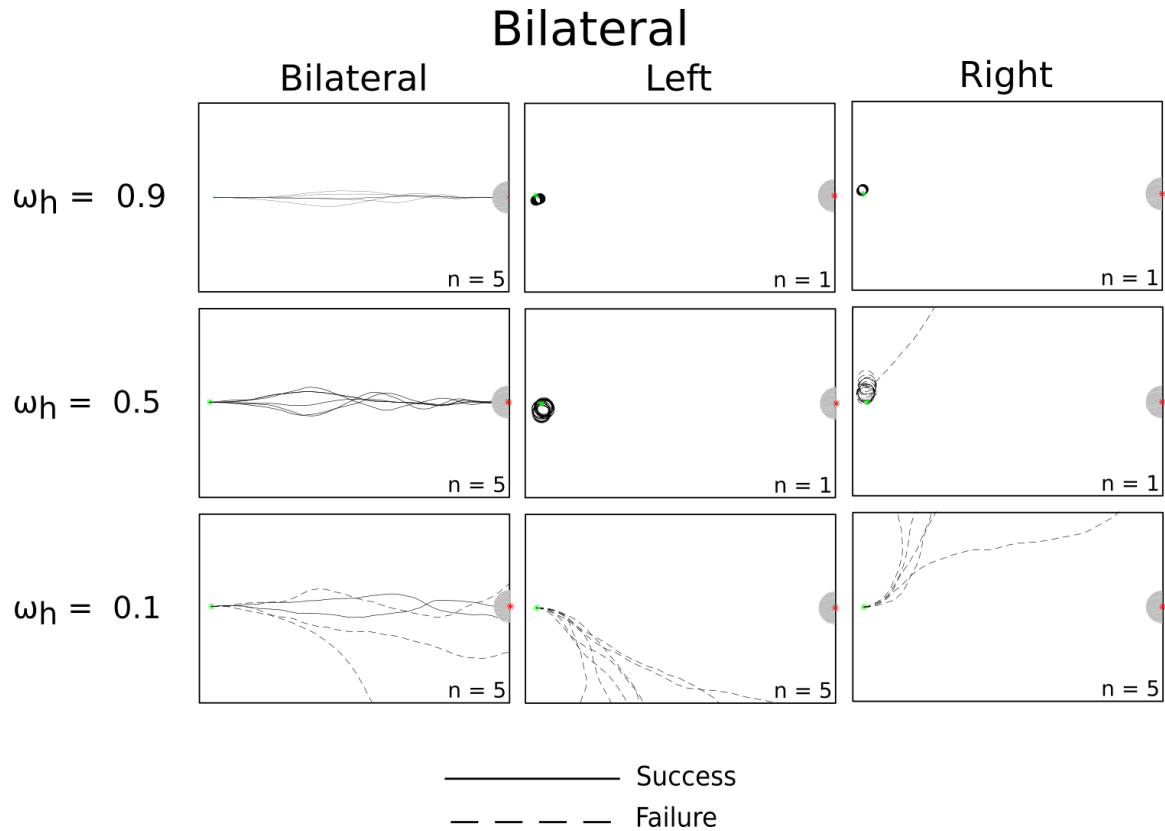


Fig. 4.03 - Examples of the behavior of individual simulation runs from three odor gains across the three antenna configurations from the bilateral heuristic.

The setup is the same as [figure 4.02](#). This figure shows the bilateral heuristic (see also [Figure 4.02A](#) - Random, [4.02B](#) - Limited, [figure 4.04A](#) - Temporal, and [4.04B](#) - Integration). Each box shows a random selection of 5 tracks (there is at least one success and one failure—if any existed), of the agents with full length antennae in the configuration indicated at the top of each column and the odor gain factor indicated at the start of each row.

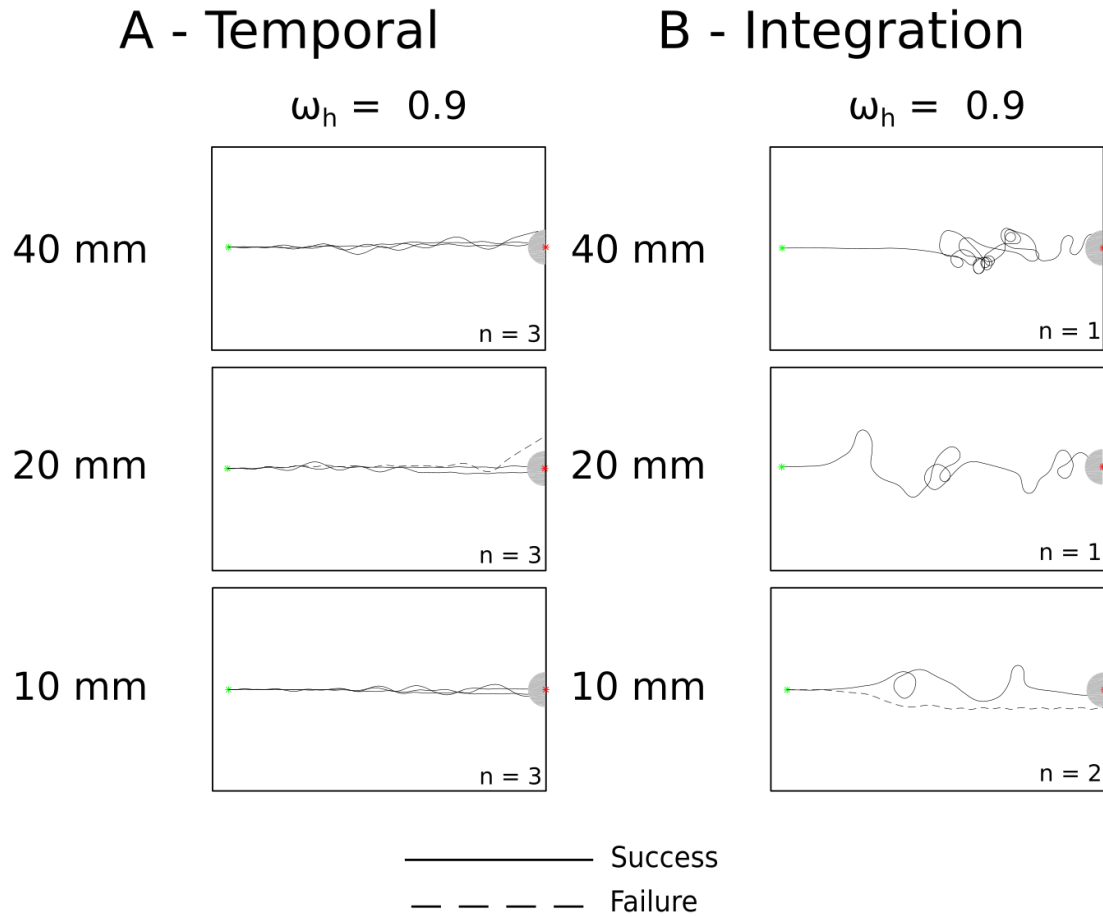


Fig. 4.04 - Examples of the behavior of individual simulation runs from two odor gains from the two random heuristics.

The setup is the same as [figure 4.02](#). The corresponding heuristic is indicated by the subfigure letter: A - Temporal, B - Integration (see also [figure 4.02A](#) - Random, [4.02B](#) - Limited, [4.03](#) - Bilateral). A shows a sampling of 3 tracks, B shows a single track (except in the case of the 10mm antenna condition, there are two to show a randomly selected failure); fewer tracks are shown to make the winding tracks more readable. Each row is with antennae of different lengths as indicated to the left of the charts, and the ω_h indicated at the top of the column.

The tracks generated by the Bilateral heuristic are relatively straight until the plume boundary is met, then the agent turns back towards the center of the plume. As soon as the agent is embedded in the plume again the turn stops and the agent continues in the upwind directions. Because the plume is narrower further upwind, this causes the agent to leave the plume, and commence a turn back into the plume again. This leads to an overall appearance of the agent following the edge of the plume ([Fig. 4.02C](#)). Also, as the size of the sensor increases, so does the success rate, but this has a limited impact with increasing odor gain factors ([Table 4.02](#), [Fig. 4.01](#)).

Table 4.02 - predicting success rate from total antenna length in the Bilateral heuristic.

GF_h	β -weight	Adjusted R^2	p -value
0.1	0.0018	0.96	0.088
0.3	0.0030	0.90	0.14
0.5	0.00029	0.14	0.45

The Temporal and Integration heuristics show the same propensity for generating straight tracks until the edge of the plume is encountered, as is the case the with the Bilateral heuristic. The main difference is in the frequency in which the heuristic-derived component of the angular velocity (ω_h) is altered and by how much. Once a plume edge is encountered, a regular pattern of counter-turns resulting from repeated odor onsets and losses begins. The frequencies are dependent on the gain factors ([Table 4.03](#)).

Table 4.03 - predicting inter-turn duration from the odor gain factor

Heuristic	β -weight	Adjusted R^2	p-value
Temporal	-0.26	0.13	<0.01
Integration	29.	0.44	<<0.001

The Integration heuristic was at least 20% successful across the gain factors we tested. However, as the dependence on odor increased (ω was constituted with more and more ω_h), the linearity decreased ([Fig. 4.01](#), bottom row, notice the darker grey squares as the gain factors shift to favor ω_h), meaning that while successful, the agents took a longer route to get there. Indeed, the total distance walked increased on average by 162 mm with each 0.1 step in the odor gain factor over a baseline of 1281 mm (linear model: intercept = 1281.4, β = 1617.6, adjusted R^2 = 0.30, p << 0.001).

DISCUSSION:

The tracking strategies presented here demonstrate how different types of information can impact behavior. While simple left-vs-right comparisons are sufficient, the loss of one input can be fatal to successful odor localization if that is your only control rule. The evidence gathering strategies (Temporal, Integration) used here withstand the loss of inputs better, but

are more sensitive to noise (small variations in the signal that do not necessarily convey larger meaning).

The Bilateral heuristic is the simplest strategy considered here. Through instantaneous comparisons of only two spatially distinct inputs the agent is able to locate the odor source. As the size of the sensors increase, the more odor they are able to detect over a larger space, increasing the likelihood that the agent will find the source.

The Bilateral heuristic could be modified to a more general spatial strategy that takes more inputs. Having more than two inputs (i.e., multiple spatially distinct sampling points per antenna) *could* save the agent from crashing when one antenna is lost, but comes at the expense of having additional sensors that aren't necessary under normal circumstances, and requires more processing to make turning decisions. Rather than simply taking the difference between two inputs, a more complicated algorithm is needed to process the information. One possibility would be to use the integration model, but with no temporal component: simply find the center of mass and turn in a direction that would put it in the center of the agent's sensory array. An early version of this model was tested in this fashion and found that unless there is a temporal component, this model performed very poorly (data not shown), and this model would be useless with only one antennae, unless the agent knew it was missing an antenna (e.g., by taking whatever bit of antenna remains, dividing it in half and comparing the left-most half to the right-most half).

The Temporal heuristic overcomes the shortcomings of the Bilateral heuristic (probably any exclusively spatial heuristic) by forgoing information about relative locations of sensors and their stimuli and instead creates information by tracking changes in time. This has the benefit of not requiring as many resources to collect information—only one input is needed—but comes at the expense of needing more resources in processing the input. The input needs to be stored, then compared later in time to a newly inputted information. The difference, in combination with wind information, is counted as “evidence” suggesting how best to adjust the angular velocity (or to make no adjustment at all). Once enough evidence is collected to cross some threshold, a decision is made and the appropriate actions are done. This is similar to the integration decision-making schema described by (Shadlen and Newsome, 1996).

The threshold for sufficient evidence and what counted as a given weight for that evidence was arbitrarily set here. It would be interesting to develop a more rigorous system, preferably one that can adjust itself dynamically (i.e., not a value selected from a list based on a collection of conditions, but perhaps defining a function that accrues evidence in proportion to the magnitude and sign of the various stimuli).

The Integration heuristic consumes the most resources. It requires the same memory as the Temporal heuristic, but instead of a simple sum, it is storing a center of mass. Calculating the center of mass is a more complicated spatial calculation than what the Bilateral heuristic

uses. These extra resources should come as a net benefit to the agent. However, that does not appear to be the case here.

Agents using the Integration heuristic never had better success rates than other heuristics with the same gain factors. When they did find the source, they often took longer getting there, as evidenced by the lower linearity scores ([Fig 4.01](#)). This is an unexpected result, as increasing the amount of information should increase the accuracy (Kruschke, 2015). Based on this, it can be concluded that the model proposed in Lockey and Willis (Lockey and Willis, 2015) may not be a good representation of the controller used by real cockroaches.

It makes little sense for *P. americana* to have an anatomy that collects such detailed spatial information (see comments in the introduction) and not use said information. The results of Bell and Tobin (Bell and Tobin, 1981) further contradict the notion that this is a purely temporal strategy. When they crossed the antennae of *P. americana* males in an “X”, the cockroaches were unable to locate an odor source. This configuration provides left information to the right antenna, and right information to the left antenna. This prevented the animal from finding the source, indicating that correct spatial information is required for odor localization.

There are at least two things that would go a long way in helping improve odor tracking modeling. The first is having a clearer idea of exactly what each sensor along the antennae experiences during odor tracking; the second is an understanding of how information is

encoded and passed along to a higher center of the brain to make turning decisions. A particularly important goal might be to link antennal inputs to the activity described in the central complex that controls turning behaviour (Guo and Ritzmann, 2013).

While there is a basic understanding of the response dynamics of olfactory sensilla, it is unknown how many of them act in concert when being driven through a plume, as is the case when the animal moves through or along a plume. Devices for conducting single sensillum recordings in the field have been demonstrated (Van der Pers and Minks, 1993), but nothing appears to be published on what a plume looks like in the field, especially comparing multiple locations in space captured simultaneously. Studies like Murlis and Jones (Murlis and Jones, 1981) have provided an understanding of plumes over larger distances that an animal may travel (i.e., on the order of several meters), but we lack clarity of what differences might be detected between the span of an animals antennae (i.e., a few millimeters or less).

METHODS:

The basic structure of a trial is given in [figure 4.05](#). After initial setup, the program loops through the following five steps: First, the plume is updated. Second, sensory information is collected and processed. Third, the agent updates its turning rate, ω , by combining an angular velocity based on the current heuristic in use, ω_h , with a random angular velocity drawn from a normal distribution ($\mu = 0$, $\sigma = 1$), ω_r (different proportions of ω_h and

ω_r are tested). Fourth, the agent's heading and position are updated. And lastly, fifth, termination conditions are checked. If the agent hasn't reached a termination condition, the program loops back to step one, updating the plume. If termination conditions have been met, the data is printed to a file, and the trial is terminated. The agent takes one step per loop, each step representing 0.01 s of elapsed time.

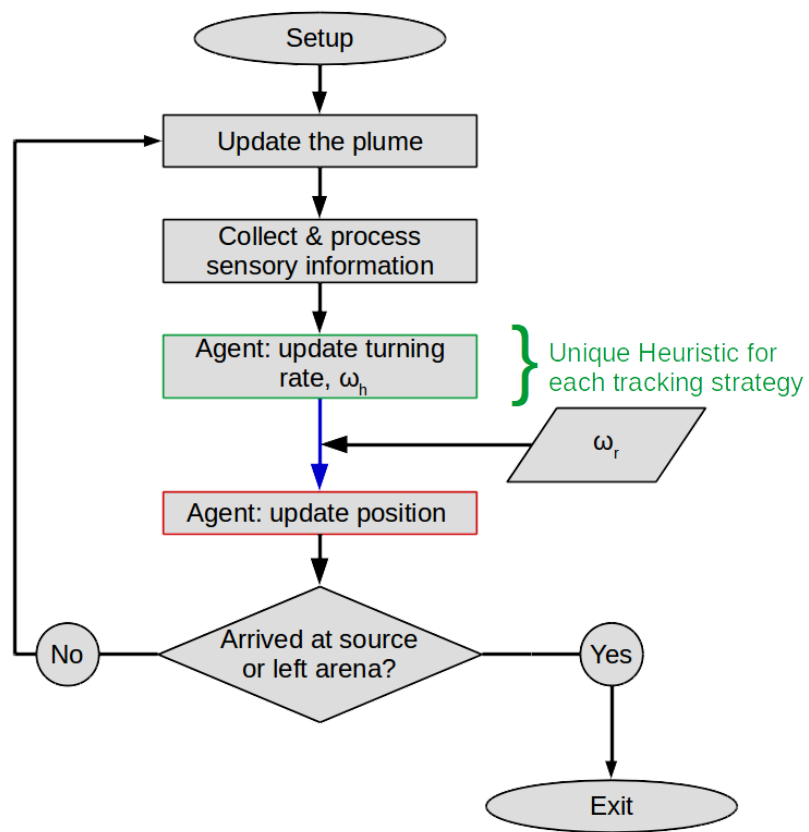


Fig. 4.05 - The overarching flow of a trial.

After the trial is set up, the simulation loops through five basic steps: updating the plume, updating the agent's location, updating the agent's angular velocity through a unique decisions-making heuristic (which calculates ω_h , and combined with a random noise component, ω_r , to yield the overall angular velocity, ω), and then the agent's position and elapsed time is checked for termination conditions.

For the data presented here, 100 trials were conducted with each set of parameters. The software is designed to select a set of parameters, run a predefined number of trials (100), then select another set of parameters. The parameters include nine different sensor configurations, five different proportions of ω_h and ω_r , and five different heuristics, giving a total of 22,500 individual trials sampled here.

Setup, the inner workings of each of the five heuristics, and an explanation of the other parameters are given below. The overall layout of the program is given in [figure 4.06](#), with details of the individual heuristics given in figures 4.07-4.12. All the code is available for download on github (<https://github.com/jklocport/roachSim>), also, see [appendix ii](#).

Setup

Overall, the program is derived from a simple random walk described in Shiffman’s Nature of Code (Shiffman, 2012), where the “walker” is created as an object and holds its own properties and has its own internal functions. This organization allows for the creation of subclasses that extend and modify the basic Walker class with unique methods implementing the heuristics described here. While preliminary versions of this simulation were written in Matlab (MathWorks, Natick, MA, USA) and Processing (Processing.org), the code used here was ultimately written in Java.

Initial conditions

The arena is defined as a rectangle matching the behavioral arena used in (Lockey and Willis, 2015), at 1525 mm x 925 mm, with the origin being in the lower left hand corner and the

long axis extending in the $+x$ direction. A “plume” is generated centered on the upwind edge of the arena ($x = 1525$, $y = 462.5$) through a `PlumeFactory` object. This is a factory-method, a single object programed to control many `OdorParticle` objects. The wind moves at 25 cm s^{-1} in the $-x$ direction.

`OdorParticle` objects are circles meant to represent a “blob” or “cloud” of odor in the environment. They each have a center position ($\vec{P}_{x,y}$), a velocity ($\vec{V}_{x,y}$), a radius (r), and a concentration (c). In each timestep of the simulation (each “frame”), there is a 90% chance of a new `OdorParticle` being generated. Each odor particle is moved downwind at the appropriate velocity, diffusing at a rate determined through detailed mapping of an ethanol plume in the same arena used in the previous behavioral studies (See [Chapter 2](#)). The r is adjusted such that as c diminishes, the total amount of mass in the `OdorParticle` is held constant:

$$\frac{c'}{A'} = \frac{c}{A}$$

Where $A = \pi r^2$, and c' & A' are the is the starting concentration and the starting area of the `OdorParticle`, respectfully.

The agent’s head begins centered laterally ($y = 462.5$), 5% of the way upwind of the end of the arena ($x = 76.25$), with an initial heading of due upwind ($\theta = 0 \text{ rad}$), and not moving (speed, $s = 0$). The wind speed is set at 25 cm s^{-1} . The plume starts generating in in frame 1. Once the plume has extended all the way downwind to the far end of the arena, the method `startTracking()` is called setting s to 23 cm s^{-1} (the mean value of intact

controls in the behavioral study), and movement begins.

Agent: abstract walker object

All agents are created as “walker” objects. The abstract class these objects extend contains and tracks the agent’s position and orientation. The structure of the classes are described in [figure 4.06](#). Key methods include an abstract method for adjusting the angular velocity that is written over by each heuristic, a step method for updating the agent’s position and orientation, and methods for checking termination conditions. The trial is terminated when the agent either finds the source or leaves the arena, or more than 5 minutes of simulated time runs out.

Collecting and processing sensory information

The agent's position is tracked by the “head point,” and the heading angle is determined by the long axis of the body (as created by the tail point to head point vector). The agent’s antennae bases are situated on either side of the headpoint by half the inter-antennal distance on a cockroaches head (3.278 mm). The antennae each extend from their base points to the tip points, 40 mm away (the average length of an intact antenna), at an angle of plus or minus $\pi/4$ for right and left antennae, respectfully. The antennae are each divided into 40 bins (1 mm long each), to “collect” odor information, the concentration of the `odor_particles` that overlap with the center point of each bin is recorded in an array

representing the antenna. To “process” this information, a threshold is set, and each bin in the antenna array is checked if the odor concentration in that location exceeds the threshold, if it is, the value is set to a binary 1 (odor-ON) or 0 (odor-OFF), akin to the odor-ON/OFF sensors the cockroach receptors have been described as by (Tichy et al., 2005).

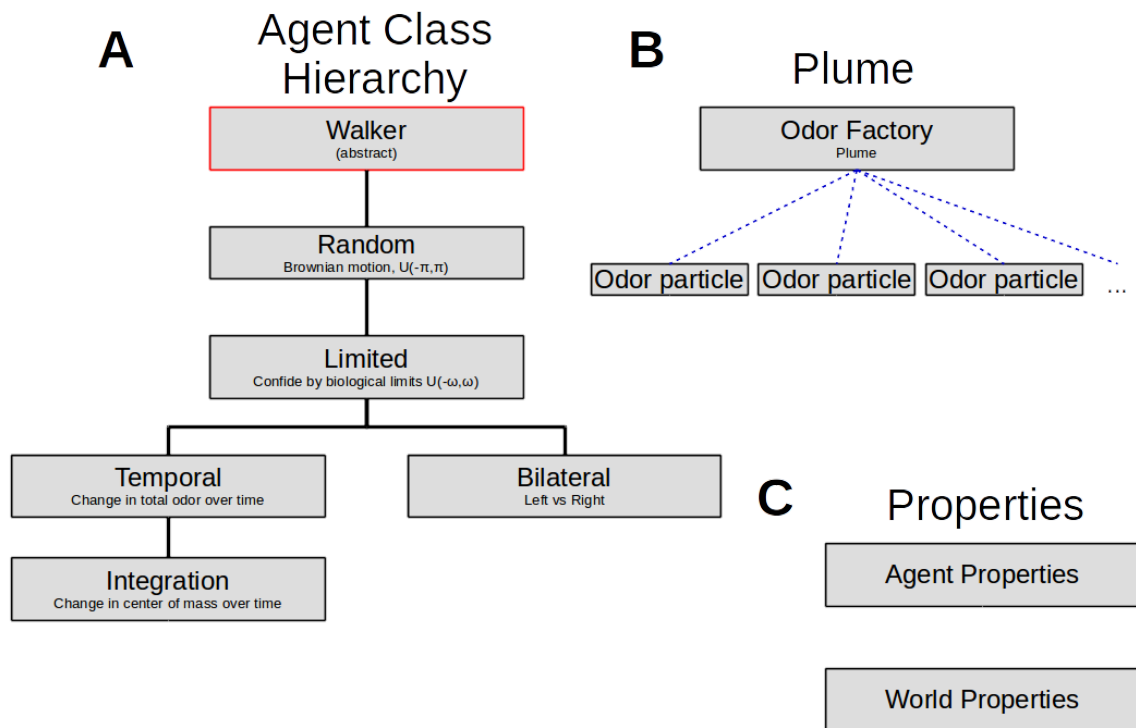


Fig. 4.06 - Class Structures

The simulation code is organized these major classes. (a) At the core is the abstract Walker class. This is extended by the Random_Walker subclass, which defines a random heuristic. The Limited_Walker subclass extends the Random_Walker class by overwriting the method for calculating ω and imposing limits on how much the agent can turn in a step. The Bilateral_Walker subclass extends Limited_Walker in much the same way, overwriting the method for calculating ω_h . The Temporal_Walker subclass adds methods for evaluating evidence in determining when to modify ω_h and by how much. Finally, The Integration_Walker subclass extends the Temporal_Walker, using the same methods for evaluating evidence; the difference is in what evidence is gathered (pattern of activation vs total stimulation across the sensory array). (b) The odor plume that the agent tracks is constructed through a factory object, which controls many Odor_Particle objects. These objects together make up the plume. (c) Two other key object classes are the Agent_Properties, which hold a collection of variables defining different aspects of the agent (antenna length, body length, ω_{max} , etc.), and World_Properties, which defines the the properties of the plume, the size of the arena, wind speed, etc.

Heuristic 1: random walk

The `Walker_Random` subclass describes by far the simplest heuristic: ω_h is selected from a uniform distribution, $U(-\pi, +\pi)$, meaning the agent can turn by any angle (average being 0 rad). There are no restrictions on how much the agent can turn in one step.

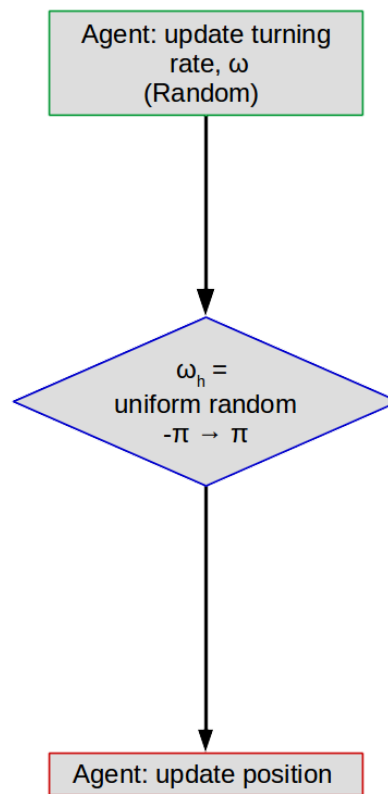


Fig. 4.07 - Random Heuristic

ω_h is selected randomly from a uniform distribution describing a full circle. Note that the first module outlined in green is the same as the module outlined in green in [Fig. 4.05](#). Likewise for the red module.

Heuristic 2: limited random walk

The `Walker_Limited` subclass has a heuristic that draws ω_h from a uniform distribution limited to the maximum & minimum ω estimated from the behavioral experiments, $U_{(-\omega_{max}, \omega_{max})}$. After ω_h is combined with ω_r , but before the step is calculated the total rotation is limited to what was observed in the behavioral experiments ($\omega_{max} = \mu_{\omega} + 3\sigma_{\omega}$).

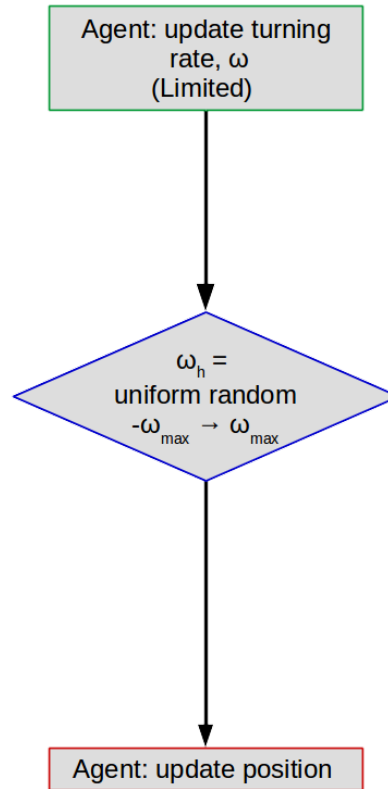


Fig. 4.08 - Limited Heuristic

ω_h is selected from a uniform distribution between $\pm \omega_{max}$, limiting the turning rate to what was observed in the behavioral experiments.

Heuristic 3: bilateral

The `Walker_Bilateral` subclass extends the `Walker_Limited` subclass and has a heuristic that calculates the total “mass” of odor on each antenna (the number of bins with odor over the detection threshold, 0 to 40) and turns based on difference in mass between the two antennae:

$$\omega_h = \omega_{max} \frac{M_r - M_l}{n}$$

Where M_r is the mass on the right antenna, M_l is the mass on the left antenna, and n is the total number of bins per antenna (40). Thus, if every bin on the right has odor ($M_r = 40$), and every bin on the left has no odor ($M_l = 0$), then the agent would turn maximally to the right, $+\omega_{max}$, and $-\omega_{max}$ if the reverse occurs.

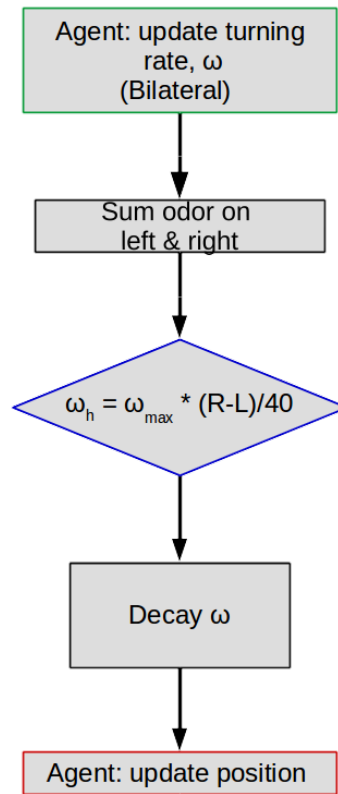


Fig. 4.09 - Bilateral Heuristic

Stimulation on the left is compared to stimulation on the right and ω_h is decided in proportion to the difference between the two.

Heuristic 4: temporal

The `Walker_Temporal` subclass extends the `Walker_Limited` subclass and has a heuristic based on evidence gathering. In each step of the simulation, the present sensory conditions are examined (orientation to the wind, amount of odor everywhere on both antennae relative to the previous step), and a small amount is added to one of three variables: `goLeft`, `goStraight`, or `goRight`. Once a threshold is met, ω_h is changed

accordingly: `goLeft` is evidence to turn more to the left ($\omega < \omega'$), `goRight` is evidence to turn more to the right ($\omega > \omega'$), and `goStraight` is evidence to turn less ($|\omega| < |\omega'|$).

This is meant to resemble an “integrate and fire” system where several neurons sample from many inputs and slowly depolarise as the appropriate inputs are activated. If any one of the neurons receives enough input to push the membrane potential above the firing threshold, the integrating neuron fires an action potential. This can be thought of as representing a decision (Shadlen and Newsome, 1996).

This heuristic specifically has the following criteria for assigning evidence:

If the amount of odor is increasing (i.e., the agent is moving into the plume):

And the wind is behind and to the right, `goRight` += 0.02.

And the wind is ahead and to the right, `goRight` += 0.01.

And the wind is ahead and to the left, `goLeft` += 0.01.

And the wind is behind and to the left, `goLeft` += 0.02.

If the amount of odor is decreasing (i.e., the agent is moving out of the plume):

And the wind is behind and to the right, `goLeft` += 0.04.

And the wind is ahead and to the right, `goRight` += 0.02.

And the wind is ahead and to the left, `goLeft` += 0.02.

And the wind is behind and to the left, `goRight` += 0.04.

Otherwise (the amount of odor must be constant):

`goStraight` += 0.01.

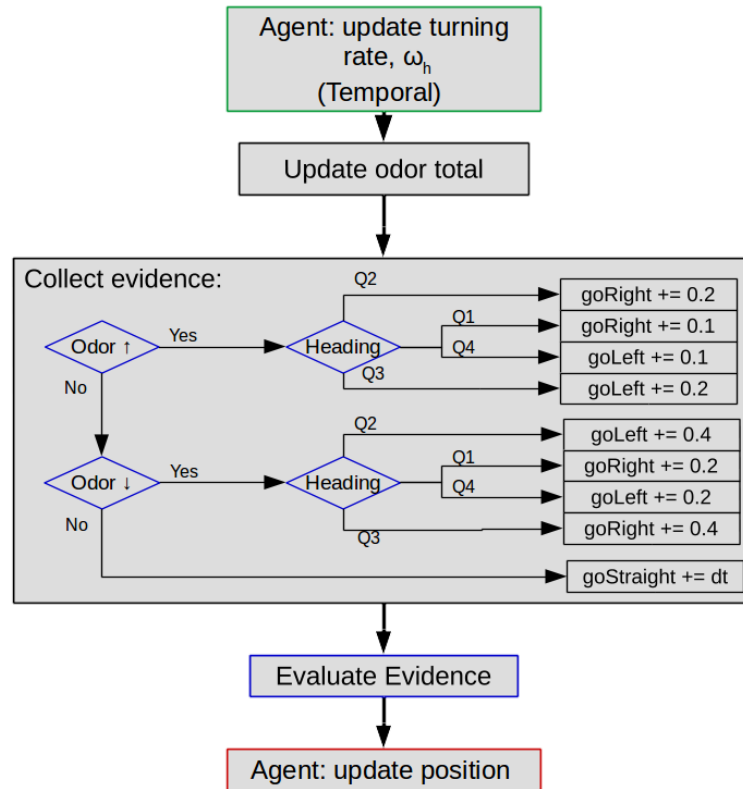


Fig. 4.10 - Temporal heuristic

Evidence is collected based on the change in total odor and wind direction, the evidence is evaluated in a segment described in [figure 4.11](#) to decide ω_h .

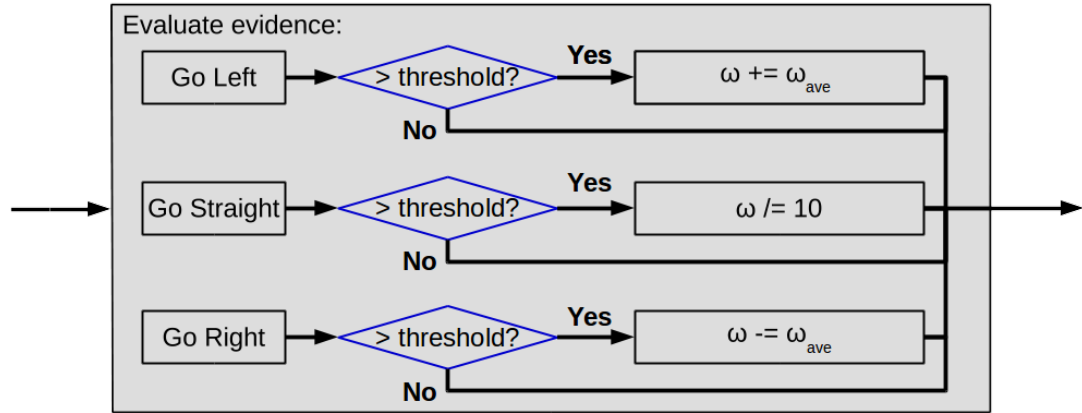


Fig. 4.11 - Evaluating evidence.

If any evidence counter exceeds a threshold, the corresponding action is taken (e.g., if enough evidence for turning right is obtained, ω_h is adjusted more to the right). Note this is the blue module in [figures 4.10 & 4.12](#).

Heuristic 5: integration

The `Walker_Integration` subclass extends the `Walker_Temporal` subclass and its heuristic uses the same evidence-based system, only here evidence is based on wind direction and rather than change in total odor amount, change in the location of odor along the antenna. The antenna is treated as a single dimensional object with weights on it representing odor. The center-of-mass is calculated and its change in position is used in combination with the wind direction to provide evidence for turning or going straight.

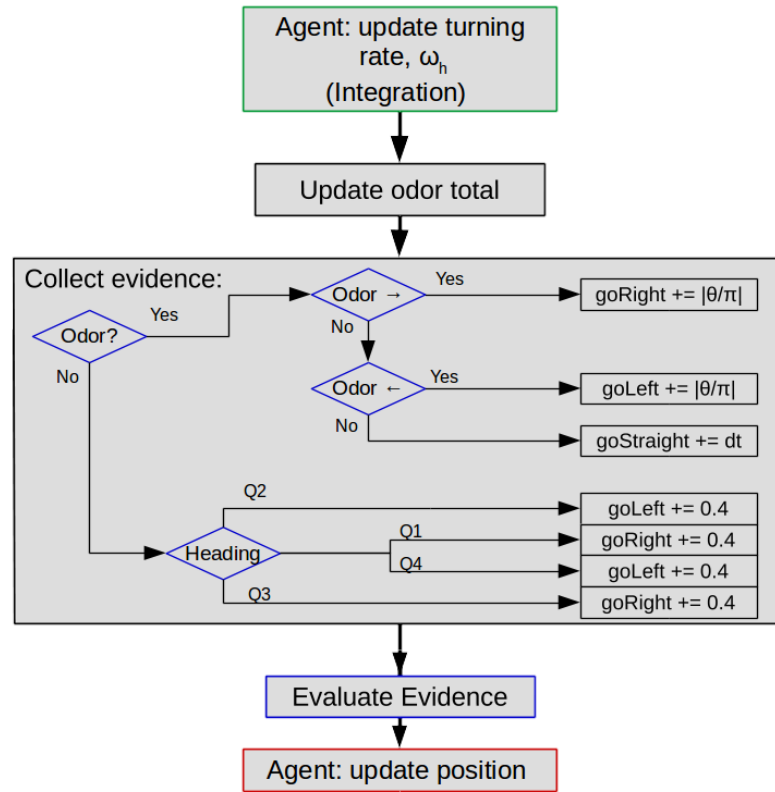


Fig. 4.12 - Integration heuristic

Evidence is collected based on the change in center of mass of the stimulation. See Fig. 4.09 for the evaluate evidence module.

Sensor configurations

The configuration of the sensors are taken directly from the behavioral work that inspired this project (Lockey and Willis, 2015). The sensors are represented by two 40-element arrays, meant to represent the two c.a. 40 mm long antennae of *P. americana*; one array element represents 1 mm of antenna. The base and the tip of the agent's "antennae" are given coordinates and the locations of the 40 units on each antenna are then interpolated. The amount of odor present in the location of the unit is then measured. If the odor

concentration meets or exceeds the detection threshold, the corresponding array element gets a score of 1; otherwise it's scored 0, not unlike the thresholding described in cockroaches by Tichy et al. (Tichy et al., 2005).

The sensors are positioned such that the base is 1.639 mm to the left or right of the head point (half the average distance between antennae of a *P. americana* head, $n = 5$), and the tip is 40 mm out from there, $\pm 45^\circ$ off of the long axis of the body projecting forward. This relative orientation between the body and the sensors is fixed. For simplicity there is no relative movement of the sensors relative to the body or each other.

The sensors are “cut” to different lengths: 40 mm, 20 mm, and 10 mm, either symmetrically (i.e., the “bilateral” treatments), or unilaterally (e.g., “left” treatments refer to the length of the left sensor, the right has been completely removed). The removed portions of the sensors are always scored 0: no odor is detected.

Angular velocity proportions

Two different angular velocities are used to control the agent's heading (θ , rad): a random component (ω_r , rad s⁻¹), and a heuristic component (ω_h , rad s⁻¹). The random component is selected from a normal distribution ($\mu = 0$, $\sigma = 1$, in rad s⁻¹), and the heuristic component is calculated in one of the heuristics described above. These are each multiplied by a gain factor and used to update θ , thusly:

$$\theta + = (\omega_h * g_h + \omega_r * g_r) * d_t$$

Where g_h and g_r are the gain factors on the angular velocity components (dimensionless), and d_t (s) is the duration of one timestep through the simulation. Each timestep, θ is updated by the amount appropriate for the intervening length of time between cycles through the program based on the information gathered and processed by the heuristic (in the form of ω_h) and some random noise (in the form of ω_r).

The gain factors are constrained such that:

$$g_h + g_r = 1$$

Evidence based decisions (temporal and integration)

This is a method in the `Temporal_Walker` subclass that is also used in the `Integration_Walker` subclass. Each subclass' method for determining ω_h has three “evidence counting” variables (ECVs): `goLeft`, `goStraight`, `goRight` that it adds small amounts to based on the sensory inputs and the inner workings of the heuristics described above. It checks if the activation threshold has been reached; if it has, ω_h is adjusted and all the ECVs are reset to zero.

For the sake of simplicity, a decay rate of 0 has been used here. This can be adjusted and manipulated in a future study.

Statistical analysis

Correlations with success rates were calculated using simple linear models in R. For example, line 1 of [table 4.01](#) was calculated by asking how well the success rate, S_r (each pie chart), can be predicted from the odor gain factor, O_{GF} :

$$S_r = \beta_1 + \beta_2 O_{GF}$$

Where β_1 is the intercept, and β_2 is the estimate on the contribution O_{GF} makes in predicting S_r .

Chapter 5

Concluding remarks

To the best of my understanding, cockroach olfactory navigation can be summed up as follows: Odor is dispersed through the environment and this information is collected by the antennae and processed through the brain, and behaviour is altered accordingly. I have primarily focused on the antennae's collection of information and the resultant behavior. We know from Hösl's work (Hösl, 1990) that there are interneurons in the antennal lobe that report the approximate location of stimulation along the antenna through changes in firing frequency, and that these neurons have partially overlapping receptive fields. These overlapping receptive fields ought to create a map showing which sensors on the antennae are detecting odor, meaning the animal could be able to resolve an instantaneous snapshot of the odor distribution across the span of the antennae at that location in space. If the odor moves in predictable ways through the environment, the animal can make appropriate changes to its trajectory. I call this the map, or odor-map hypothesis.

It is important to understand what the stimulus is that the cockroach is tracking, so I first present a detailed understanding of the fluid environment and show that there is little (if any) intermittency in the plume cockroaches track in our wind tunnel ([chapter 2](#)). This shows that the cockroaches are likely experiencing a solid “stripe” of odor through the environment.

If the animal is using a spatial map to track an odor, altering the map should impact tracking performance. Specifically, if the map were scrambled, we should expect the animal to be unable to reliably track an odor. If the size of the map is reduced, we might expect a reduction in success or an increase in the time it takes the animal to find the source.

Bell and Tobin (Bell and Tobin, 1981) did something very similar to this. They didn't reduce the length of the antennae, but they did cross the antennae. *Periplaneta americana* with crossed antennae were unable to locate an odor source. Individuals with crossed antennae made fewer forays away from the wall of the arena towards the center where the odor source was located, and when they made sharp turns, they were rarely in the correct direction. Other than to say that "Males with crossed antennae were unable to locate the pheromone source, suggesting that the fixed position of their antennae interfered with sensory information input," they offered no discussion or explanation for why this might be. In light of Hösl's work, I'd argue it supports the map hypothesis. By misplacing the map (intentionally inverting or moving the various portions of the map around) the information gathered from that map would be miss-allocated if the animal has no way of unscrambling the map (e.g., if right and left are flipped and the animal doesn't know that right and left have been flipped, all the decisions should be backwards from what the system would normally intend).

In building off of Bell and Tobin's work, I undertook a similar study, but rather than crossing the antenna or simply removing one, I challenged animals to track with different

length antennae. There ought to be a predictable relationship between antennae length and performance. Indeed, there was (Lockey and Willis, 2015) ([chapter 3](#) above).

The immediately obvious result was that animals with shorter antennae did worse: they were less likely to find the source, and if they did, they took longer, more circuitous routes. The more interesting result was a lack of any difference between missing a right or a left antenna. The behavior of an animal with only a right antenna X mm long was identical to that of an animal with a left antenna X mm long. What's more, animals with two antennae, each $\frac{1}{2}X$ mm long (so a total of X , distributed across the two separate antennae) were also identical in their behavior.

To me, this suggested that the system is taking advantage of the size of the spatial distribution of odor it is able to detect, and not caring about where that is coming from. It is as if you were looking through a window trying to steer a vehicle: the size of the window is the important part, not the precise location on the front of the vehicle. This led to a proposed model of how I thought the system might be working (see the end of [chapter 3](#)).

The proposed model focused on changes in pattern of odor presented to the antennae. Lacking a clear way to test this in live animals, I turned to building a computer simulation ([chapter 4](#)). I created an environment similar to the one I know the cockroaches to be experiencing, informed by careful measurement of odor plumes in our wind tunnel—we know the structure of the environment alters the structure of the behavior (Willis and

Avondet, 2005). I then created an agent to explore that environment, and programmed a number of heuristics for the agent to use in exploring that environment.

Not only did I program a heuristic based on the proposed model from the behavioral experiments, but built several heuristics based on classic models of orientation based primarily on (Fraenkel and Gunn, 1961).

The model is sufficient to show that a controller that operates on changes in spatial odor distributions is able to track an odor plume reasonably well. Simple bilateral comparisons are the most effective, but also the most fragile. The loss of one sensor renders the system incapable of finding the source by any odor-guided means.

This contribution will serve as a foundation that will be refined and tested under a barrage of different simulated environments, the results of which will, with any luck, provide a useful framework to ask future questions that we can test in cockroaches or other insects, furthering our understanding of how these systems function.

Supplementary material for [Chapter 3](#)

Table A.i.01 – Credibility intervals (Highest Density Intervals – HDIs) on the difference in means between animals with only a left or right antenna (used to form [figure 3.03](#)). A negative credibility interval (the lower (HDI-lo) and upper (HDI-up) bounds are both negative) indicates that first group in the comparison is smaller than the second group, whereas a positive credibility interval (HDI-lo and HDI-up are both positive) indicates first group is larger than the second. A credibility interval that contains zero indicates the groups are the same. In this case, we compared left to right, and all groups are equal for all track parameters. Significant differences are highlighted.

	4 cm		2 cm		1 cm	
	HDI-low	HDI-up	HDI-low	HDI-up	HDI-low	HDI-up
Time to Source (s)	-12.9	10.9	-33.8	36.6	-112	106
Walking Speed (cm/s)	-4.83	4.68	-4.55	4.25	-18.47	6.75
Track Width (cm)	-2.00	1.81	-1.57	1.23	-5.63	4.50
Walking Distance (cm)	-248	200	-390	371	-1450	780
Linearity	-0.22	0.20	-0.11	0.22	-0.097	0.26
No. Stops	-6.52	6.68	-11.4	27.7	-82.8	75.7
Stop Duration (s)	-0.065	0.13	-0.039	0.11	-0.13	0.17
Total Stop Time (s)	-1.53	1.76	-2.52	7.58	-17.8	17.7
No. Backtracks	-4.16	4.31	-7.77	6.98	-21.8	16.3
No. Left Turns	-6.99	5.78	-9.84	15.8	-31.7	15.2
No. Right Turns	-9.18	6.16	-11.2	14.5	-28.7	7.32
Interturn Duration	-0.22	0.61	-0.50	1.05	-1.12	3.52
Mag. Body Angle (°)	-15.9	21.9	-20.1	12.2	-29.6	18.5
Body Angle (°)	-10.2	8.75	-11.7	6.12	-23.5	17.2
Angular Velocity (°/s)	-7.72	24.4	-0.67	27.32	-40.4	40.1

Angular Acceleration ($^{\circ}/s^2$) -5.65 5.44 -4.92 1.79 -9.24 5.79

Table A.i.02 – Credibility intervals on the difference in means between animals with two antennae vs one antenna (used to form [figure 3.04](#)). See [table A.i.01](#) for information on how to interpret HDIs. Significant differences are highlighted.

	4 cm		2 cm		1 cm	
	HDI-low	HDI-up	HDI-low	HDI-up	HDI-low	HDI-up
Time to Source (s)	-17.9	-6.28	-40.8	-11.7	-62.6	-15.9
Walking Speed (cm/s)	1.27	9.56	3.34	10.9	4.82	11.9
Track Width (cm)	-3.31	-0.84	-3.09	-0.59	-3.18	-0.25
Walking Distance (cm)	-252	-79.9	-500.	-82.9	-761	142
Linearity	0.12	0.42	0.021	0.37	-4.59E-5	0.20
No. Stops	-8.44	-1.35	-29.9	-11.1	-32.0	-0.17
Stop Duration (s)	-0.12	-0.01	-0.12	-0.01	-0.12	0.0058
Total Stop Time (s)	-1.86	-0.21	-6.08	-1.30	-4.66	-0.24
No. Backtracks	-5.13	-1.35	-10.8	-2.13	-17.0	1.73
No. Left Turns	-7.71	-2.16	-15.0	2.95	-18.2	11.8
No. Right Turns	-7.93	-1.79	-16.0	-2.34	-16.5	8.84
Interturn Duration	-0.39	0.44	-1.05	-0.23	-1.96	-0.13
Mag. Body Angle ($^{\circ}$)	-35.8	-8.63	-31.1	-0.17	-20.6	6.27
Body Angle ($^{\circ}$)	-4.90	8.94	-8.89	2.45	-12.0	2.14
Angular Velocity ($^{\circ}/s$)	-12.9	13.1	-5.14	16.3	-14.9	12.7
Angular Acceleration ($^{\circ}/s^2$)	-9.38	0.82	-3.97	3.30	-3.27	3.20

Table A.i.03 – Credibility intervals on the difference in means between animals with different length antennae, by treatment (used to form [figure 3.06](#)). See [table A.i.01](#) for information on how to interpret HDIs. Significant differences are highlighted.

	Bilateral				Antennectomy			
	4 cm vs 2 cm		2 cm vs 1 cm		4 cm vs 2 cm		2 cm vs 1 cm	
	HDI-low	HDI-up	HDI-low	HDI-up	HDI-low	HDI-up	HDI-low	HDI-up
Time to Source (s)	-17.4	-0.72	-21.7	1.83	-43.2	-11.7	-48.2	6.10
Walking Speed (cm/s)	-2.68	7.05	-4.08	4.01	0.97	6.80	-2.23	4.32
Track Width (cm)	-2.32	0.43	-2.55	0.02	-1.80	0.37	-2.61	0.25
Walking Distance (cm)	-244	-10.7	-515	14.8	-491	-99.6	-693	71.0
Linearity	0.043	0.43	0.030	0.38	0.043	0.28	5.6E-05	0.15
No. Stops	-3.27	2.18	-5.44	2.20	-26.0	-5.63	-26.6	17.7
Stop Duration (s)	-0.062	0.039	-0.082	0.039	-0.071	0.036	-0.71	0.043
Total Stop Time (s)	-0.39	0.44	-0.60	0.25	-5.63	-0.72	-5.14	4.79
No. Backtracks	-5.20	-0.32	-10.4	-0.30	-10.4	-2.90	-16.4	1.09
No. Left Turns	-12.4	-0.89	-16.6	3.28	-15.4	-3.09	-17.2	4.64
No. Right Turns	-9.60	-0.24	-16.52	.54	-15.8	-3.75	-14.6	7.43
Interturn Duration	-0.033	0.78	-0.21	0.24	-0.63	0.17	-1.21	0.45
Mag. Body Angle (°)	-35.7	-1.79	-31.8	-0.58	-23.7	-0.59	-19.5	3.99
Body Angle (°)	-3.11	9.97	-4.34	7.54	-7.63	4.24	-6.99	6.67
Angular Velocity (°/s)	-8.68	18.0	-14.0	14.6	0.77	20.4	-16.6	3.75
Angular Acceleration (°/s ²)	-7.41	3.27	-5.25	3.16	-1.29	4.25	-3.05	1.56

Table A.i.04 – Credibility intervals on the difference in means between animals with the same net antenna length, bilateral (B) vs antennectomy (A) (used to form [figure 3.07](#)). See [table A.i.01](#) for information on how to interpret HDIs. Significant differences are highlighted.

	2 cm B vs 4 cm A		1 cm B vs 2 cm A	
	HDI-low	HDI-up	HDI-low	HDI-up
Time to Source (s)	-10.4	5.98	-10.4	5.98
Walking Speed (cm/s)	-0.61	6.95	4.03	10.42
Track Width (cm)	-2.48	0.26	-1.58	0.34
Walking Distance (cm)	-181	114	-326	380
Linearity	-0.15	0.21	-0.12	0.10
No. Stops	-7.59	-0.61	-27.4	-6.31
Stop Duration (s)	-0.11	0.01	-0.10	0.01
Total Stop Time (s)	-1.57	-0.17	-5.14	-0.86
No. Backtracks	-3.16	3.26	-6.12	6.46
No. Left Turns	-4.55	8.92	-8.58	15.6
No. Right Turns	-5.48	4.63	-9.51	10.8
Interturn Duration	-0.56	-0.08	-1.14	-0.39
Mag. Body Angle (°)	-19.6	12.6	-9.85	11.5
Body Angle (°)	-7.32	4.24	-10.9	1.28
Angular Velocity (°/s)	-15.9	5.72	-8.27	19.1
Angular Acceleration (°/s ²)	-5.75	2.17	-2.43	3.90

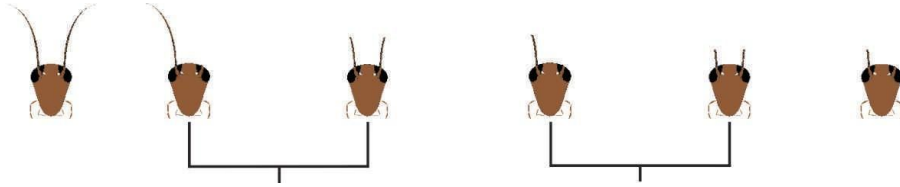
Table A.i.05 – Grand means \pm S.D. of parameters measured from the trajectories of *P.americana* males with antennae of different lengths as they walked upwind in plumes of female pheromone. Means across rows with no letters or symbols in common are significantly different according to a one-way ANOVA ($P \leq 0.05$) followed by a Tukeys-Kramer multiple comparison test (JMP ver. 11.1.1). Roman letters indicate significant groups in the ANOVA length comparisons, Greek letters (α , β , and γ) indicate significant groups in the length comparisons in the Bayesian hierarchical model.

	4 cm	2 cm	1 cm
Time to Source (s)	17.0 \pm 13.3 ^{bα}	45.0 \pm 44.7 ^{aβ}	52.9 \pm 42.5 ^{aγ}
Walking Speed (cm/s)	20.6 \pm 6.9 ^{aα}	17.4 \pm 6.81 ^{bβ}	18.4 \pm 6.05 ^{abβ}
Track Width (cm)	4.49 \pm 2.32 ^{bα}	5.29 \pm 2.17 ^{ab$\alpha\beta$}	6.13 \pm 1.86 ^{aβ}
Walking Distance (cm)	318 \pm 247 ^{bα}	707 \pm 797 ^{aβ}	914 \pm 808 ^{aγ}
Linearity	0.52 \pm 0.27 ^{aα}	0.34 \pm 0.2 ^{bβ}	0.22 \pm 0.18 ^{bγ}
No. Stops	7.84 \pm 7.58 ^{bα}	17.9 \pm 20.6 ^{aβ}	19.2 \pm 25.6 ^{a$\alpha\beta$}
Stop Duration (s)	0.14 \pm 0.13 ^{α}	0.14 \pm 0.09 ^{α}	0.15 \pm 0.09 ^{α}
Total Stop Time (s)	1.50 \pm 2.25 ^{bα}	3.75 \pm 5.28 ^{aα}	3.79 \pm 5.89 ^{aα}
No. Backtracks	3.29 \pm 4.48 ^{bα}	10.5 \pm 12.4 ^{aβ}	15.2 \pm 13.0 ^{aγ}
No. Left Turns	7.63 \pm 7.90 ^{bα}	21.3 \pm 27.3 ^{aβ}	25.6 \pm 23.2 ^{aβ}
No. Right Turns	8.04 \pm 9.33 ^{bα}	21.2 \pm 24.5 ^{aβ}	26.7 \pm 27.8 ^{aγ}
Interturn Duration	1.40 \pm 1.05 ^{α}	1.27 \pm 0.85 ^{α}	1.46 \pm 2.00 ^{α}
Mag. Body Angle (°)	44.4 \pm 24.7 ^{bα}	58.3 \pm 24.2 ^{aβ}	68.1 \pm 17.1 ^{aγ}
Body Angle (°)	1.60 \pm 11.5 ^{α}	1.36 \pm 9.84 ^{α}	-0.69 \pm 9.20 ^{α}
Angular Velocity (°/s)	5.36 \pm 20.3 ^{α}	-3.33 \pm 17.7 ^{α}	-0.09 \pm 19.1 ^{α}
Angular Acceleration (°/s ²)	-0.27 \pm 8.27 ^{α}	-0.39 \pm 5.37 ^{α}	0.57 \pm 4.5 ^{α}

Table A.i.06 - Grand means \pm S.D. of parameters measured from the trajectories of *P.americana* males with 1 and 2 antennae as they walked upwind in plumes of female pheromone. * is given in the 2 antennae column if there was a significant difference between groups by number of antennae in the ANOVA and [†] is given to denote a significant difference between 1 and 2 antennae individuals in the Bayesian Hierarchical model.

	2 antennae	1 antennae
Time to Source (s)	25.9 \pm 34.6* [†]	44.4 \pm 39.4
Walking Speed (cm/s)	22.4 \pm 6.48* [†]	16.0 \pm 5.55
Track Width (cm)	4.28 \pm 2.04* [†]	5.92 \pm 2.14
Walking Distance (cm)	597 \pm 896 [†]	615 \pm 456
Linearity	0.46 \pm 0.30 [†]	0.32 \pm 0.24
No. Stops	6.83 \pm 9.16* [†]	20.4 \pm 22.4
Stop Duration (s)	0.11 \pm 0.11 [†]	0.16 \pm 0.10
Total Stop Time (s)	1.18 \pm 2.41* [†]	4.28 \pm 5.50
No. Backtracks	7.52 \pm 12.8 [†]	9.89 \pm 9.81
No. Left Turns	18.2 \pm 29.0 [†]	16.2 \pm 14.1
No. Right Turns	18.0 \pm 29.1 [†]	17.0 \pm 14.9
Interturn Duration	1.02 \pm 0.83 [†]	1.65 \pm 1.50
Mag. Body Angle (°)	48.6 \pm 25.8* [†]	60.7 \pm 22.4
Body Angle (°)	-0.03 \pm 9.87	1.75 \pm 10.7
Angular Velocity (°/s)	1.87 \pm 21.2	-0.05 \pm 17.7
Angular Acceleration (°/s ²)	-1.42 \pm 7.87	0.54 \pm 4.94

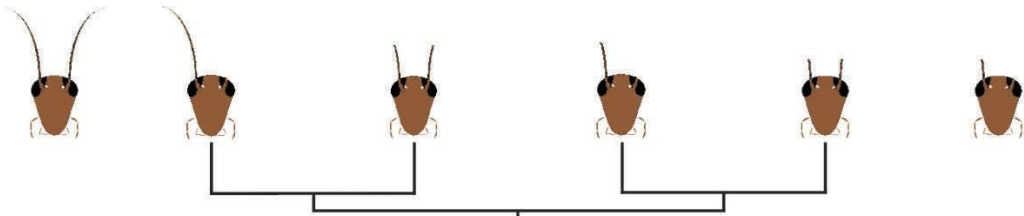
Table A.i.07. Least squares contrast between the mean track parameters measured from cockroaches with one or two antenna but with equal total length of antenna. Values listed are p-values.



Track parameter	4cm uni- vs bi- contrast	2cm uni- vs bi- contrast	Effect of side w/ respect to length
Walking distance (cm)	0.07	0.36	No effect of “side” on distance walked. [Tracks of roaches w/ one longer antenna marginally shorter.]
Time to Source (sec)	0.44	0.1	No effect of “side” on time to source.
Walking speed (cm/s)	0.06	0.0001*	Symmetrical roaches walk faster.
Track width (cm)	0.05	0.30	No effect of “side” on track width. [Roaches w/ one long antenna generate wider tracks than symmetrical roaches.]
Linearity index	0.69	0.75	No effect of “side” on directness of track.
Mean # stops	0.35	0.001*	Roaches w/ only one short antenna stop more.
Stop duration (sec)	0.12	0.20	No effect of side on stop duration.
Total stops time (sec)	0.31	0.005	No effect of “side” on total time stopped. [Roaches w/ only one short antenna stop more.]
# of Backtracks	0.12	0.71	No effect of “side” on backtracking.
# of Left turns	0.02	0.27	No effect of “side” on # of left turns. [Fewer L turns with longer antenna.]
# of Right turns	0.07	0.23	No effect of “side” on # of right turns.
Inter-turn duration (sec)	0.13	0.03	No effect of “side” on inter-turn durations. [Shorter inter-turn dur. w/ two short antennae.]
X body angle (degrees)	0.58	0.80	No effect of “side” on body angle
Body angle	0.69	0.08	No effect of “side” on body angle
Angular velocity (degrees/sec)	0.37	0.41	No effect of “side” on angular velocity
Angular acceleration (deg./s/s)	0.31	0.63	No effect of “side” on angular acceleration

Significance was designated after a Bonferroni correction for multiple comparisons. For this design the post-correction probability level indicating a statistically significant difference is $p < 0.002$

Table A.i.08. Least squares contrast of the effect of antennal length across all of the mean track parameters measured from cockroaches with one or two antenna equaling the same total length. Values listed are p-values.



Track parameter	4cm vs 2cm contrast	Effect of length regardless of symmetry
Walking distance (cm)	0.12	No effect of length regardless of symmetry on angular acceleration
Time to Source (sec)	0.002*	Significant effect of antennal length regardless of symmetry. [Cockroaches with longer antennae take less time to reach the source.]
Walking speed (cm/s)	0.10	No effect of length regardless of symmetry on angular acceleration
Track width (cm)	0.01	No effect of length regardless of symmetry on angular acceleration. [Roaches w/ one long antenna generate wider tracks than symmetrical roaches.]
Linearity index	0.0003*	Significant effect of antennal length regardless of symmetry. [Cockroaches with longer antennae generate a more direct track to the source.]
Mean # stops	0.002*	Significant effect of antennal length regardless of symmetry. [Cockroaches w/ only one short antenna stop more.]
Stop duration (sec)	0.43	No effect of side on stop duration.
Total stop time (sec)	0.005	No effect of "side" on total time stopped. [Roaches w/ only one short antenna stop more.]
# of Backtracks	0.021	No effect of "side" on backtracking.
# of Left turns	0.17	No effect of "side" on # of left turns.
# of Right turns	0.04	No effect of "side" on # of right turns.
Inter-turn duration (sec)	0.80	No effect of "side" on inter-turn durations. [Shorter inter-turn duration w/ two short antennae.]
Magnitude of body angle (degrees)	0.002*	Significant effect of antennal length regardless of symmetry. [Cockroaches with longer antennae steer more directly into the wind.]
Mean Body angle	0.96	No effect of length regardless of symmetry on angular acceleration
Angular velocity (degrees/sec)	0.20	No effect of length regardless of symmetry on angular acceleration

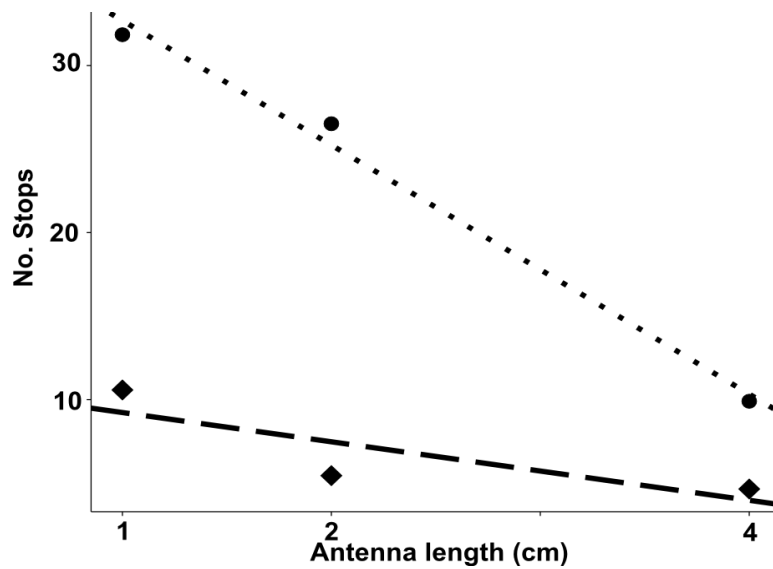
Angular acceleration
(deg./s/s)

0.84

No effect of length regardless of symmetry on
angular acceleration

Significance was designated after a Bonferroni correction for multiple comparisons. For this design the post-correction probability level indicating a statistically significant difference is $p < 0.003$.

Fig. A.i.01 – Interaction of antenna length and number of antennae with the number of stops: length ($F_{2,2}=7.31$, $p=0.001$), side ($F_{1,1}=28.0$, $p<0.001$), length-side interaction ($F_{2,2}=3.47$, $p=0.034$). The dotted line and circles are for 1 antenna, and the dashed line and diamonds are for 2 antennae.



Glossary:

- **algorithm** - the underlying calculus that drives a heuristic
- **heuristic** - an idea for how to accomplish something
- **model** - a description of how one would go about using that idea to accomplish the task
- **simulation** - turned that idea into a computer program and ran it a bunch (this seems to be what simulation means in scientific literature in other disciplines also)

Code used in [chapter 4](#).

All code is available on github.

Please See my git repository: <https://github.com/jklocport/roachSim>

References

- Anderson, J. D., Jr.** (2010). *Fundamentals of Aerodynamics*. 5th ed. McGraw-Hill.
- Andersson, P., Löfstedt, C. and Hambäck, P. A.** (2013). How insects sense olfactory patches – the spatial scaling of olfactory information. *Oikos* **122**, 1009–1016.
- Ariew, R. and Watkins, E.** (2009). *Modern Philosophy (Second Edition): An Anthology of Primary Sources*. Hackett Publishing Company.
- Baker, T. C. and Haynes, K. F.** (1989). Field and laboratory electroantennographic measurements of pheromone plume structure correlated with oriental fruit moth behaviour. *Physiol. Entomol.* **14**, 1–12.
- Bell, W. J. and Kramer, E.** (1979). Search and anemotactic orientation of cockroaches. *J. Insect Physiol.* **25**, 631–640.
- Bell, W. J. and Kramer, E.** (1980). Sex pheromone-stimulated orientation of the American cockroach on a servosphere apparatus. *J. Chem. Ecol.* **6**, 287–295.
- Bell, W. J. and Tobin, T. R.** (1981). Orientation to sex pheromone in the American cockroach: Analysis of chemo-orientation mechanisms. *J. Insect Physiol.* **27**, 501–508.
- Bell, W. J. and Tobin, T. R.** (1982). Chemo-orientation. *Biol. Rev. Camb. Philos. Soc.* **57**, 219–260.
- Berg, H. C. and Brown, D. A.** (1972). Chemotaxis in *Escherichia coli* analysed by three-dimensional tracking. *Nature* **239**, 500–504.
- Borst, A. and Heisenberg, M.** (1982). Osmotropotaxis in *Drosophila melanogaster*. *Journal of Comparative Physiology A* **147**, 479–484.
- Campbell, G. S.** (1977). *An Introduction to Environmental Biophysics*. Springer New York.
- COSEWIC** (2002). COSEWIC assessment and update status report on the Blue Whale *Balaenoptera musculus* in Canada. *Committee on the Status of Endangered Wildlife in Canada, Ottawa* vi + 32 pp.
- Crimaldi, J. P., Wiley, M. B. and Koseff, J. R.** (2002). The relationship between mean and instantaneous structure in turbulent passive scalar plumes. *J. Turbul.* **3**, N14.
- Daly, K. C., Kalwar, F., Hatfield, M., Staudacher, E. and Bradley, S. P.** (2013). Odor detection in *Manduca sexta* is optimized when odor stimuli are pulsed at a frequency matching the wing beat during flight. *PLoS One* **8**, e81863.
- De Freitas R. N., Littlejohn T. S., Clarkson I. S., Kristament, C. R.** (1982). Cave climate: Assessment of airflow and ventilation. *international journal of climatology* **2**, 383–397.
- Duistermars, B. J., Chow, D. M. and Frye, M. A.** (2009). Flies require bilateral sensory input to

- track odor gradients in flight. *Curr. Biol.* **19**, 1301–1307.
- Dusenbery, D. B.** (1997). Minimum size limit for useful locomotion by free-swimming microbes. *Proc. Natl. Acad. Sci. U. S. A.* **94**, 10949–10954.
- Eaton, J. L.** (1988). *Lepidopteran anatomy*.
- Fraenkel, G. S. and Gunn, D. L.** (1961). *The orientation of animals: kineses, taxes and compass reactions*. New York: Dover Publications Inc.
- Gettier, E. L.** (1963). Is Justified True Belief Knowledge? *Analysis* **23**, 121–123.
- Girling, R. D. and Cardé, R. T.** (2007). Analysis and manipulation of the structure of odor plumes from a piezo-electric release system and measurements of upwind flight of male almond moths, *Cadra cautella*, to pheromone plumes. *J. Chem. Ecol.* **33**, 1927–1945.
- Grünbaum, D. and Willis, M. a.** (2015). Spatial memory-based behaviors for locating sources of odor plumes. *Movement Ecology* **3**, 11.
- Guo, P. and Ritzmann, R. E.** (2013). Neural activity in the central complex of the cockroach brain is linked to turning behaviors. *J. Exp. Biol.* **216**, 992–1002.
- Hodgson, E. S.** (1958). ELECTROPHYSIOLOGICAL STUDIES OF ARTHROPOD CHEMORECEPTION. III. CHEMORECEPTORS OF TERRESTRIAL AND FRESH-WATER ARTHROPODS. *Biol. Bull.* **115**, 114–125.
- Hösl, M.** (1990). Pheromone-sensitive neurons in the deutocerebrum of *Periplaneta americana*: receptive fields on the antenna. *Journal of Comparative Physiology A* **167**, 321–327.
- Jackson, J. L., Webster, D. R., Rahman, S. and Weissburg, M. J.** (2007). Bed roughness effects on boundary-layer turbulence and consequences for odor-tracking behavior of blue crabs (*Callinectes sapidus*). *Limnol. Oceanogr.* **52**, 1883–1897.
- Kaissling, K.-E.** (2009). The Sensitivity of the Insect Nose: The Example of *Bombyx Mori*. In *Biologically Inspired Signal Processing for Chemical Sensing* (ed. Gutiérrez, A.) and Marco, S.), pp. 45–52. Springer Berlin Heidelberg.
- Kanaujia, S. and Kaissling, K. E.** (1985). Interactions of pheromone with moth antennae: Adsorption, desorption and transport. *J. Insect Physiol.* **31**, 71–81.
- Karman, T. V.** (1934). Turbulence and Skin Friction. *J. Aeronaut. Sci.* **1**, 1–20.
- Kennedy, J. S.** (1978). The concepts of olfactory “arrestment” and “attraction.” *Physiol. Entomol.* **3**, 91–98.
- Koch, U. T., Lüder, W., Andrick, U., Staten, R. T. and Cardé, R. T.** (2009). Measurement by electroantennogram of airborne pheromone in cotton treated for mating disruption of *Pectinophora gossypiella* following removal of pheromone dispensers. *Entomol. Exp. Appl.* **130**, 1–9.

- Koehler, O.** (1932). Beiträge zur Sinnesphysiologie der Süßwasserplanarien. *Z. Vgl. Physiol.*
- Kowalczyk, A. J. and Froelich, P. N.** (2010). Cave air ventilation and CO₂ outgassing by radon-222 modeling: How fast do caves breathe? *Earth Planet. Sci. Lett.* **289**, 209–219.
- Kraus-Epley, K. E. and Moore, P. A.** (2002). Bilateral and unilateral antennal lesions alter orientation abilities of the crayfish, *Orconectes rusticus*. *Chem. Senses* **27**, 49–55.
- Kruschke, J. K.** (2015). *Doing Bayesian Data Analysis: A Tutorial with R, JAGS, and Stan*. Academic Press.
- Lochmatter, T. and Martinoli, A.** (2009). Theoretical analysis of three bio-inspired plume tracking algorithms. In *2009 IEEE International Conference on Robotics and Automation*, pp. 2661–2668. ieeexplore.ieee.org.
- Lockey, J. K. and Willis, M. A.** (2015). One antenna, two antennae, big antennae, small: total antennae length, not bilateral symmetry, predicts odor-tracking performance in the American cockroach *Periplaneta americana*. *J. Exp. Biol.* **218**, 2156–2165.
- Magariyama, Y., Sugiyama, S. and Kudo, S.** (2001). Bacterial swimming speed and rotation rate of bundled flagella. *FEMS Microbiol. Lett.* **199**, 125–129.
- Manson, M. D.** (1992). Bacterial motility and chemotaxis. *Adv. Microb. Physiol.* **33**, 277–346.
- Marden, J. H., Wolf, M. R. and Weber, K. E.** (1997). Aerial performance of *Drosophila melanogaster* from populations selected for upwind flight ability. *J. Exp. Biol.* **200**, 2747–2755.
- Mast, S. O.** (1911). *Light and the Behavior of Organisms*. Wiley.
- Mitchell, B. K.** (2009). Chemoreception. In *Encyclopedia of Insects*, pp. 148–152. Elsevier.
- Moore, P. and Crimaldi, J.** (2004). Odor landscapes and animal behavior: tracking odor plumes in different physical worlds. *J. Mar. Syst.* **49**, 55–64.
- Moore, P. A. and Lepper, D.** (1997). Role of Chemical Signals in the Orientation behavior of the Sea Star *Asterias forbesi*. *Biol. Bull.* **192**, 410–417.
- Moore, P. A. and Weissburg, Marc J.** (1994). BENTHIC BOUNDARY LAYER FLOWS. *J. Chem. Ecol.* **20**,.
- Murlis, J. and Jones, C. D.** (1981). Fine-scale structure of odour plumes in relation to insect orientation to distant pheromone and other attractant sources. *Physiol. Entomol.* **6**, 71–86.
- Murlis, J., Willis, M. A. and Cardé, R. T.** (1990). Odour signals: patterns in time and space. In *Proceedings of the X International Symposium on Olfaction and Taste, Oslo*, pp. 6–17.
- Murlis, J., Elkinton, J. S. and Cardé, R. T.** (1992). Odor Plumes and How Insects Use Them. *Annu. Rev. Entomol.* **37**, 505–532.
- Murlis, J., Willis, M. A. and Cardé, R. T.** (2000). Spatial and temporal structures of pheromone plumes in fields and forests. *Physiol. Entomol.*

- Nishino, H. and Mizunami, M.** (2007). Sensilla position on antennae influences afferent terminal location in glomeruli. *Neuroreport* **18**, 1765–1769.
- Nishino, H., Watanabe, H., Kamimura, I., Yokohari, F. and Mizunami, M.** (2015). Coarse topographic organization of pheromone-sensitive afferents from different antennal surfaces in the American cockroach. *Neurosci. Lett.* **595**, 35–40.
- Nishino, H., Iwasaki, M., Paoli, M., Kamimura, I., Yoritsune, A. and Mizunami, M.** (2018). Spatial Receptive Fields for Odor Localization. *Curr. Biol.* **28**, 600–608.e3.
- Pflitsch, A. and Piasecki, J.** (2003). DETECTION OF AN AIRFLOW SYSTEM IN NIEDZWIEDZIA (BEAR) CAVE, KLETNO, POLAND. *Journal of Cave and Karst Studies* **65**, 160–173.
- Prandtl, L.** (1925). Bericht über Untersuchungen zur ausgebildeten Turbulenz. *ZAMM Z. Angew. Math. Mech.*
- Pritchard, D. T. and Currie, J. A.** (1982). Diffusion of coefficients of carbon dioxide, nitrous oxide, ethylene and ethane in air and their measurement. *J. Soil Sci.* **33**, 175–184.
- Rajan, R., Clement, J. P. and Bhalla, U. S.** (2006). Rats smell in stereo. *Science* **311**, 666–670.
- Riffell, J. a., Lei, H. and Hildebrand, J. G.** (2009). Neural correlates of behavior in the moth *Manduca sexta* in response to complex odors. *Proc. Natl. Acad. Sci. U. S. A.* **106**, 19219–19226.
- Roth, L. M. and Willis, E. R.** (1960). *The Biotic Associations of Cockroaches: Smithsonian Miscellaneous Collections, V. 141*. Washington: Smithsonian Institution.
- Schaller, D.** (1978). Antennal Sensory System of *Periplaneta americana* L. *Cell Tissue Res.* **191**, 121–139.
- Schneider, D.** (1957). Elektrophysiologische Untersuchungen von Chemo- und Mechanorezeptoren der Antenne des Seidenspinners *Bombyx mori* L. *Zeitschrift für Vergleichende Physiologie* **40**, 8–41.
- Shadlen, M. N. M. N. and Newsome, W. T. T.** (1996). Motion perception: seeing and deciding. *Proceedings of the National ...* **93**, 628–633.
- Shiffman, D.** (2012). *The Nature of Code*. D. Shiffman.
- Steck, K., Hansson, B. S. and Knaden, M.** (2009). Smells like home: Desert ants, *Cataglyphis fortis*, use olfactory landmarks to pinpoint the nest. *Front. Zool.* **6**, 5.
- Streeter, V. L. and Benjamin Wylie, E.** (1975). *Fluid mechanics*. McGraw-Hill.
- Takasaki, T., Namiki, S. and Kanzaki, R.** (2012). Use of bilateral information to determine the walking direction during orientation to a pheromone source in the silkmoth *Bombyx mori*. *J. Comp. Physiol. A Neuroethol. Sens. Neural Behav. Physiol.* **198**, 295–307.
- Tichy, H., Hinterwirth, A. J. and Gingl, E.** (2005). Olfactory receptors on the cockroach antenna signal odour ON and odour OFF by excitation. *Eur. J. Neurosci.* **22**, 3147–3160.

- Tobin, T. R.** (1981). Pheromone orientation: role of internal control mechanisms. *Science* **214**, 1147–1149.
- Trinh, K. T.** (2010). On the Karman constant. *arXiv [physics.flu-dyn]*.
- Van der Pers, J. N. C. and Minks, a. K.** (1993). Pheromone monitoring in the field using single sensillum recording. *Entomol. Exp. Appl.* **68**, 237–245.
- Vogel, S.** (1966). Flight in *Drosophila*. *J. Exp. Biol.* **44**, 567–578.
- Vogel, S.** (1994). *Life in Moving Fluids: The Physical Biology of Flow*. Princeton University Press.
- Wasserman, S., Lu, P., Aptekar, J. W. and Frye, M. A.** (2012). Flies dynamically anti-track, rather than ballistically escape, aversive odor during flight. *J. Exp. Biol.* **215**, 2833–2840.
- Webster, D. R. and Weissburg, M. J.** (2001). Chemosensory guidance cues in a turbulent chemical odor plume. *Limnol. Oceanogr.* **46**, 1034–1047.
- Wehner, R., Michel, B. and Antonsen, P.** (1996). Visual navigation in insects: coupling of egocentric and geocentric information. *J. Exp. Biol.* **199**, 129–140.
- Weissburg, M. J.** (2000). The fluid dynamical context of chemosensory behavior. *Biol. Bull.* **198**, 188–202.
- Weissburg, M. J. and Dusenbery, D. B.** (2002). A multidisciplinary study of spatial and temporal scales containing information in turbulent chemical plume tracking. *Environmental Fluid ...* **2**, 65–94.
- Weissburg, M. J. and Zimmer-Faust, R. K.** (1994). Odor plumes and how blue crabs use them in finding prey. *J. Exp. Biol.* **197**, 349–375.
- Willis, M. a. and Avondet, J. L.** (2005). Odor-modulated orientation in walking male cockroaches *Periplaneta americana*, and the effects of odor plumes of different structure. *J. Exp. Biol.* **208**, 721–735.
- Willis, M. a., Avondet, J. L. and Finnell, A. S.** (2008). Effects of altering flow and odor information on plume tracking behavior in walking cockroaches, *Periplaneta americana* (L.). *J. Exp. Biol.* **211**, 2317–2326.
- Willis, M. a., Avondet, J. L. and Zheng, E.** (2011). The role of vision in odor-plume tracking by walking and flying insects. *J. Exp. Biol.* **214**, 4121–4132.
- Willis, M. a., Ford, E. a. and Avondet, J. L.** (2013). Odor tracking flight of male *Manduca sexta* moths along plumes of different cross-sectional area. *J. Comp. Physiol. A Neuroethol. Sens. Neural Behav. Physiol.* **199**, 1015–1036.
- Yen, J.** (2000). Life in transition: balancing inertial and viscous forces by planktonic copepods. *Biol. Bull.* **198**, 213–224.

